



THE ACADEMY OF MANAGEMENT  
AND ADMINISTRATION IN OPOLE

---

**AGROTRONICS  
AND OPTIMAL CONTROL  
OF CRANES AND HOISTING  
MACHINES**

---

THE ACADEMY OF MANAGEMENT AND ADMINISTRATION IN OPOLE

Viatcheslav Loveikin, Yuriy Romasevych, Lyubov Shymko, Mikola Ohienko,  
Wojciech Duczmal, Witold Potwora, Liudmyla Titova, Ivan Rogovskii

**AGROTRONICS AND OPTIMAL CONTROL  
OF CRANES AND HOISTING MACHINES**

*Monograph*

Opole 2020

ISBN 978-83-66567-10-8

**Agrotronics and optimal control of cranes and hoisting machines.**  
Monograph. Opole: The Academy of Management and Administration in Opole,  
2020; ISBN 978-83-66567-12-2; pp. 164, illus., tabs., bibls.

Editorial Office:

Wyższa Szkoła Zarządzania i Administracji w Opolu 45-085 Polska, Opole, ul.  
Niedziałkowskiego 18 tel. 77 402-19-00/01 E-mail: info@poczta.wszia.opole.pl

Recommended for publication

by the Academic Council of Research Institute of Engineering and Technology  
of National University of Life and Environmental Science of Ukraine  
(Protocol No. 7 of February 21, 2020)

Reviewers

*prof. dr hab. Marian Duczmal, prof. dr hab. Waclaw Romaniuk,  
prof. dr hab. Eugeniusz Krasowski*

Authors of Monograph

*Viatcheslav Loveikin, Yuriy Romasevych, Lyubov Shymko, Mikola Ohiienko,  
Wojciech Duczmal, Witold Potwora, Liudmyla Titova, Ivan Rogovskii*

Publishing House:

Wyższa Szkoła Zarządzania i Administracji w Opolu 45-085 Polska, Opole,  
ul. Niedziałkowskiego 18 tel. 77 402-19-00/01

200 copies

Authors are responsible for content of the materials.

ISBN 978-83-66567-10-8

© Authors of Monograph, 2020  
© Publishing House WSZiA, 2020

**TABLE OF CONTENTS**

|  |     |
|--|-----|
| PREFACE.....   | 5   |
| CHAPTER 1. OPTIMAL CONTROL OF MINE WINDER.....   | 8   |
| 1.1 Dynamic optimization of a mine winder acceleration mode.....   | 8   |
| 1.2 Regime-parametric optimization of a mine winder deceleration.....  | 20  |
| 1.3 Energy optimization of a mine winder acceleration mode.....  | 32  |
| Conclusions to chapter 1.....  | 43  |
| References to chapter 1.....   | 44  |
| CHAPTER 2. AGROTRONICS AND OPTIMAL CONTROL<br>OF TOWER CRANE MECHANISMS.....   | 50  |
| 2.1 Dynamical analysis of the tower crane slewing mechanism (the case of<br>the steady velocity of the crane trolley)..... | 50  |
| 2.2 Optimization of the tower crane slewing (the case of the steady<br>velocity of the crane trolley).....                 | 63  |
| 2.3 Optimization of the slewing of the boom crane upon a complex<br>integral criterion.....                                | 78  |
| 2.4 Optimization of tower crane luffing and slewing.....   | 88  |
| Conclusions to chapter 2.....  | 101 |
| Reference to chapter 2.....  | 102 |
| CHAPTER 3. MANAGEMENT AND OPTIMAL CONTROL<br>OF OVERHEAD CRANES.....   | 109 |
| 3.1 Optimization of bridge crane movement control.....   | 109 |

*TABLE OF CONTENTS*

---

|   |     |
|---|-----|
| 3.2 Management and closed-loop optimal control of the system „crane-load” (minimum time control).....               | 120 |
| 3.3 Management and closed-loop optimal control of the system „crane-load” (minimum integral criterion control)..... | 129 |
| 3.4 Management and optimal control of the system „crane-load” as a function of time (minimum time control).....     | 143 |
| Conclusions to chapter 3.....   | 153 |
| References to chapter 3.....  | 155 |

## **PREFACE**

Cranes and hoisting machines are widely used in many areas of modern production. Transportation of different loads at the sea and river ports, warehouses, building yards as well as at machine-building and metallurgical factories is impossible without them. Thus, the improvement of their operational efficiency is a significant issue to study.

In the monograph authors have investigated the dynamic, energetic, and electric processes, which take place in the different types of cranes and hoisting machines. It led them to the grounded recommendations, which allowed to exploit cranes and hoisting machines mechanisms in optimal modes. It, undoubtedly, positively impacts machines' performance.

In chapter 1 authors described the results of a mine winder dynamics and optimal control investigations. They have used a three-mass dynamical model of a hoisting machine (mine winder). The researched modes were the starting (acceleration) and the braking (deceleration) of the mine winder during lifting and lowering of the final load (skip). The obtained results, which are in both analytical and numerical forms, refer to the dynamic and energetic indicators of the machine. They may be used for: calculation of dynamical loads in the elements of the mine winder under different methods of control (rheostatic or with a frequency inverter); improving the energy efficiency of the hoist machine exploitation; increasing of the mine winder operational life; developing or modernization of drive control systems, etc.

The main goal of chapter 2 is connected with revealing the influence of optimal (or suboptimal) control to the initiation and evolution of dynamic and energetic processes that take place in a tower crane (particularly in the slewing mechanism and the trolley movement mechanism). Authors have used both linear and nonlinear mathematical models of the mentioned mechanisms. In the carried out calculations

analytical and numerical approaches have been used. The obtained dynamic and energetic characteristics have been analyzed via maximal and RMS values, plots, and phase plots (refer to loads oscillations). In chapter 2 authors have approved that optimization of the slewing and trolley movement modes has a quite positive effect on the overall performance of the crane operation. Indeed, they cause the load pendular oscillations elimination, decreasing the overall level of dynamical loads and energy losses in the mechanisms' drives.

In chapter 3 authors focused on the impact of optimal control of bridge and gantry cranes on their efficiency indicators. The distinguishing feature of the presented results relates to the taking into account the electrical processes in the cranes' drive. They were accounted in the conducted calculations as constrains and as electro-dynamical forces. In chapter 3 have been shown the results, which may be used for a reducing of a crane motion cycle duration (even under unpredicted wind rushes), elimination of the load pendular oscillations, and improvement of energetic and dynamic characteristics of a crane.

The common feature of the researches, which is presented in the monograph, is a wide range of the used optimization criteria. They all are grounded by theoretical and practical goals. The first and foremost is connected with the desire of showing the different approaches, that allowed authors to find the solutions of the quite difficult (constrained, nonlinear) optimization problems.

These insights may be used in the allied sciences.

The practical usefulness of the research relates to the recommendations for: adjusting of different options of frequency-controlled cranes' and mine winders' drives; selection one or another optimal mode of a mechanism motion (according to the exploitation conditions and practical requirements); illustrations of performance reserves (in terms of capacity, energy efficiency, and reliability), etc. Their application provides decreasing of undesired (dynamic and energetic) features of cranes' and mine winders' mechanisms.

In the presented research were used classical (analytical dynamics, mathematical analysis, variation calculus, dynamic programming etc.) and modern

## *PREFACE*

---

(particle swarm optimization and its modifications, differential evolution, etc.) methods. Their combinations allowed to achieve the set goals and to develop new approaches to the problems of optimal control of mechanisms of cranes and mine winders.

Most of the monograph's content has been obtained in the frame of scientific research supported by the public grant of Ukraine „Scientific substantiation and development of methods of dynamic modeling and mode-parametric optimization of modern load-lifting machines” (registration number 0119U100848). It was conducted by scholars of National University of Life and Environmental Sciences of Ukraine.

The monograph is useful for specialists in the area of dynamics and optimal control, scientists, workers, and operators of cranes and hoisting machines, developers of the control systems, students, and graduate students of higher technical institutions.

## **CHAPTER 1. OPTIMAL CONTROL OF A MINE WINDER**

### **1.1 Dynamic optimization of a mine winder acceleration mode**

The issue of the mine winders' efficient operation is particularly relevant in modern conditions of mining. This is due to the fact that one can increase the technical and economic indicators of the whole production process by carrying out certain activities (machine design modernization; flexible and damping and/or inertial elements introduction into the machine structure, replacement of the old relay control systems by the modern computer-integrated ones, etc.) The mentioned activities should be carried out primarily for the technically outdated mine winders. It is possible to extend its service life, and in some cases to improve the energy efficiency performance of hoisting by reducing the dynamic loads in the machine's elements.

In order to study the mine winder operation dynamics, in the scientific papers [1, 2] was presented a multi-mass dynamical system with visco-flexible links. This has allowed taking into account wave processes in the ropes and estimating loads they caused [1]. The calculations of rope complex spatial fluctuations have been carried out in scientific papers [3, 4]. There has been proved. Those dynamic loads depend on the skip's speed diagram. A developed in [5] approach has made it possible to offer recommendations on preventing ropes severe wear. The issue of ropes dynamic calculation using approximate methods by applying the non-linear models is presented in the scientific paper [6]. These results can be used for approximate evaluation of dynamic processes in the mine winders.

Experimental research results of loads initiating in machine's components at different operation modes are presented in scientific paper [7], as well as the main factors affecting the machine dynamics are specified there. The parametric and operating parameters can be conditionally marked out among them [8]. The inertial, stiffness, and some other parameters of individual machine components, as well as

machine structure (components placement order in its structure), belong to the first group. The operating parameters include acceleration and deceleration durations, nature of external force impact and its magnitude [9].

Hoisting machines' motion modes optimization causes a significant improvement in their technical and economic indicators [10].

However, the optimization problems of mine winders have been studied in a few scientific papers [2, 11]. It means that there are unused reserves in improving of efficiency of a mine winder operation.

The issue of mine winder motion optimization is important. Nowadays, there is no its final solution. That is why the scientific researches in this area is continuing. Moreover, considering the progress in the field of controlled electric drive, the realization of mine winder optimal motion laws is not the subject of the principal difficulties.

Thus, the development of the algorithmic part of the modern mine winder motion control system should be carried out taking into account the nature of dynamic and energetic processes.

Since the mine winder is a complex mechatronic system, several factors should be considered during the synthesis of optimal motion control. Therefore, the most appropriate (in terms of machine efficiency improvement) is control that relates to the complex optimization problems' solutions (problems with complex optimization criteria). In addition, the very important issue is optimal control simulation, which allows to set optimal motion impact on dynamic and energetic indicators of the mine winder operation. This provides recommendations for implementation of optimal control on practice.

The objective of the current study is a synthesis of the mine winder optimal acceleration mode whereby its energetic and dynamic technical and performance indicators are increasing.

For study, we take a mine winder dynamic model, which is shown in fig. 1.1.

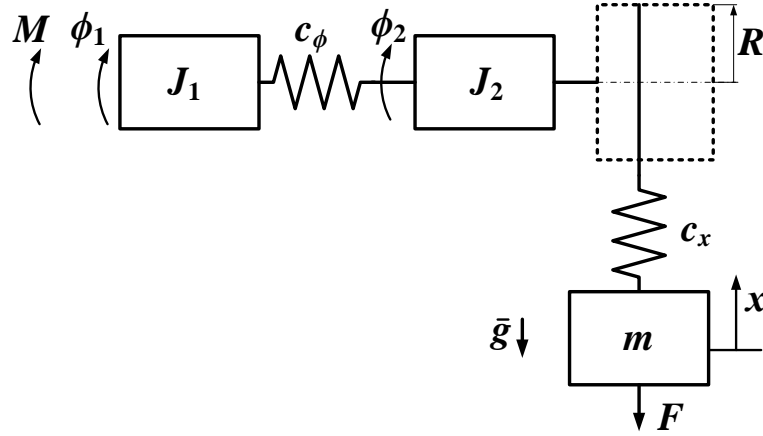


Fig. 1.1 The dynamic model of a mine winder

The scheme in the fig. 1.1 shows:  $J_1$  – reduced (equivalent) load inertia of the motor rotor and connecting halfcoupling;  $J_2$  – reduced load inertia of connecting halfcoupling, reduction unit, and rope drum;  $m$  – reduced mass of the final load;  $R$  – rope drum radius;  $c_\phi$  – reduced ratio of a coupling stiffness;  $c_x$  – reduced ratio of rope stiffness;  $M$  – reduced torque of the mine winder drive;  $F$  – reduced resistance force. Reduced mass of the final load  $m$  includes the skip and the rope masses: according to the Rayleigh method, it is sufficient to add a third part of the rope mass to the final load for calculating the rope mass when vibrating. All of the mine winder dynamic parameters are reduced to the rope drum. The following assumptions were used to build the model (fig. 1):

- 1) all components, except the flexible rope and flexible coupling, are absolutely rigid bodies with the same masses (moments of inertia);
- 2) when hoisting the load the reduced stiffness ratio  $c_x$  changes slightly, That is why it is a constant;
- 3) all the resistance forces and skip weight are reduced to the force  $F$ ;
- 4) elastic properties of the coupling and rope are subject to Hooke's law.

The mathematical model which refers the mine winder dynamic model (fig. 1.1) can be represented as follows:

$$\begin{cases} M = J_1 \ddot{\phi}_1 + c_\phi (\phi_1 - \phi_2); \\ c_\phi (\phi_1 - \phi_2) = J_2 \ddot{\phi}_2 + c_x (\phi_2 R - x) R; \\ c_x (\phi_2 R - x) = m \ddot{x} + F. \end{cases} \quad (1.1)$$

The point above the symbol means differentiation by time. The model shown in fig. 1.1 allows to study the dynamic loads in the flexible coupling and rope.

In order to carry out the machine acceleration mode optimization we use the complex criterion which is presented in the following form:

$$I = \frac{1}{T} \int_0^T (\delta_1 M^2 + \delta_2 \dot{M}^2) dt = \frac{1}{T} \int_0^T \left( \delta_1 (A_0 + \sum_{i=1}^3 A_i x^{(2i)})^2 + \delta_2 (\sum_{i=1}^3 A_i x^{(2i+1)})^2 \right) dt, \quad (1.2)$$

where  $T$  – duration of the system's acceleration to the steady rate  $v$ ;  $\delta_1$  and  $\delta_2$  – coefficients which reduce the corresponding components (driving torque and its change rate) to the dimensionless form and determine the importance of each of the components in the criteria structure;  $A_0 \dots A_3$  – constants ratios which are determined with the following expressions:

$$\begin{cases} A_0 = FR; \\ A_1 = \frac{J_1 + J_2}{R} + mR; \\ A_2 = \frac{1}{c_\phi} \left( mR J_1 + \frac{J_1 J_2}{R} \right) + \frac{m}{c_x R} (J_1 + J_2); \\ A_3 = \frac{J_1 J_2 m}{c_x c_\phi R}. \end{cases} \quad (1.3)$$

Criterion (1.2) is a complex one: expression at  $\delta_1$  shows the mean square value of driving torque during the machine acceleration. Choosing this component in the criterion structure is grounded by the need of reducing the variable electrical losses in the mine winder electric drive. In addition, it decreases the level of unwanted dynamic loads in the machine components. Expression at  $\delta_2$  shows the change rate of the motor torque. Quick change of the drive electromagnetic torque requires applying considerable voltages to its windings. It can damage the windings' insulation. Therefore, the rate of drive motor torque increasing and decreasing should be minimized; that determines the second term in the integrand of the optimization criterion (1.2).

The system's reduced masses boundary conditions should be set to complete the statement of the optimization problem:

$$\begin{cases} x(0) = x_0; \phi_1(0) = \phi_2(0) = 0; \\ \dot{x}(0) = \dot{\phi}_1(0) = \dot{\phi}_2(0) = 0; \\ x(T) = x_0 + \frac{vT}{2}; \phi_1(T) = \phi_2(T) = \frac{vT}{2R}; \\ \dot{x}(T) = v; \dot{\phi}_1(T) = \dot{\phi}_2(T) = \frac{v}{R}, \end{cases} \quad (1.4)$$

where  $x_0$  – is the final load position at the motion start;  $v$  – is the steady speed of the final load. All boundary conditions (1.4) may be expressed through higher derivatives of the function  $x(t)$  by time, whereby we obtain:

$$\begin{cases} x(0) = x_0; \dot{x}(0) = \ddot{x}(0) = \overset{IV}{x}(0) = \overset{V}{x}(0) = 0; \\ x(T) = x_0 + \frac{vT}{2}; \dot{x}(T) = v; \ddot{x}(T) = \overset{IV}{x}(T) = \overset{V}{x}(T) = 0. \end{cases} \quad (1.5)$$

We try to use variations calculus to minimize the expression (1.2). For this purpose we have written the Euler-Poisson formula [12], which for the integral functional (1.2) looks like as follows:

$$\sum_{i=2}^7 (-1)^i B_i x^{2i} = 0, \quad (1.6)$$

where  $B_i$  – are constant coefficients which may be expressed via coefficients  $A_0 \dots A_3, \delta_1, \delta_2$ . In order to find the solution of the homogeneous differential equation (1.6) one should obtain a corresponding characteristic equation. By substitution  $x^2=z$  we have presented it in the following form:

$$z^2 \cdot \left( B_2 + \sum_{i=1}^5 (-1)^i B_{i+2} z^i \right) = 0. \quad (1.7)$$

In order to find the roots of the equation (1.7) it is necessary to solve the fifth-degree algebraic equation, which can not be done analytically (in radicals) [13].

Therefore, we will find an approximate solution of the variational problem (1.1-1.5). For this purpose, we use direct variational method [14]. The first step of the method consists in finding solution of the boundary problem:

$$\left\{ \begin{array}{l} x = 0; \\ \left\{ \begin{array}{l} x(0) = x_0; \dot{x}(0) = \ddot{x}(0) = \overset{IV}{x}(0) = \overset{V}{x}(0) = 0; \\ x(\frac{jT}{4}) = q_j, \quad j = 1, 2, 3; \\ x(T) = x_0 + \frac{vT}{2}; \dot{x}(T) = v; \ddot{x}(T) = \overset{IV}{x}(T) = \overset{V}{x}(T) = 0, \end{array} \right. \end{array} \right. \quad (1.8)$$

where  $q_j$  – are unknown coefficients (they should be used to minimize the value of the functional (1.2)).

The solution of the boundary problem (1.8) has a significant volume and therefore is not presented here. In order to minimize the functional (1.2) we found its integrand, which is represented through higher derivatives by time of the boundary problem (1.8) solution. Thereafter, we take definite integral (1.2), which is a function of unknown coefficients  $q_j$ . In order to minimize the functional  $I(q_j)$  it is necessary to solve a system of linear equations:

$$\frac{\partial I}{\partial q_j} = 0. \quad (1.9)$$

Having found coefficients  $q_j$  from the system of equations (1.9) and having substituted them into the solution of the boundary problem (1.8), we obtain an approximate solution of the variational problem (1.1-1.5).

Choosing only three coefficients  $q_j$ , under which the functional (1.2) minimization has been performed, is substantiated by the fact that further complications of calculations due to the increasing of the number  $j$  only slightly affects the problem solution accuracy. On the other hand, the use of two or only one coefficient  $q_j$  does not allow to find an adequate approximation to the exact solution of variational problem (1.1-1.5).

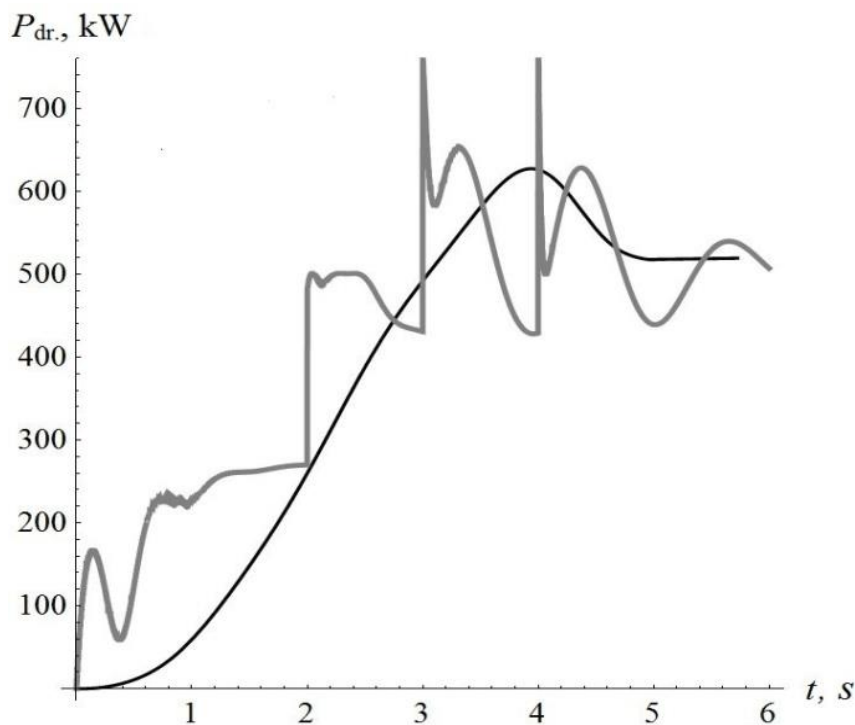
Let us compare the found optimal motion mode with that which was implemented using the rheostat resistance change of the machine's asynchronous drive. Actuation of the mine winder is carried out by AKH-2-16-39-12YXJ14 500 kW

high voltage asynchronous motor with phase rotor. The change of the engine is simulated as a effect of the three-stage change of rotor circle resistance.

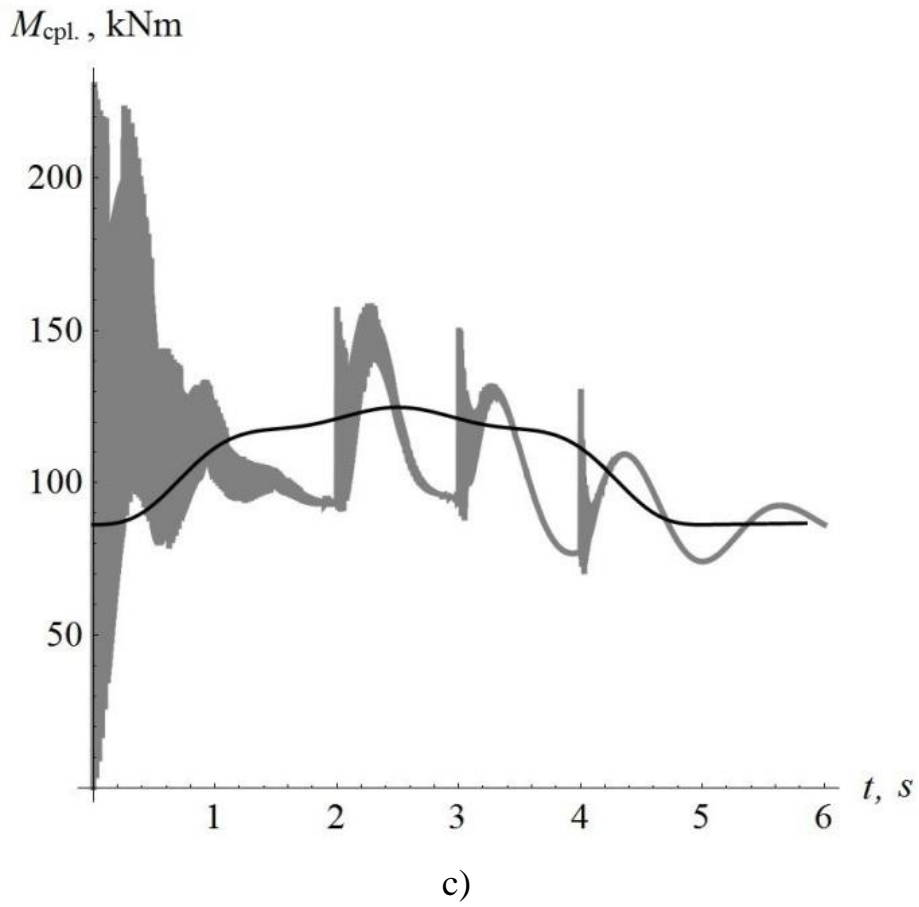
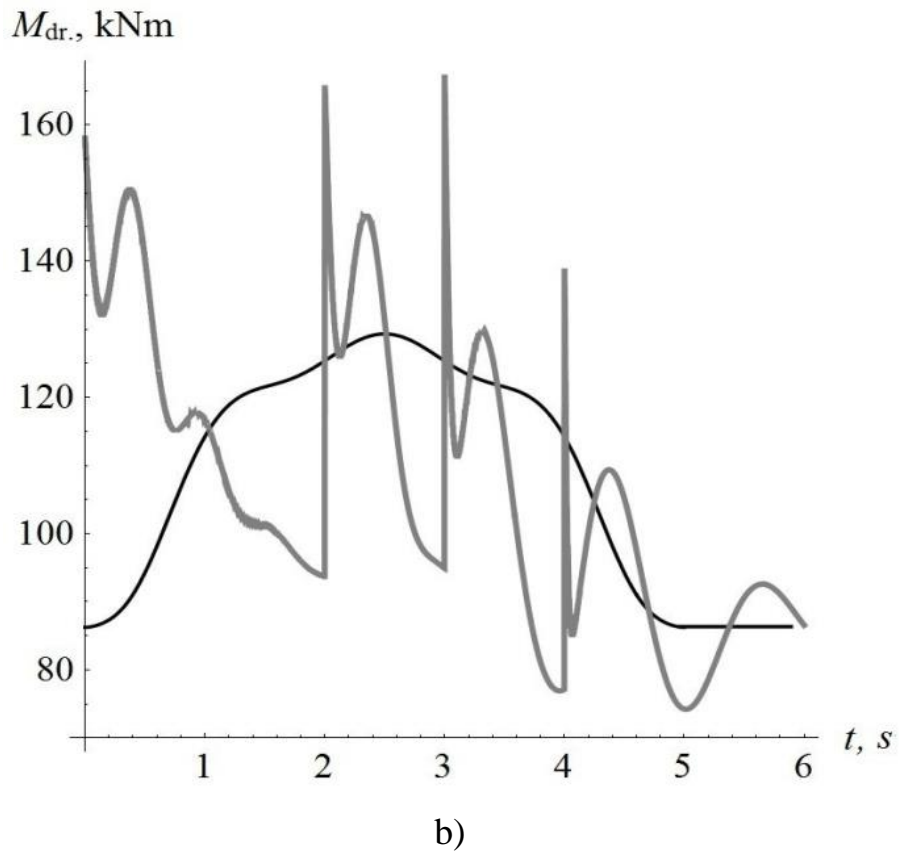
Fig. 1.2 shows the plots of the mine winder dynamical and energetic functions during its acceleration. All the plots are built for the following parameters of the mine winder:  $T=5$  s;  $\delta_1=0.5$ ;  $\delta_2=0.5$ ;  $v=12$  m/s;  $m=4400$  kg;  $J_1=2400$  kg·m<sup>2</sup>;  $J_2=2000$  kg·m<sup>2</sup>;  $R=2$  m;  $c_x=1,06 \cdot 10^5$  N/m;  $c_\phi=1,2 \cdot 10^9$  Nm/rad.

Grey diagrams on the fig. 1.2 correspond to the mine winder acceleration during rheostat control of the electric drive, and black diagrams correspond to suboptimal control. Analysis of the plots (fig. 1.2) shows that in conditions of identical acceleration time the energetic and dynamical indicators of mine winder during optimal motion control are much better than those corresponding to the drive motor rheostat control.

For example, the maximum power consumption during suboptimal control is 22.5% less than the same indicator refers to the rheostat control. The maximum torques of the engine and coupling are respectively 29.9% and 84.0% less than those obtained via rheostat control. Suboptimal control cause reducing the maximum force in the rope by 40.0%.



a)



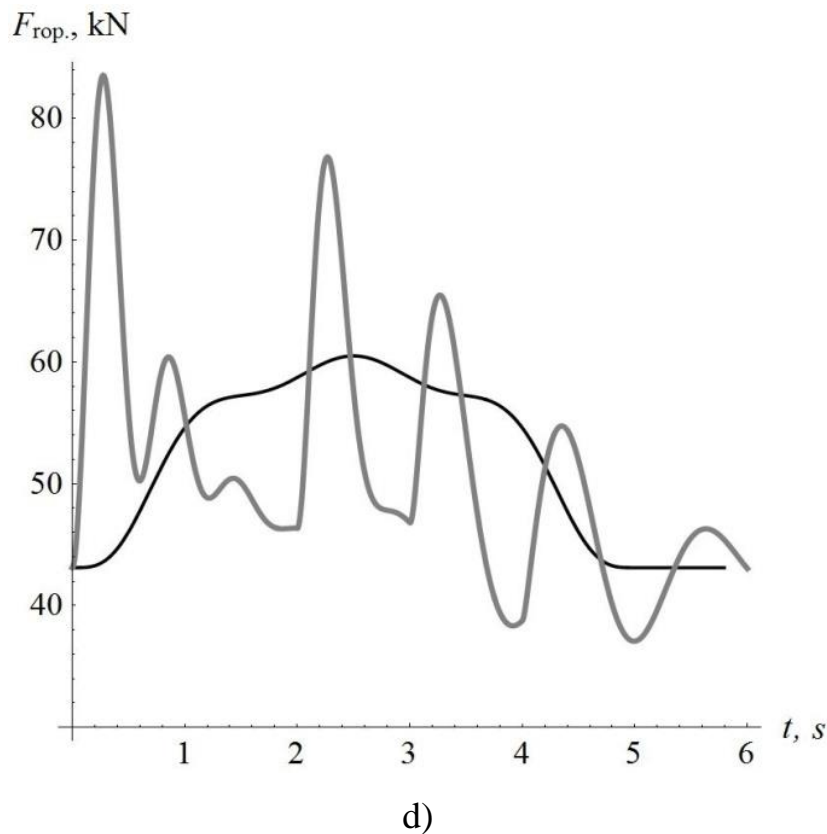


Fig. 1.2 Plots of mine winder motion characteristics during its acceleration: a) engine capacity; b) machine drive torque; c) torque in the flexible coupling; d) force in the rope

In addition, fig. 1.2 shows that at the end of acceleration (which lasts 5 seconds) according to the suboptimal law the machine motion energetic and dynamic indicators are constant. Under rheostat-controlled start these characteristics continue to fluctuate.

Hence, the effect of suboptimal control is in reducing the unwanted dynamic loads in machine's components (in rope and flexible coupling), as well as in minimization of drive motor peak of power.

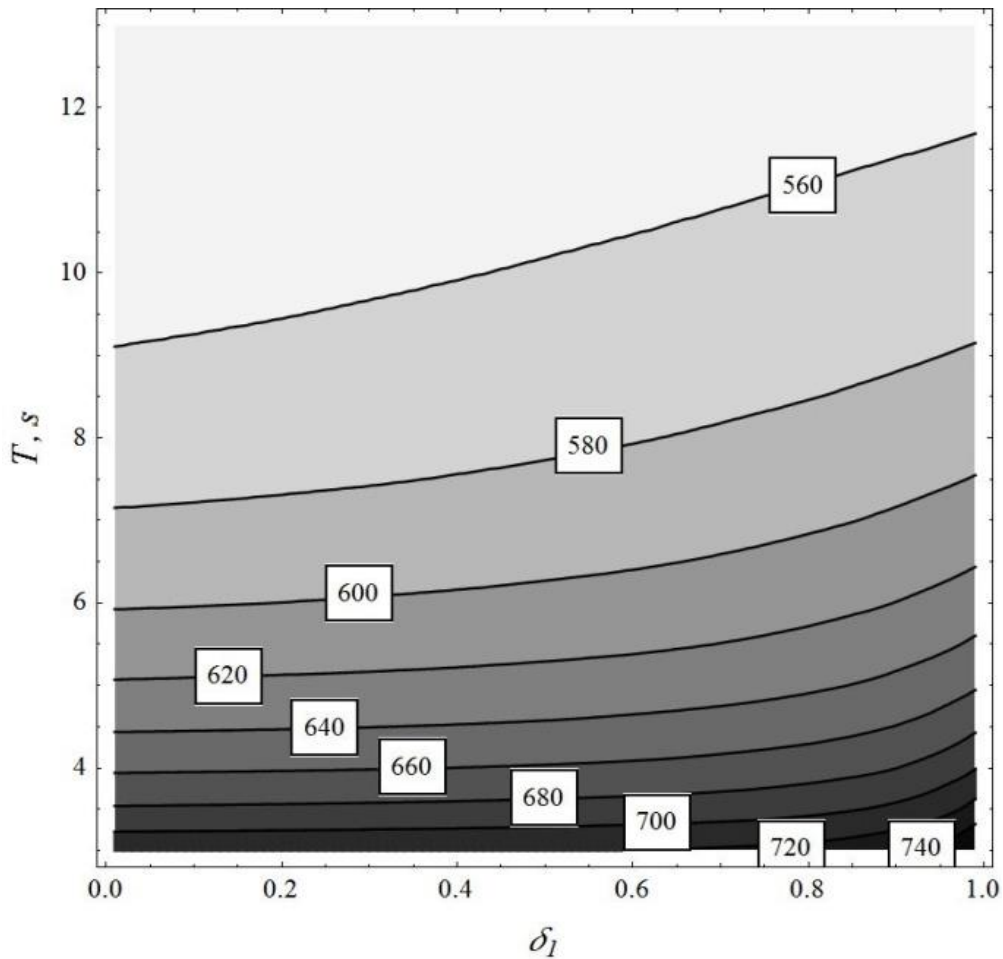
In order to determine its practical value of the study we have carried out additional study. For this purpose, we choose the indicators under which the analysis of the estimation of the system motion. Such indicators include:

- 1) maximal drive motor capacity  $P_{\max}$ , kW;
- 2) maximal torque in coupling  $M_{\text{cpl.}\max}$ , kNm;
- 3) maximal drive motor torque  $M_{\text{dr.}\max}$ , kNm;

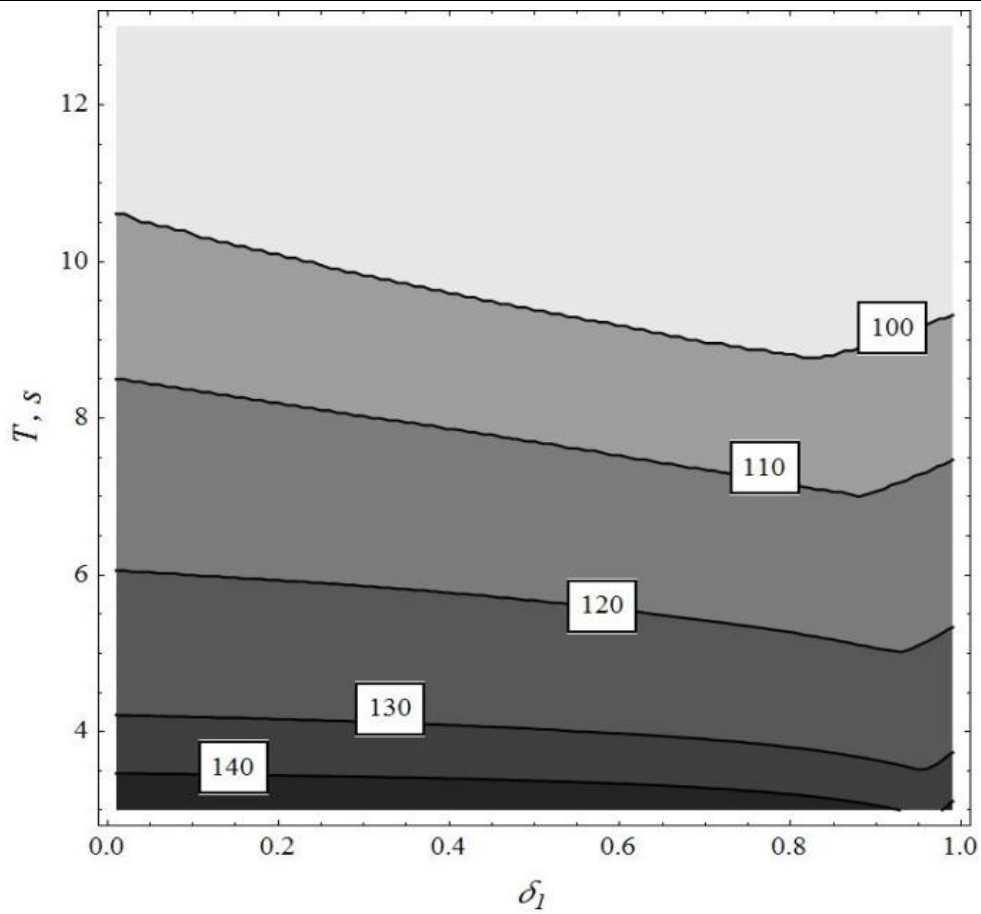
4) maximal force in the rope,  $F_{\text{rop,max}}$ , kN.

Independent factors were  $\delta_1$  and  $T$ . Value  $T$  was being varied in the range 3-13 s with increment 0.5 s. Coefficient  $\delta_1$  was being varied in the range of 0.01-0.99 with increment of 0.01. Thus, 2079 computer experiments have been carried out to evaluate the approximate solution of optimization problem (1.1-1.5). In each experiment six estimated indicators were determined. Calculation results are shown in fig. 1.3.

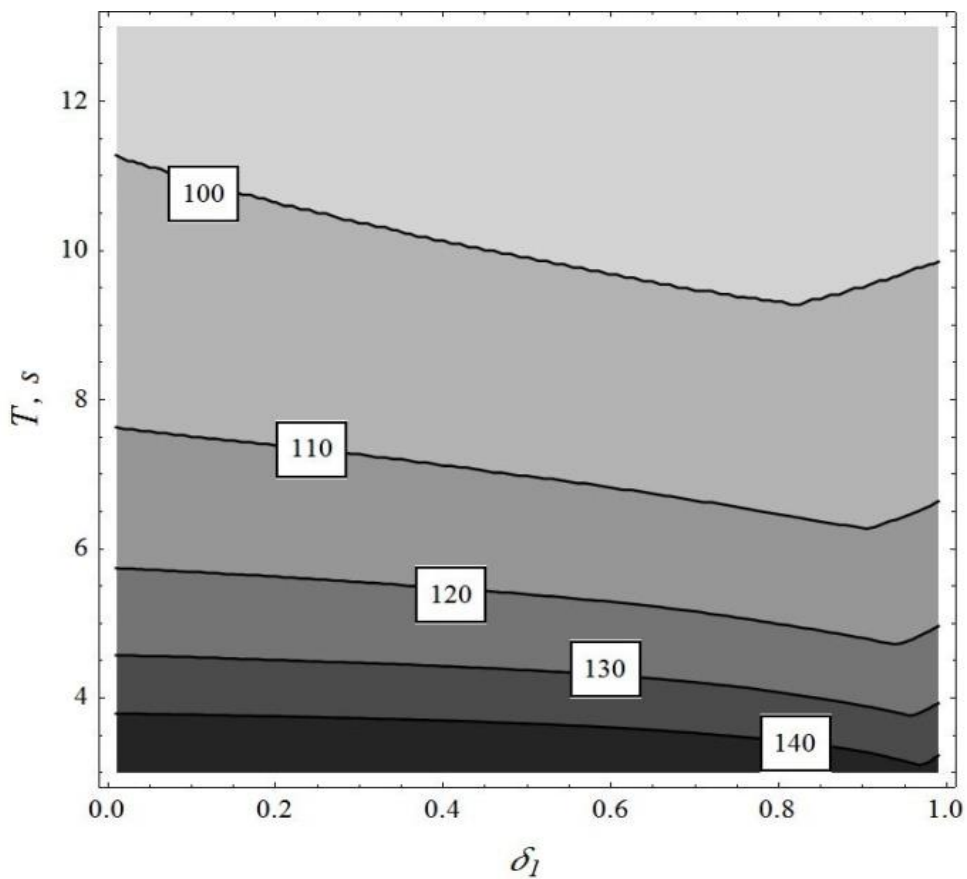
In order to determine the rational parameter settings of  $\delta_1$  and  $T$  during the mine winder operation, we carry out an analysis of the obtained data. First of all, we noted that increasing the acceleration time  $T$  causes intensive reduction of all unwanted evaluation indicators. However, further increasing of  $T$  does not influence on them (fig. 1.3). Thus, rationally substantiated acceleration duration  $T$  is in the range of 5-6 s. In this case, the engine is overloaded in 1.21-1.17 times and dynamic factors of the coupling and the rope are 1.45-1.33 and 1.46-1.37 respectively.



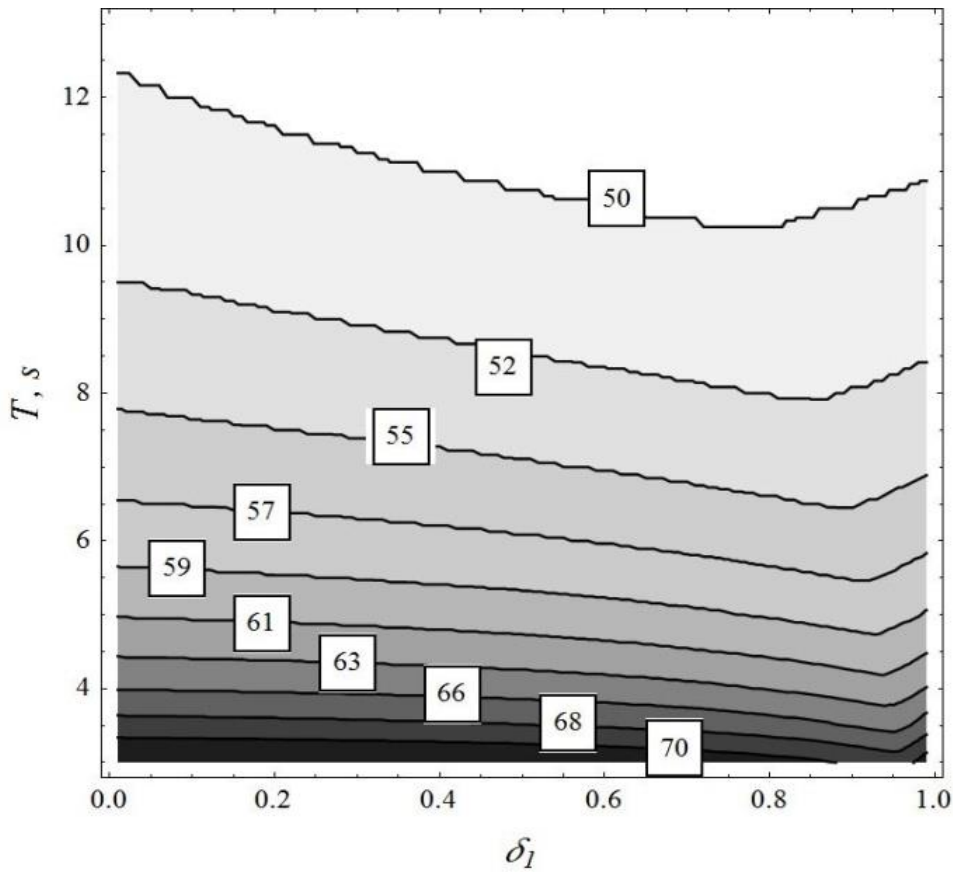
a)



b)



c)



d)

Fig. 1.3 Contour graphics that illustrate dependencies of estimated indicators from values  $\delta_1$  and  $T$ : a)  $P_{\max}$ , kW; b)  $M_{\text{cpl.max}}$ , kNm; c)  $M_{\text{dr.max}}$ , kNm; d)  $F_{\text{rop.max}}$ , kN

It should be noted that the implementation of the machine acceleration suboptimal mode is carried out by using the frequency inverter, which can withstand overload current 1.5 times for 60 s [15]. Thus, the overload of the engine and the frequency inverter at  $T=5$  s is in the acceptable limits.

Using fig. 1.3, it is possible to determine the impact of the parameter  $\delta_1$  on the dynamic and energetic indicators of the mine winder operation. While increasing  $\delta_1$  the indicator  $P_{\max}$  is slightly increasing. For example, when  $T=5$  s changing coefficient  $\delta_1$  from 0.01 to 0.99 increases value  $P_{\max}$  only by 4.8%. The opposite situation for estimated dynamic indicators: when  $T=5$  s changing coefficient  $\delta_1$  from 0.01 to 0.99 decreases  $M_{\text{cpl.max}}$  and  $M_{\text{dr.max}}$  by 5.9% and  $F_{\text{rop.max}}$  by 5.1% respectively. For large values  $T$  the impact of the coefficient  $\delta_1$  is not significant. In order to reduce the criterion value, it is desirable to set the value  $\delta_1$  in the range 0.01...0.1. The

performance should be given to the reducing of the root-mean-square value of the driving torque change rate [16].

## **1.2 Regime-parametric optimization of a mine winder deceleration**

The state-of-art mine winders work in quite hard regimes. Basically, it is connected with the demands of their high productivity and load capacity. At another point a mine winder should be reliable; its operation life must be as long as possible. Mentioned above demands are contradictory. In order to meet them (to a greater or a lesser extent), designers of a mine winder should find compromises.

One of the ways to find such compromises is to design a mine winder with optimal parameters. Moreover, designers of the mine winder's system of control should develop the speed diagrams for different regimes of mine winder motion. The solutions of both problems in aggregate allow improving the processes' effectiveness of the hoist machine.

Dynamic effects in elements of mine winders have been studied in many works. In articles [17, 18] the analytical expressions of maximum loads in rope in different operation conditions were obtained. In many articles, numerical simulation was used [19, 20]. It has been stated that rope tension is the function of a machine movement regime [20] and machine's parameters [21] (some of them may be non-linear [22]).

Researchers in the mentioned works used mathematical models based on ordinary [19] and partial [17] differential equations.

In the article [18] correlation between rope tensions, fretting and fatigue parameters was established. The results of the investigation [23] show the danger of collision between two adjacent ropes. It is caused by large axial fluctuating displacements of head sheaves. Dangerous dynamic loads in the mine hoisting rope are also connected with its internal spiral components [21]. In the work [24] the connection between the dynamic loads and safety of exploitation of shafts has been researched.

In the analyzed works only peak (maximum and minimum) values of the rope tension were taken into calculations. The indicators which reflect the overall load (for instance, the root-mean-square value) during the transient regime have not used. Moreover, the loads in other elements of a mine winder are still unstudied.

There are many scientific works in which mine winder control problems have been studied. For these purposes use classical [25] and non-classical [26, 27] methods of automatic control theory. They allow to obtain a control of the mine winder final (terminal) load movement. It is notable that in the work [27] the problem statement of the mine winder optimal control has been shown. But its solution has not given. In the article [28] the speed curve of the mine hoist has been obtained. It is smooth and piecewise. Obviously, the character of the speed curve is attended with a low level of dynamic loads which is desirable.

In conclusion, it is necessary to mention the works [29, 30] in which the implementation of a mine winder control has been studied. The state-of-the-art approach in such a field is using the programmable industrial controllers with specific communication channels and protected sensors.

Nowadays, a mine winder, as well as other lifting machinery [11], is a complex mechatronic system. The movement control of a mine winder is connected with industrial controllers using. These devices can be programmed by some means or other. The software of a mine winder control system should include the optimal (in some sense) laws of its motion. The implementation of the optimal laws can be performed with the high-capacity frequency inverters.

Thus, the main problem at the stage of the previous calculation of the mine winder motion regimes is a selection of the „right” optimization criterion and the effective method for a problem solution.

The general approach to improvement of a mine winder operation should take into account the processes of different nature (dynamic, energy, electrical, and information). That broad problem statement allows obtaining the increasing of mine winder efficiency by mean of rational changing of its construction and/or control system software. However, the carried out analysis showed that deep studies of mine

winders considered the effects which are caused only a few factors. It is desirable to study the mine winder movement from the regime and the parametric perspective.

Moreover, the results which will be obtained should be compared with the results of known scientific works and the best practice.

The objectives of the current work are improving the mine winder operation efficiency during deceleration of the final load lowering due to regime-parametric optimization and study the obtained results with dynamic and energetic indicators.

In order to carry out the study, we have used a mine winder dynamic model, which is described in the previous study (fig. 1.1).

The mathematical model, which meets the mine winder dynamic model, can be presented in the form of three differential equations (1.1).

The important part of the research is the choice of the optimization criterion. We have chosen the complex – integral-terminal – criteria  $Cr$ , which can be presented in the following form:

$$\left\{ \begin{array}{l} Cr = Ter_0 + Ter_T + Int \rightarrow \min; \\ Ter_0 = \delta_{\dot{M}} \dot{M}^2(0); \\ Ter_T = \delta_{\dot{M}} \dot{M}^2(T); \\ Int = T^{-1} \int_0^T (\delta_1 M^2 + \delta_2 (c_x (\phi_2 R - x))^2 + \delta_3 (c_\phi (\phi_1 - \phi_2))^2 + \delta_4 \dot{M}^2) dt, \end{array} \right. \quad (1.10)$$

where  $T$  – duration of the system deceleration to the quiescent state;  $\delta_1$ ,  $\delta_2$ ,  $\delta_3$  and  $\delta_4$  – coefficients, which reduce the respective components to dimensionless form and determine the importance of each of the components in the criterion structure;  $\delta_{\dot{M}}$  – coefficient, which reduces the terminal criteria  $Ter_0$  and  $Ter_T$  to the dimensionless form.

Minimization of terminal criteria  $Ter_0$  and  $Ter_T$  allows avoiding the „soft” force interaction between the mine winder transmission elements.

Minimization of the expression at  $\delta_1$  causes increasing in energy efficiency of the mine winder drive and dynamic loads in the machine decrease as well. The components at  $\delta_2$  and  $\delta_3$  reflect the force in the rope and torque in the coupling respectively.

The expression at  $\delta_4$  shows the rate of the drive torque changing. Its minimization is required under conditions of the normal operation of the mine winder drive.

All the coefficients can be presented as follows:

$$\begin{cases} \delta_1 = k_1(\nu R^{-1}P^{-1})^2; \\ \delta_2 = k_2(mg)^{-2}; \\ \delta_3 = k_3(\nu R^{-1}P^{-1})^2; \\ \delta_4 = (1 - k_1 - k_2 - k_3)T^4 \left( 2(FRT - 2R(mr^2 + J_1 + J_2)) \right)^{-2}; \\ \delta_{\dot{M}} = T^4 \left( 2(FRT - 2R(mr^2 + J_1 + J_2)) \right)^{-2}, \end{cases} \quad (1.11)$$

where  $k_1, k_2, k_3$  – weight coefficients which show the significance of the corresponding components at the criterion *Int* structure;  $P$  – rated power of the mine drive;  $\nu$  – the constant final load motion speed. Criteria (1.10) may be presented in another form:

$$\begin{cases} Ter_0 = \delta_{\dot{M}} \left( \sum_{i=1}^3 A_i x^{(2i+1)}(0) \right)^2; \\ Ter_T = \delta_{\dot{M}} \left( \sum_{i=1}^3 A_i x^{(2i+1)}(T) \right)^2; \\ Int = T^{-1} \int_0^T \left( \delta_1 \left( A_0 + \sum_{i=1}^3 A_i x^{(2i)} \right)^2 + \delta_2 (F + m\ddot{x})^2 + \right. \\ \left. + \delta_3 \left( B_0 + \sum_{j=1}^2 B_j x^{(2j)} \right)^2 + \delta_4 \left( \sum_{i=1}^3 A_i x^{(2i+1)} \right)^2 \right) dt, \end{cases} \quad (1.12)$$

where  $A_0 \dots A_3$  and  $B_0 \dots B_2$  – constants which are determined as follow:

$$\begin{cases} A_0 = FR; \\ A_1 = (J_1 + J_2)R^{-1} + mR; \\ A_2 = (mRJ_1c_\phi^{-1} + J_1J_2(c_\phi R)^{-1}) + m(J_1 + J_2)(c_x R)^{-1}; \\ A_3 = J_1J_2m(c_x c_\phi R)^{-1}; \\ B_0 = FJ_2; \\ B_1 = m + J_2R^{-1}; \\ B_2 = mJ_2(c_x R)^{-1}. \end{cases} \quad (1.13)$$

The boundary conditions of the system follow:

$$\begin{cases} \phi_1(0) = 0; \phi_2(0) = -FRc_\phi^{-1}; x(0) = -FR^2c_\phi^{-1} - Fc_x^{-1}; \\ \dot{x}(0) = -v; \dot{\phi}_1(0) = \dot{\phi}_2(0) = -vR^{-1}; \\ x(T) = -FR^2c_\phi^{-1} - Fc_x^{-1} - s; \phi_2(T) = -FR^2c_\phi^{-1} - sR^{-1}; \\ \phi_1(T) = -sR^{-1}; \dot{x}(T) = \dot{\phi}_1(T) = \dot{\phi}_2(T) = 0, \end{cases} \quad (1.14)$$

where  $s$  – the distance which the load passes during the deceleration regime. The boundary conditions (1.14) can be expressed through higher derivatives of  $x(t)$  by time, whereby we have obtained:

$$\begin{cases} x(0) = FR^2c_\phi^{-1} + Fc_x^{-1}; \dot{x}(0) = -v; \ddot{x}(0) = \overset{IV}{\ddot{x}}(0) = \overset{V}{x}(0) = \overset{V}{\dot{x}}(0) = 0; \\ x(T) = FR^2c_\phi^{-1} + Fc_x^{-1} + s; \dot{x}(T) = \ddot{x}(T) = \overset{IV}{\ddot{x}}(T) = \overset{V}{x}(T) = \overset{V}{\dot{x}}(T) = 0. \end{cases} \quad (1.15)$$

The analysis of the expressions (1.12) and (1.15) shows that taking into calculation the extra boundary conditions:

$$\begin{cases} \overset{VI}{x}(0) = \overset{VII}{x}(0) = 0; \\ \overset{VI}{x}(T) = \overset{VII}{x}(T) = 0 \end{cases} \quad (1.16)$$

allows meeting the absolute minimums of the terminal criteria  $Ter_0$  and  $Ter_T$ .

In work [16] we have found that the integral criterion of seventh order (the highest derivative of the function  $x(t)$  in the integrand) cannot be used in order to find the exact solution of the optimization problem. It connected with the fact that the characteristic equation of the Euler-Poisson's equation is fifth-order. It is impossible to find the solution of that kind of equation [13].

We can only find the approximate solution of the problem (1.10)-(1.15). We will use Euler's direct variation method [31]. In order to find the approximate solution, we have to use discrete values of the functions.

Moreover, the approximate solution should be found in conjunction of the regime and parametric domains. It allows obtaining a minimum of the criterion (1.11) compared with the value obtained only in the regime domain. In the study we have used the simplest approximation of the derivative:

$$x(t_i + 2^{-1}(t_i - t_{i-1})) = \lim_{t_i - t_{i-1} \rightarrow 0} \frac{x_i - x_{i-1}}{t_i - t_{i-1}} \approx \frac{x_i - x_{i-1}}{t_i - t_{i-1}} \quad (1.17)$$

if the remainder  $t_i - t_{i-1}$  is sufficiently small.

In expression (1.17) symbol  $n$  means the order of derivative by time and  $i$  – is the index which corresponds to the discrete moment of time  $t_i$ . So, we will consider the discrete function  $x_i(t_i)$  (in the subsequent the notation  $x_i$  will be used). Discrete function  $x_i$  must meet the conditions, which can be obtained from boundary conditions (1.15) and (1.16). These conditions are as follow:

$$\left\{ \begin{array}{l} x_0 = FR^2 c_\phi^{-1} + Fc_x^{-1}; (x_1 - x_0)\Delta t^{-1} = -v; \\ (x_2 - 2x_1 + x_0)\Delta t^{-2} = 0; \\ (x_3 + 3x_2 - 3x_1 - x_0)\Delta t^{-3} = 0; \\ (x_4 - 4x_3 + 6x_2 - 4x_1 + x_0)\Delta t^{-4} = 0; \\ (x_5 - 5x_4 + 10x_3 - 10x_2 + 5x_1 - x_0)\Delta t^{-5} = 0; \\ (x_6 - 6x_5 + 15x_4 - 20x_3 + 15x_2 - 6x_1 + x_0)\Delta t^{-6} = 0; \\ (x_7 - 7x_6 + 21x_5 - 35x_4 + 35x_3 - 21x_2 + 7x_1 - x_0)\Delta t^{-7} = 0; \\ x_{N-1} = FR^2 c_\phi^{-1} + Fc_x^{-1} + s; (x_{N-2} - x_{N-1})\Delta t^{-1} = 0; \\ (x_{N-3} - 2x_{N-2} + x_{N-1})\Delta t^{-2} = 0; \\ (x_{N-4} + 3x_{N-3} - 3x_{N-2} - x_{N-1})\Delta t^{-3} = 0; \\ (x_{N-5} - 4x_{N-4} + 6x_{N-3} - 4x_{N-2} + x_{N-1})\Delta t^{-4} = 0; \\ (x_{N-6} - 5x_{N-5} + 10x_{N-4} - 10x_{N-3} + 5x_{N-2} - x_{N-1})\Delta t^{-5} = 0; \\ (x_{N-7} - 6x_{N-6} + 15x_{N-5} - 20x_{N-4} + 15x_{N-3} - 6x_{N-2} + x_{N-1})\Delta t^{-6} = 0; \\ (x_{N-8} - 7x_{N-7} + 21x_{N-6} - 35x_{N-5} + 35x_{N-4} - 21x_{N-3} + 7x_{N-2} - x_{N-1})\Delta t^{-7} = 0, \end{array} \right. \quad (1.18)$$

where  $N$  – the number of the discretization steps;  $\Delta t$  – the time step i.e. the distance between nearest-neighbor moments at the discrete-time axis (values  $N$ ,  $\Delta t$  and  $T$  connected with following expression  $\Delta t = TN^{-1}$ ). The system of algebraic equations (1.18) allows finding the fourteen values  $x_0, \dots, x_7, x_{N-8}, \dots, x_{N-1}$ .

Using the discrete values of the function  $x(t)$  allows to formulate the next optimization problem – it is necessary to find the  $N-14+2$  unknown values, which minimize the Riemann sum:

$$\begin{aligned}
 Int \approx Sum_{Int} = & \sum_{k=7}^{N-8} \left( \delta_1 \left( A_0 + A_1 \Delta t^{-2} (x_{k+2} - 2x_{k+1} + x_k) + A_2 \Delta t^{-4} (x_{k+4} - 4x_{k+3} + \right. \right. \\
 & + 6x_{k+2} - 4x_{k+1} + x_k) + A_3 \Delta t^{-6} (x_{k+6} - 6x_{k+5} + 15x_{k+4} - 20x_{k+3} + 15x_{k+2} - 6 \times \\
 & \times x_{k+1} + x_k) \left. \right)^2 + \delta_2 \left( F + m \Delta t^{-2} (x_{k+2} - 2x_{k+1} + x_k) \right)^2 + \left( \delta_3 \left( B_0 + B_1 \Delta t^{-2} (x_{k+2} - \right. \right. \\
 & - 2x_{k+1} + x_k) + B_2 \Delta t^{-2} (x_{k+4} - 4x_{k+3} + 6x_{k+2} - 4x_{k+1} + x_k) \left. \right)^2 + \delta_4 \left( A_1 \Delta t^{-3} \times \right. \\
 & \times (x_{k+3} + 3x_{k+2} - 3x_{k+1} - x_k) + A_2 \Delta t^{-5} (x_{k+5} - 5x_{k+4} + 10x_{k+3} - 10x_{k+2} + 5x_{k+1} - \\
 & \left. - x_k) + A_3 \Delta t^{-7} (x_{k+7} - 7x_{k+6} + 21x_{k+5} - 35x_{k+4} + 35x_{k+3} - 21x_{k+2} + 7x_{k+1} - x_k) \right)^2. \quad (1.19)
 \end{aligned}$$

The two extra values which minimizing the  $Sum_{Int}$  are  $s$  and  $c_\phi$ .

For numerical calculation, the parameters of the mine winder were used as they are in the previous calculations. The regime parameters assumed are following:  $T=4$  s;  $v=12$  m/s;  $k_1=k_2=0.4$ ;  $k_3=0.15$ . These weight coefficients are assumed on a compromise basis. The significance of the corresponding components in the criterion (1.12) was taken into consideration as well.

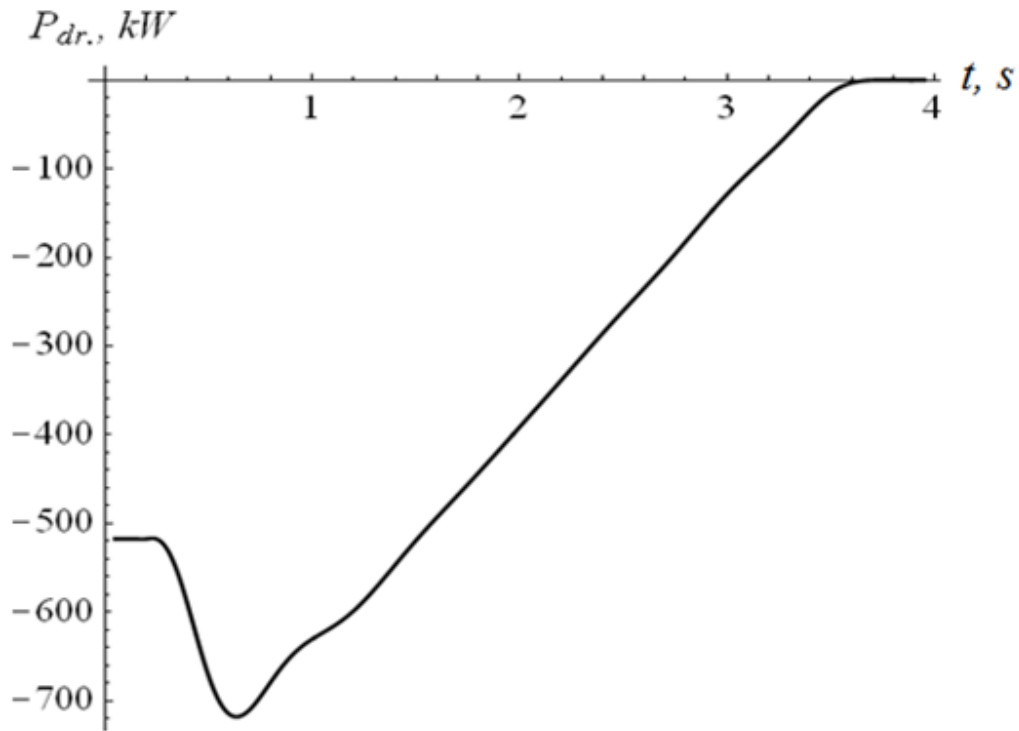
The stated problem has been solved with the differential evolution method [32]. As a result, the values  $x_8, \dots, x_{N-8}, s$ , and  $c_\phi$  were found. The optimal values of  $s$  and  $c_\phi$  are  $s=vT2^{-1}$  and  $c_\phi=1.55 \cdot 10^9$  Nm/rad.

The basic construction of the mine winder has the coupling with reduced coefficient of stiffness which is equal to  $1.2 \cdot 10^9$  Nm/rad. Thus, within the framework of the study that value of the coefficient  $c_\phi$  is not optimal.

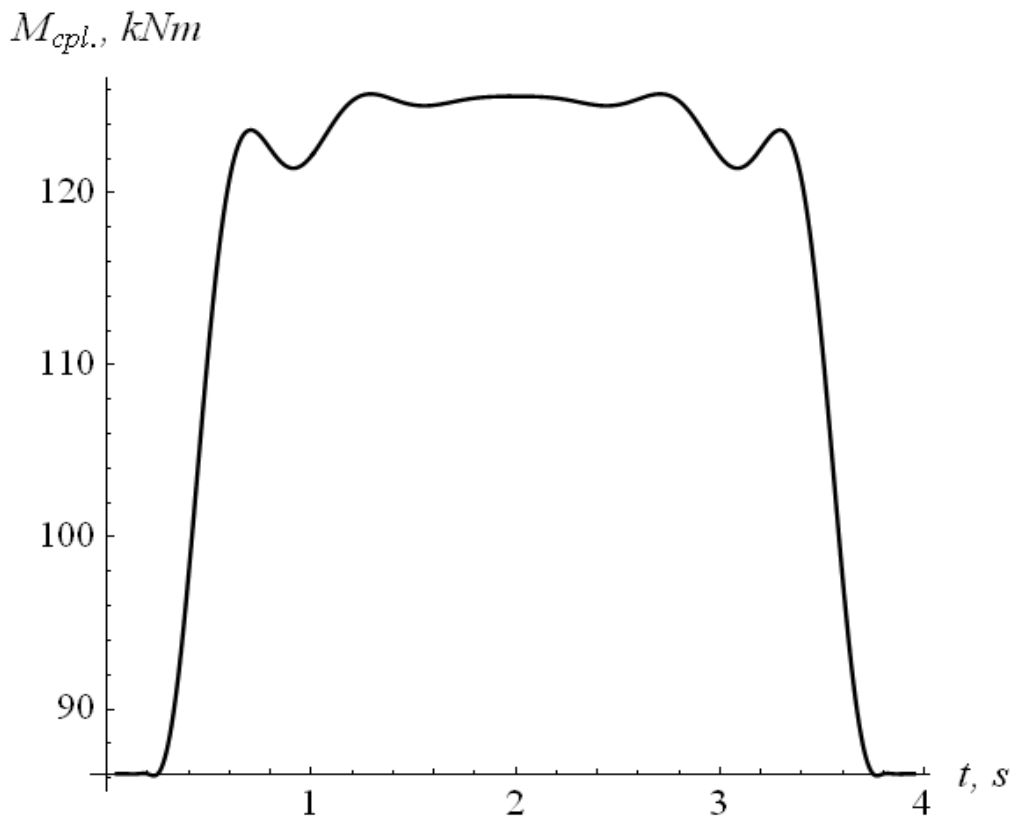
The drive of the considered mine winder includes the high voltage asynchronous motor with phase rotor AKH-2-16-39-12YXJI4 (rated-power output is 500 kW). The mine winder drive can work in braking mode (regenerative braking). It is possible due to the state-of-the-art inverters (they act as the mine winder drive power source) [33].

In order to illustrate the main characteristics of the optimal law of the mine winder motion their plots have been built (fig. 1.4). As the optimal law is discrete

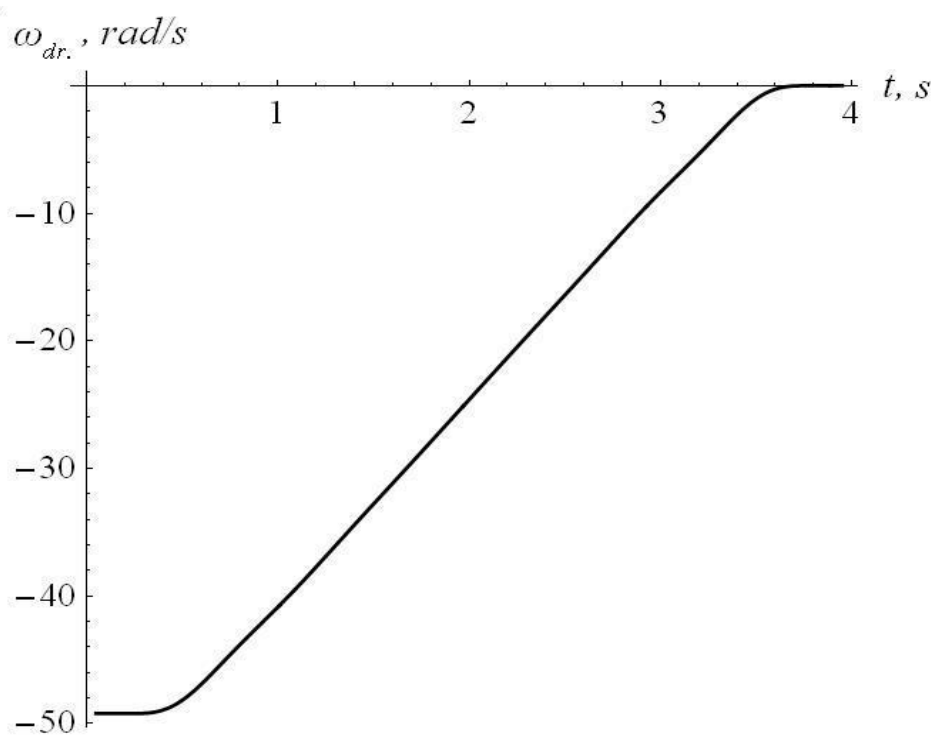
function  $x_i$  we have found the discrete function of angular velocity, drive power, rope force, and coupling torque. Then we built the third-order spline functions of the mentioned characteristics (fig. 1.4).



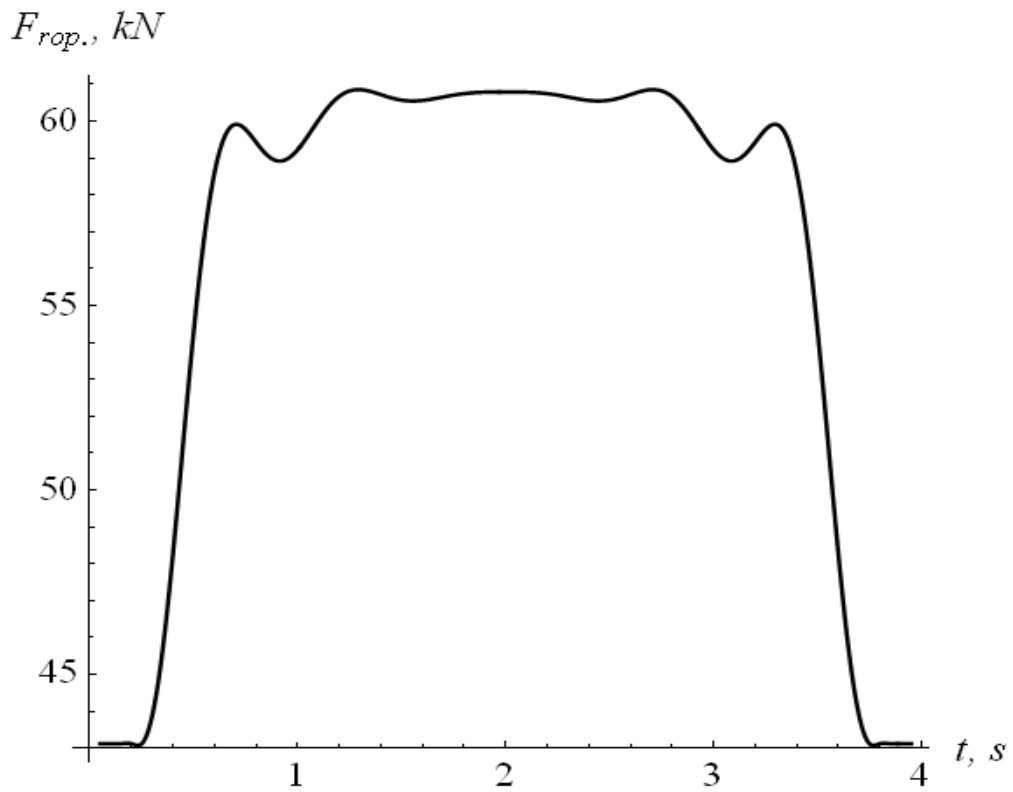
a)



b)



c)



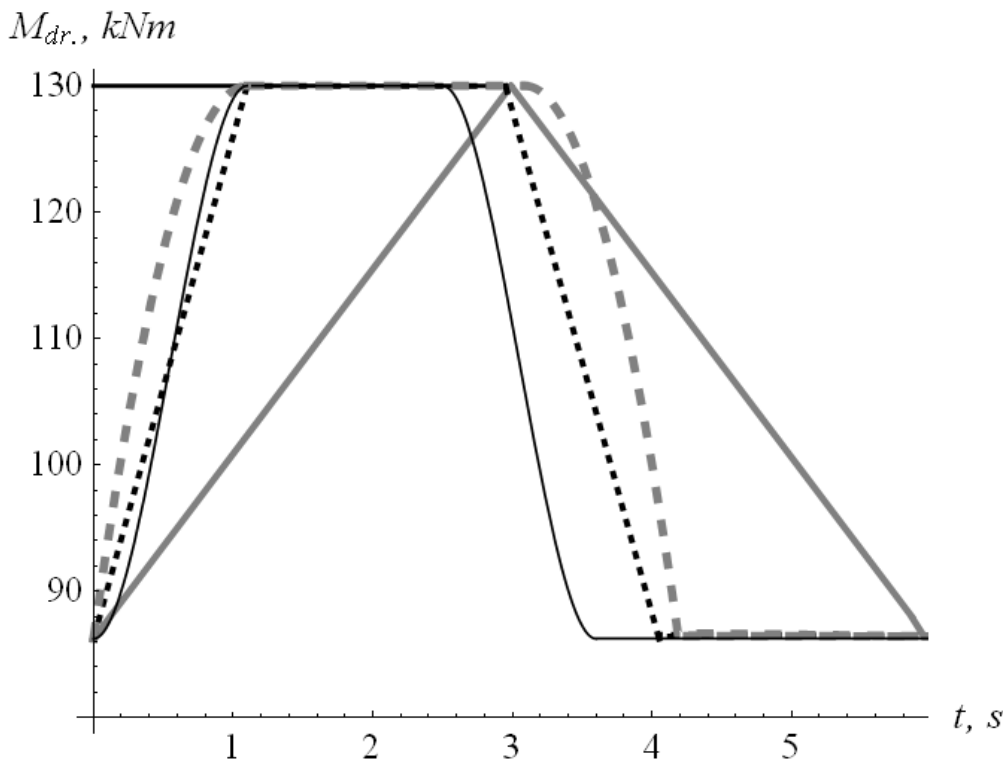
d)

Fig. 1.4 Diagrams of mine winder motion characteristics during its deceleration:  
 a) drive power; b) torque in the flexible coupling; c) drive angular velocity; d) force  
 in the rope

We should notice that all diagrams are smooth. Moreover, the increasing and decreasing of the functions near initial and final moments of time are very slow. It is the result of the minimization of the terminal criteria  $Ter_0$  and  $Ter_T$ . The advantages of that approach to problem solving will be shown in the following.

The residual oscillations of the coupling and the load (skip) do not exist. That means that dynamic forces in the rope and coupling after deceleration are minimized and (as consequence) the operation life of the mine winder will increase.

As has been noted above, modern inverters can implement the diagram of the deceleration torque. They might implement other shapes of deceleration torque as well. In order to carry out the comparative analysis, the different shapes of deceleration torque were selected. They are: constant, triangle-shaped, trapezium-shaped, U-shaped, and S-shaped. The following calculations were carried out for two cases (fig. 1.5): 1) the deceleration torque is constant (130 kNm) and the deceleration duration is variable; 2) the deceleration torque is variable and the deceleration duration (4 s) is constant. These constant values selected as the parameters of the found optimal law.



a)

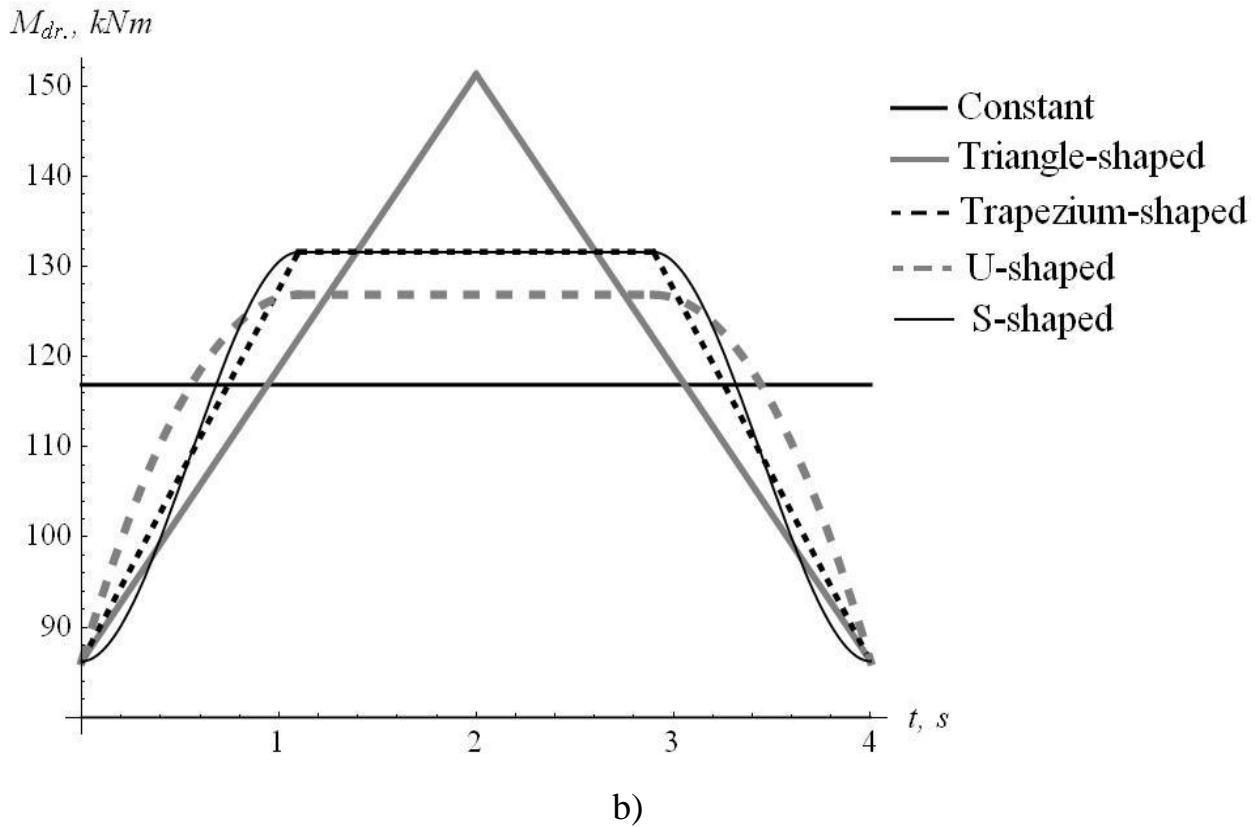


Fig. 1.5 Diagrams of drive deceleration torque shapes which selected for comparative analysis: a) for the first case; b) for the second case

The variable values for each deceleration torque law and for each case were calculated on the basis of the mine winder braking.

The diagrams of the deceleration torque for both cases have been shown in fig 1.5. In fig. 1.5 (a) assumed that increasing and decreasing duration is equal to 1.1 s. These durations for optimal law of deceleration torque is about the same.

The results of carried out calculations are in Table 1.1. The biggest values are marked with gray, and the smallest ones – with bold. Comparing analysis of the coupling torque allowed to state: using the optimal control is the best way to reduce the load in this element of the mine winder transmission. The reduction of unwanted dynamic loads is within 15.4...82.7%.

The maximum of the load in the rope is not big. It is equal to the value which corresponds to triangle-shaped deceleration torque. But for the last case the duration of the deceleration almost in one and a half times bigger. The reducing of unwanted dynamic loads in the rope for all considered deceleration torque laws is up to 28.4%.

Table 1.1. The dynamic and energetic indicators which correspond to different laws of the deceleration torque

| Deceleration torque law | Deceleration duration, s | Deceleration torque maximum, kNm | Drive power maximum ratio | Force rope maximum ratio | Coupling torque maximum ratio | RMS* drive power, kW | RMS* force rope, kN | RMS* coupling torque, kNm | Residual oscillations of the coupling and the load |
|-------------------------|--------------------------|----------------------------------|---------------------------|--------------------------|-------------------------------|----------------------|---------------------|---------------------------|--|
| Optimal                 | 4.00                     | 130.0                            | 1.43                      | <b>1.41</b>              | <b>1.46</b>                   | 427.0                | 57.0                | <b>116.0</b>              | <b>do not exist</b>                                |
| <b>The first case</b>   |                          |                                  |                           |                          |                               |                      |                     |                           |  |
| Constant                | <b>2.89</b>              | 130.0                            | 1.56                      | 1.81                     | 2.44                          | 459.9                | 61.7                | 133.9                     | exist  |
| Triangle-shaped         | <b>5.86</b>              |                                  | <b>1.15</b>               | <b>1.41</b>              | 2.41                          | 397.8                | <b>52.3</b>         | 122.0                     |  |
| Trapezium-shaped        | 4.05                     |                                  | 1.28                      | 1.42                     | 2.45                          | 426.1                | 56.7                | 130.8                     |  |
| U-shaped                | 4.19                     |                                  | 1.33                      | 1.44                     | 2.46                          | <b>419.4</b>         | 56.0                | 129.7                     |  |
| S-shaped                | 3.60                     |                                  | 1.35                      | 1.48                     | <b>2.48</b>                   | 436.9                | 58.1                | 133.7                     |  |
| <b>The second case</b>  |                          |                                  |                           |                          |                               |                      |                     |                           |  |
| Constant                | 4.00                     | <b>116.9</b>                     | 1.41                      | 1.57                     | <b>2.31</b>                   | 416.7                | <b>55.9</b>         | 124.3                     | exist  |
| Triangle-shaped         |                          | 151.3                            | <b>1.25</b>               | 1.65                     | 2.66                          | 421.8                | 56.2                | 129.9                     |  |
| Trapezium-shaped        |                          | 131.6                            | 1.29                      | <b>1.44</b>              | 2.47                          | 427.4                | 56.7                | 131.0                     |  |
| U-shaped                |                          | 126.8                            | 1.33                      | <b>1.44</b>              | 2.44                          | <b>413.9</b>         | 56.3                | 131.1                     |  |
| S-shaped                |                          | 131.5                            | 1.36                      | 1.46                     | 2.47                          | 422.1                | 56.4                | 130.4                     |  |

\*RMS is a root mean-square value

Thus, the optimal law shows advantages in terms of reducing the dynamic loads in elements of the mine winder. The energetic indicators show that the optimal law of the deceleration torque does not case the decreasing of the unwanted energetic losses. In the study, we have not used the energy component of the criterion (1.12).

Thus, the energetic indicators have not improved compared with taken in the calculations laws of the deceleration torque.

Summing everything up, we have stated: the main factors for the mine winder dynamics are the regime duration and the character of the increasing and decreasing of the deceleration torque [34].

### **1.3 Energy optimization of mine winder acceleration mode**

An important problem of the mine winder exploitation is to provide high energy efficiency [35]. This problem is becoming increasingly urgent because of the constant increase of the cost of electricity tariffs. The variable energy losses of the electric engines of the hoisting machines are one of the main factors, which can be minimized and provides improvement of the cycle efficiency of the machine [36]. Intensive and long-lasting exploitation of the mine winder with high cycle efficiency allows increasing the mining profitability.

One of the important aspects connected with the energy efficiency of the mine winder exploitation is the long-term work of its elements. Electrical losses in the mine winder drive cause the electrical motor winding heating and deterioration of the drive electrical insulation. It, in turn, reduces the durability of the machine's electric drive.

The requirement of the mechanical elements (coupling, wire rope) durability is connected with the level of the dynamical forces they bear. The minimization of this level is an important issue to investigate.

One of the ways to increase the energy efficiency of the mine winder is to optimize its parameters and operating modes. Investigations, which have been conducted in the work [37], are connected with the optimization of the mine winder drum weight (its strength remained on the same level). In the article [38] with the use of a finite-element method, an approach concerning the optimal configuration of machine's drive has been developed. The similar research, which is presented in the work [39], allows reducing the concentrations of the local stresses of the mine winder

drum. It provides the ability to reduce the weight of the drum and the probability of cracks in it. In the work, for optimization purposes, the special software OptiStruct has been used.

The problem of optimal reliability of a main-shaft device of a mine hoist was investigated in the work [40]. The authors identified the most significant factors that affect the reliability of the mechanism. In addition, the universal method, which allows obtaining an optimal construction of the main-shaft device of a mine hoist, has been developed.

In the article [34] the solution of the mine winder optimization problem has been found. The search domain was a conjunction of the mine winder motion modes and parameters' domains. The criterion of optimization was integral-terminal functional, which reflected undesired dynamic indicators of machine's exploitation. Such an approach allowed improving the dynamic and energetic indicators of the machine during its design and exploitation.

In the research paper [41], the problem of a few mine hoisting machines scheduling is formalized. The consumed energy is used as a criterion. Using the wide range of mathematical methods authors have obtained an approximate problem solution. However, the problem of optimization of each mine winder is unsolved.

Currently, the unsolved problem in the field of the high energy efficiency of the mine winder is the synthesis of such laws of its motion that would enable to minimize the energy consumption while providing the minimum dynamic loads in its elements. Results, which have been obtained in the previous studies, allow improving the construction of hoisting machines or their particular dynamics or energetic efficiency indicators.

Mine winders are characterized by oscillatory features [42, 43]. That is why energetic optimal control of the mine winder motion should be found with the imposed conditions of the elimination of its elements oscillations. Such a problem must be solved by using effective mathematical methods that ensure the requirements.

Thus, the complex increasing of energetic and dynamic indicators of the mine winder is an unsolved scientific and practical problems. The solution of the mentioned problem provides high reliability and energy efficiency of the mine winder.

In order to perform optimization of the mine winder motion, its characteristics should be taken into account. It is rational to consider the machine's movement at three stages: acceleration – steady motion – deceleration. In the statement of the optimal control problems of the machine's motion, characteristics of the transient mode (acceleration or deceleration) and direction of the final load movement are related to the boundary conditions of the machine elements.

This investigation explores the acceleration of the mine winder during the hoisting of the final load. However, the approach developed in the research may be used for optimization of other modes of machine's motion.

The goal of the investigation is to increase energetic features of the mine winder acceleration during the final load hoisting due to its optimization and analysis of the obtained results in terms of energetic and dynamic indicators.

In order to synthesize the optimal acceleration mode of the mine winder, we have used a dynamical model (fig. 1.1). The mathematical model, which is related to the machine's dynamical model, is presented in the form of a system of three differential equations (1.1). Note, that it is very common to use differential equations in the simulation of technical systems [44]. This statement may be applied to the hoisting machines as well [45].

All numerical parameters which are in the equation system (1.1) are reduced to rope drum. The point above the symbol means differentiation by time.

Note, that the mathematical model of the mine hoisting machine (1.1) reflects the oscillations of the drive elements and the final load. That is why the synthesis of energetic optimal laws of the hoisting machine with the differential equations (1.1) allows to eliminate the oscillations of these elements, decreases the level of the dynamical loads, and provides high reliability of its exploitation.

In order to carry out the optimization of the energetic characteristics of the mine winder, the criterion should be chosen. Within the framework of the current study we chose an integral criterion:

$$Int = \left( T^{-1} \int_0^T P_{dr}^2 dt \right)^{\frac{1}{2}} \rightarrow \min. \quad (1.20)$$

where  $T$  – duration of the machine acceleration to the steady velocity;  $P_{dr}$  – machine's drive power.

Criterion (1.20) reflects the root-mean-square value of the consumed power of the mine winder drive during its acceleration. Minimization of its criterion allows obtaining a mode of acceleration with a low level of energy losses. Criterion (1.20) is a non-linear integral functional. With the consideration of the system of differential equations (1.1) it may be presented as follows:

$$Int = \left( T^{-1} \int_0^T \left( A_0 + \sum_{i=1}^3 A_i x^{2i} \left( \sum_{j=0}^2 B_j x^{2j+1} \right) \right)^2 dt \right)^{\frac{1}{2}}, \quad (1.21)$$

where  $A_0 \dots A_3$  and  $B_0 \dots B_2$  – coefficients, which may be defined as follows:

$$\begin{cases} A_0 = FR; \\ A_1 = (J_1 + J_2)R^{-1} + mR; \\ A_2 = mRJ_1c_\phi^{-1} + J_1J_2(c_\phi R)^{-1} + m(J_1 + J_2)(c_x R)^{-1}; \\ A_3 = J_1J_2m(c_x c_\phi R)^{-1}; \\ B_0 = R^{-1}; \\ B_1 = (c_x J_2 + c_\phi m + c_x m R^2)(c_x c_\phi R)^{-1}; \\ B_2 = mJ_2(c_x c_\phi R)^{-1}. \end{cases} \quad (1.22)$$

For an optimal problem statement, the boundary conditions of the machine elements movement should be set. They are presented in the following form:

$$\begin{cases} \phi_1(0) = 0; \phi_2(0) = -FRc_\phi^{-1}; x(0) = \phi_2(0)R - Fc_x^{-1}; \\ \dot{\phi}_1(0) = \dot{\phi}_2(0) = \dot{x}(0) = 0; \\ \phi_1(T) = sR^{-1}; \phi_2(T) = \phi_2(0) + sR^{-1}; x(T) = x(0) + s; \\ \dot{\phi}_1(T) = \dot{\phi}_2(T) = vR^{-1}; \dot{x}(T) = v, \end{cases} \quad (1.23)$$

where  $s$  – distance, which the load passes during acceleration mode. Initial conditions (1.23) mean that the dynamical system begins to move from a quiescent state. Final conditions (1.23) relate to the steady-state movement of the machine (its steady velocity is  $v$ ), and oscillations of the elements are absent. The last factor provides reducing of the dynamical loads in the elements of the mine winder after its acceleration.

We have expressed the boundary conditions (1.23) in terms of function's  $x(t)$  higher-order derivatives:

$$\begin{cases} x(0) = FR^2 c_\phi^{-1} + Fc_x^{-1}; \dot{x}(0) = 0, r \in \overline{(1, 5)}; \\ x(T) = FR^2 c_\phi^{-1} + Fc_x^{-1} + s; \dot{x}(T) = v; \ddot{x}(T) = 0, y \in \overline{(2, 5)}. \end{cases} \quad (1.24)$$

Thus, the problem of optimal acceleration mode of the mine winder (1.21), (1.22), (1.24) is a variational one. In order to find its solution, a necessary condition of criterion (1.21) minimum has been stated. It is the Euler-Poisson [13] equation, which is a non-linear differential equation of twelfth order (it is very large and that is why we have not presented it here). It is impossible to find the analytical solution of this equation. The numerical solution of the boundary problem (1.21), (1.24) does not bring the desired result: the change of a parameter of the system causes the need for a new solution of the problem.

In order to find an approximate solution of the variational problem (1.21), (1.22), (1.24) we used a class of the continuously differentiable functions. In the class, we set basis function, which meets the boundary conditions (1.24) and includes an unknown parameter. Such function may be found as a solution of the following boundary problem:

$$\begin{cases} x_{b,1} = 0; \\ x_{b,1}(0) = FR^2 c_\phi^{-1} + Fc_x^{-1}; \dot{x}_{b,1}(0) = 0, r \in \overline{(1, 5)}; \\ x_{b,1}(T) = FR^2 c_\phi^{-1} + Fc_x^{-1} + s; \dot{x}_{b,1}(T) = v; \ddot{x}_{b,1}(T) = 0, y \in \overline{(2, 5)}, \end{cases} \quad (1.25)$$

where  $x_{a.1}$  – the first basis function, which is used as an approximate variational problem (1.21), (1.22), (1.24) solution. Let us set more boundary problems. Their solutions we will use for the same purpose – to find the approximation of the exact solution of the variational problem (1.21), (1.22), (1.24). They are:

$$\left\{ \begin{array}{l} \text{XIV} \\ x_{b.2} = 0; \\ \left\{ \begin{array}{l} x_{b.2}(0) = FR^2 c_\phi^{-1} + Fc_x^{-1}; x_{b.2}(0) = 0, r \in \overline{(1, 5)}; \\ \text{VI} \\ x_{b.2}(0) = q_1; \\ x_{b.2}(T) = FR^2 c_\phi^{-1} + Fc_x^{-1} + s; \dot{x}_{b.2}(T) = v; x_{b.2}(T) = 0, y \in \overline{(2, 5)}; \\ \text{VI} \\ x_{b.1}(T) = q_2, \end{array} \right. \end{array} \right. \quad (1.26)$$

$$\left\{ \begin{array}{l} \text{XV} \\ x_{b.3} = 0; \\ \left\{ \begin{array}{l} x_{b.3}(0) = FR^2 c_\phi^{-1} + Fc_x^{-1}; x_{b.3}(0) = 0, r \in \overline{(1, 5)}; \\ \text{u} \\ x_{b.3}(\frac{T}{2}) = 0, u \in \overline{(4, 6)}; \\ x_{b.3}(T) = FR^2 c_\phi^{-1} + Fc_x^{-1} + s; \dot{x}_{b.3}(T) = v; x_{b.3}(T) = 0, y \in \overline{(2, 5)}, \end{array} \right. \end{array} \right. \quad (1.27)$$

$$\left\{ \begin{array}{l} \text{XVII} \\ x_{b.4} = 0; \\ \left\{ \begin{array}{l} x_{b.4}(0) = FR^2 c_\phi^{-1} + Fc_x^{-1}; x_{b.4}(0) = 0, r \in \overline{(1, 5)}; \\ \text{u} \\ x_{b.4}(\frac{T}{2}) = 0, u \in \overline{(4, 8)}; \\ x_{b.4}(T) = FR^2 c_\phi^{-1} + Fc_x^{-1} + s; \dot{x}_{b.4}(T) = v; x_{b.4}(T) = 0, y \in \overline{(2, 5)}, \end{array} \right. \end{array} \right. \quad (1.28)$$

$$\left\{ \begin{array}{l} \text{XII} \\ x_{b.5} = 0; \\ \left\{ \begin{array}{l} x_{b.5}(0) = FR^2 c_\phi^{-1} + Fc_x^{-1}; x_{b.5}(0) = 0, r \in \overline{(1, 5)}; \\ \text{u} \\ x_{a.5}(\frac{T}{2}) = 0, u \in \overline{(4, 10)}; \\ x_{b.5}(T) = FR^2 c_\phi^{-1} + Fc_x^{-1} + s; \dot{x}_{b.5}(T) = v; x_{b.5}(T) = 0, y \in \overline{(2, 5)}, \end{array} \right. \end{array} \right. \quad (1.29)$$

where  $x_{b,2}$ ,  $x_{b,3}$ ,  $x_{b,4}$ ,  $x_{b,5}$  – the second, third, fourth, and fifth basis functions;  $q_1$  and  $q_2$  – unknown values of the function's  $x(t)$  sixth order derivative at  $t=0$  and  $t=T$ , which should be found.

Let us explain the selection of such specific boundary conditions in the boundary problems (1.26)-(1.29). The higher orders of the function  $x(t)$  derivatives in the moment of time  $T/2$  are equal to zero. For that, using the system of differential equations (1.1), we have written the angular acceleration of the first system's reduced element (the element with the moment of inertia  $J_1$ ):

$$\ddot{\phi}_1 = B_1 x + B_2 x. \quad (1.30)$$

The analysis of the boundary conditions, which are presented in the boundary problems (1.26)-(1.29), allows setting following expressions:

$$\begin{cases} \ddot{\phi}_{1,b,3}(\frac{T}{2}) = 0; \\ \ddot{\phi}_{1,b,4}(\frac{T}{2}) = \ddot{\phi}_{1,b,4}(\frac{T}{2}) = 0; \\ \ddot{\phi}_{1,b,5}(\frac{T}{2}) = \ddot{\phi}_{1,b,5}(\frac{T}{2}) = \phi_{1,b,5}^{IV}(\frac{T}{2}) = 0. \end{cases} \quad (1.31)$$

where  $\phi_{1,b,3}$ ,  $\phi_{1,b,4}$ ,  $\phi_{1,b,5}$  – the angular coordinate of the first reduced element of the dynamic system, which corresponds to the third, fourth, and fifth basis function respectively.

Kinematic characteristics (1.31) of the reduced element motion laws provide the desirable feature: at the moment of time  $T/2$  the torque of the inertial force, which influences the element  $J_1$ , equals zero. It cases the less severe energetic and dynamic conditions of the mine winder drive work. The third and the fourth derivatives of the function  $\phi_1$  (the second and the third expression in the system (1.31)) provides some „continuation” of this feature in time.

Solutions of the boundary problems (1.25)-(1.29) (basis functions) include free parameters that can be used to find the minimum of the criterion (1.21). In order to do that, we need to find the higher derivatives of the basis functions and substitute them

into the integrand of the criterion (1.21). By performing such mathematical transformations we obtain the following dependence:

$$Int = f(p), \quad (1.32)$$

where  $p$  – a vector of basis functions  $x_{b,1}, x_{b,2}, x_{b,3}, x_{b,4}, x_{b,5}$  free parameters. For the cases, which correspond to the boundary problems (1.25), (1.27)-(1.29), the vector reduces to a scalar  $p=s$ . For the basis function  $x_{a,2}$  the vector can be presented as following  $p=[s, q_1, q_2]^T$ .

Taking the derivative of criterion (1.21) by the components of the vector  $p$  and equating the obtained result to zero, we will find the necessary conditions for the criterion (1.21) minimum. For the basic functions, which are solutions of boundary problems (1.25), (1.27)-(1.29), such an equation has the form of a cubic equation:

$$\frac{\partial Int}{\partial s} = \sum_{w=0}^3 \alpha_w s^w = 0, \quad (1.33)$$

where  $\alpha_0, \dots, \alpha_3$  – coefficients of the equation defined in terms of coefficients  $A_0 \dots A_3$  and  $B_0 \dots B_2$ , parameters  $T, \nu$  and coefficients of the basis functions  $x_{b,1}, x_{b,3}, x_{b,4}, x_{b,5}$ . Analysis of the roots of the equation (1.33) shows, that for any (real) values of parameters  $T, \nu$  and coefficients  $A_0 \dots A_3$  and  $B_0 \dots B_2$  only one root is real. Two other are complex numbers. Taking into account physical concerns, we will choose the real root of the equation (1.33):

$$s = \frac{\nu T}{2}. \quad (1.34)$$

For the basis function, which is a solution of the boundary problem (1.26), the calculation of derivatives with respect to the vector  $p$  components leads to the system of nonlinear algebraic equations. It is impossible to find analytical solutions of the system. In order to find the numerical solution the modified particle swarm optimization method (ME-PSO) has been used [46]. It allowed finding the minimum

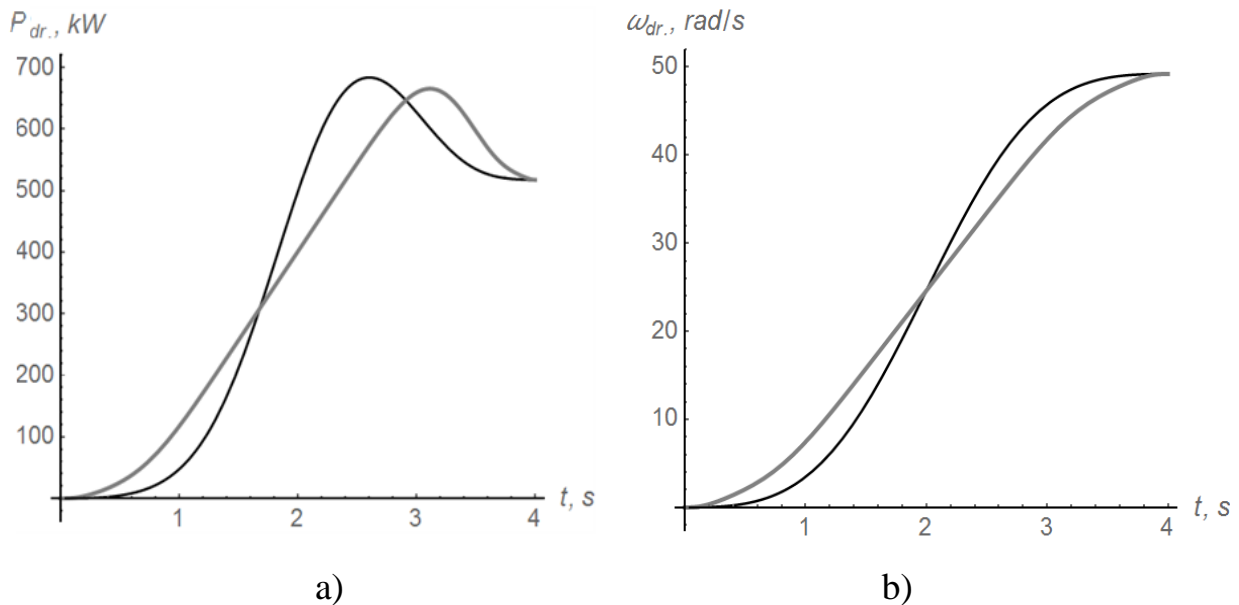
of the expression, (1.32), as the function of the arguments  $s$ ,  $q_1$ ,  $q_2$ . That method corresponds to the soft calculation techniques, which have been used for calculation of the mine winder modes [47].

All the calculations have been carried out for the values of the mine winder, which are used in the previous investigations. In the calculations, the following parameters have been used:  $T=4$  s;  $v=12$  m/s. The obtained optimal values of the mode's parameters are  $s=24$  m,  $q_1=q_2=711$  m/s<sup>6</sup>.

Substitution of the obtained results in the expressions of the basic functions  $x_{b.1}$ ,  $x_{b.2}$ ,  $x_{b.3}$ ,  $x_{b.4}$ ,  $x_{b.5}$  leads to the laws of the final load movement, which minimize the value of the criterion (1.21). We denote these as suboptimal laws. Using the system of equations (1.1) and suboptimal laws of load motion, the expressions of the kinematic, dynamic, and energetic characteristics have been found.

In order to illustrate the obtained characteristic of mine winder motion, the plots have been built. They are shown in fig. 1.6.

The black plots in fig. 1.6 correspond to the function  $x_{b.1}$ , gray plots – to the function  $x_{b.4}$ . In fig. 1.6 all the graphical dependencies are continuous. It provides the reduction of the dynamical loads in the elements of the mine winder.



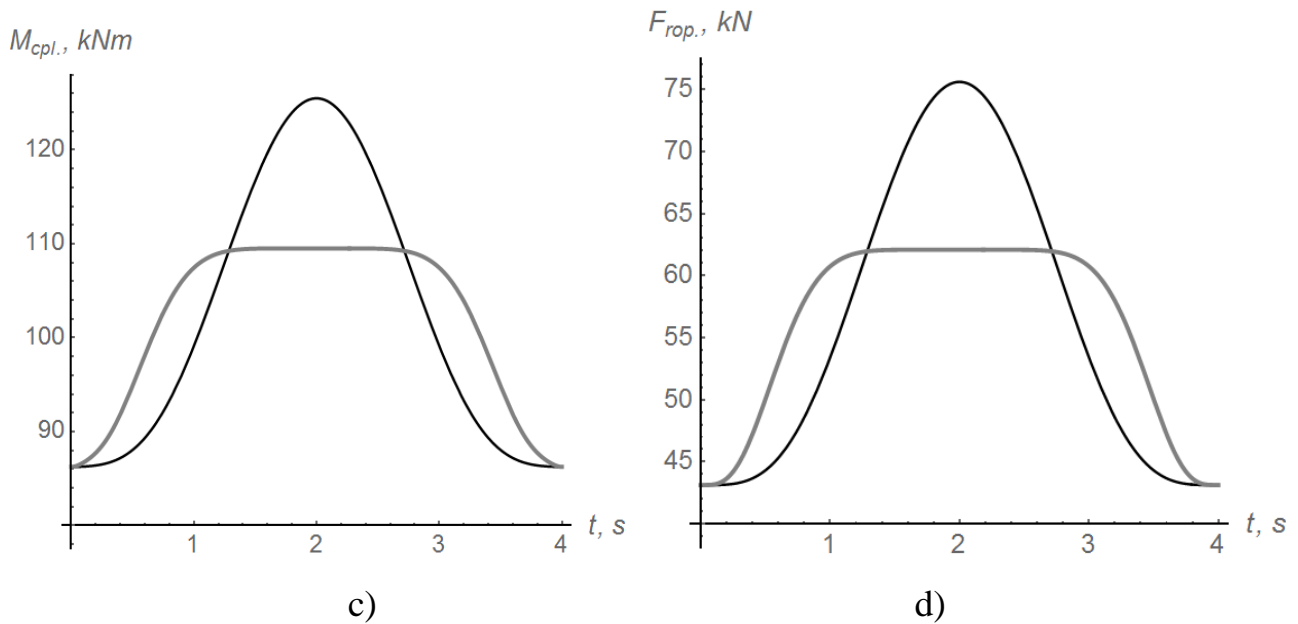


Fig. 1.6 Plots of mine winder motion characteristics during its acceleration: a) drive power; b) drive angular velocity; c) torque in the flexible coupling; d) force in the rope

Residual oscillations of the elements do not exist. It is a desirable feature as the dynamical loads during steady-state movement of the machine do not exist as well. Such characteristics increase the coupling and wire rope reliability.

Analysis of the graphical dependencies shown in fig. 1.6, reveals, that the important factor affecting the maximum loads in the mine winder elements are the features of the basis functions that have been used for finding suboptimal solutions of the variational problem. Selection of the specific features (in the frame of the current investigation such features were reached by adding the special boundary conditions in the boundary problems (1.27)-(1.29)) allows obtaining desirable characteristics of the mine winder movement. These characteristics are manifested in a significant reduction of the maximum values of the forces and torques in the machine's elements.

In order to estimate the obtained approximate solutions of the initial variational problem, we have used energetic and dynamic indicators. We have conducted the evaluation with root-mean-square values and the ratios of the maximal values. All these indicators reflect the undesirable features of the mine winder movement.

Calculated data are given in Table 1.2. The smallest values are highlighted in bold. Note, that the last column of Table 1.2 is related to the value of the optimization criterion (1.21).

Analysis of data in Table 1.2 shows that the worst energetic and dynamic features has suboptimal motion law, which corresponds to the basis function  $x_{b,1}$ . The law of motion founded with the help of basis functions  $x_{b,4}$  and  $x_{b,5}$  have the best features. In that sense, functions  $x_{b,4}$  and  $x_{b,5}$  are similar. Thus, a further complication of the basis function (i.e. adding extra boundary conditions in the middle of the acceleration interval) to obtain a more precise solution to the optimal problem is not expedient. Thus, in order to control the mine winder movement, we may recommend using the suboptimal law, which corresponds to the basis function  $x_{b,4}$ .

Table 1.2. The energetic and dynamic indicators which correspond to suboptimal control laws of the mine winder motion

| Basis function used in suboptimal motion law calculation | Dynamic response factor |             |             | Drive power maximum ratio | RMS*                  |                             |                    |                  |
|--|-------------------------|-------------|-------------|---------------------------|-----------------------|-----------------------------|--------------------|------------------|
|  | rope                    | coupling    | engine      |                           | force in the rope, kN | torque in the coupling, kNm | engine torque, kNm | engine power, kW |
| $x_{b,1}$  | 1.75                    | 1.46        | 1.93        | 1.37                      | 57.6                  | 103.4                       | 122.7              | 442.9            |
| $x_{b,2}$  | 1.53                    | 1.33        | 1.66        | 1.34                      | 57.1                  | 103.0                       | 121.3              | 434.6            |
| $x_{b,3}$  | 1.48                    | 1.29        | 1.60        | <b>1.33</b>               | 56.9                  | 102.9                       | 120.8              | 430.9            |
| $x_{b,4}$  | <b>1.42</b>             | <b>1.25</b> | <b>1.52</b> | <b>1.33</b>               | <b>56.7</b>           | <b>102.7</b>                | <b>120.3</b>       | <b>425.6</b>     |
| $x_{b,5}$  | <b>1.42</b>             | <b>1.25</b> | <b>1.52</b> | <b>1.33</b>               | <b>56.7</b>           | <b>102.7</b>                | <b>120.3</b>       | <b>425.6</b>     |

\* RMS – root-mean-square value

The analysis of the data in Table 1.2 shows that the drive power maximum ratio varies in a narrow range. The same applies to the root-mean-square values of wire rope force, coupling, and drive torques.

The root-mean-square value of the drive power for different suboptimal modes differs only on 4.0%

Dynamical response factors of the rope, the coupling, and the drive depend on features of the suboptimal laws of the hoisting machine. For example, the coefficient of the rope, which is related to the basis function  $x_{b,4}$ , on 23.2% less than the similar indicator for the basis function  $x_{b,1}$ . The dynamic response factors of the coupling for these laws vary on 16.8%, and for the drive on 27.0%. These data support the previously made conclusion regarding the rationality of using suboptimal law of the mine winder motion, which is based on the basis function  $x_{b,4}$  [48].

### **Conclusions to chapter 1**

1. For better performance of the mine winder, the drive motor rheostat control should be replaced by the frequency inverter that implements the optimal machine acceleration (deceleration) characteristics. Under similar conditions, the optimal control allows to reduce the dynamic loads of machine components up to 22.5-84.0%, as well as to minimize peak values of the drive motor power consumption [16].

2. The impact of acceleration duration  $T$  and coefficient  $\delta_1$  in the criterion (1.2) on the dynamic and energetic indicators of mine winder operation was found. Such a result allows reasonably to implement the obtained optimal acceleration mode of the mine winder and to configure the appropriate settings based on the requirements for improving the machine's operational efficiency [16].

3. In the study has been shown that the problem of increasing the dynamic performance of the mine winder is complex. Thus, its solution should be found in the complex domain. Such a domain within the framework of the study was the conjunction of regimes' and parameters' domains of the mine winder [34].

4. The implementation of the mine winder optimal control allows increasing the machine's dynamic performance. In turn, it makes the operation life of the machine is longer. The found in the study optimal value of the reduced coefficient of

the coupling stiffness may be useful during the mine winder design process. The complex approach to optimization of the mine winder deceleration has shown its efficiency [34].

5. The executed investigation develops an approach of increasing the energetic efficiency of the mine winder. It is applied to the acceleration mode of the mine winder. It can be generalized to other transient modes of the machine movement: deceleration during hoisting or lowering the final load, and acceleration during lowering of the final load. In the work, in order to find the approximate solution of the optimal control problem (based on energetic criterion), the continuous-differentiable class of functions has been used. They have a priori set of specific characteristics, which allowed eliminating the residual oscillations of the machine elements at the end of the acceleration and provide decreasing of undesirable maximal values of forces and torques in the elements of the mine winder. It, in turn, improves the energetic indicators of the machine exploitation. Calculation of the suboptimal laws of the mine winder motion (except one basis function) has been carried out in the analytical form [48].

### **References to chapter 1**

1. Stepanov A.G. Theoretical basis of the mine hoist dynamics. Mining Machinery and Electromechanics, 2013, Vol. 7, pp. 31-40.
2. Osipova T.N. To a question about the dynamics and optimization of mine hoists, Mechanical Engineering, 2014, Vol. 13, pp. 74-81.
3. Dagang W., Dekun Z., Zefeng Z., Shirong G. Effect of various kinematic parameters of mine hoist on fretting parameters of hoisting rope and a new fretting fatigue test. Engineering Failure Analysis. 2012, № 22, pp. 92-112.
4. Dagang W., Dekun Z., Shirong G. Effect of terminal mass on fretting and fatigue parameters of a hoisting rope during a lifting cycle in coal mine. Engineering Failure Analysis. 2014, № 36, pp. 407-422.

5. Jiannan Y., Xingming X. Effect of hoisting load on transverse vibrations of hoisting catenaries in floor type multirope friction mine hoists. 2016, № 36, pp. 1-15.
6. Pukach P.Ya., Kuzo I.V. Nonlinear transverse vibrations semibounded rope considering resistance. Scientific Bulletin of National Mining University, 2013, Vol. 3, pp. 82-86.
7. Ilin S.R., Trifanov G.D., Vorobel, S.V. Complex experimental studies of the dynamics of ore-lifting trunk. Mining Machinery and Electromechanics. 2011, Vol. 5, pp. 30-35.
8. Kyrychenko Y., Samusia V., Kyrychenko V. Software development for the automatic control system of deep-water hydrohoist. Geomechanical Processes during Underground Mining, 2012. pp. 81–86.
9. Popov Yu.P., Kudravytsev S.V., Stepanov S.V. Modernization of the braking system of mine hoisting plant. Mining informational and analytical bulletin (scientific and technical journal), 2015, Vol. 9, pp. 195-197.
10. Loveikin V.S., Romasevych Yu.O. Dynamika i optymizatsiia rezhymiv rukhu mostovykh kraniv, [Dynamics and optimization of movement modes of bridge cranes], 2016, Kyiv, Ukraine.
11. Loveikin V.S., Chovniuk Yu.V., Liashko A.P. The crane's vibrating systems controlled by mechatronic devices with magnetorheological fluid: the nonlinear mathematical model of behavior and optimization of work regimes. Naukovyi Visnyk Natsionalnoho Hirnychoho Universytetu, 2014, 6, pp. 97-102.
12. Eduardo S. de C., Variational methods for engineers with Matlab, 2015, London, UK; Hoboken, USA.
13. Bronshtein I.N., Semendyayev K.A. Handbook of mathematics [Reprint of the third edition]. Springer Science & Business Media, 2013.
14. Loveikin V.S., Romasevich Yu.O., Loveikin Yu.V. Analysis of the direct variational methods for solving optimal control problems, Proceedings of the National University "Lviv Polytechnic". Optimization of production processes and technical control in machine and instrument, 2012, Vol. 729, pp. 70-79.

15. FR-E700: frequency inverter instruction manual. Art. no.: 213994. Version D. Mitsubishi Electric Industrial Automation, 2011, p. 524.
16. Loveikin V.S., Romesevych Yu.O. Dynamic optimization of a mine winder acceleration mode. *Naukovyi Visnyk Natsionalnoho Hirnychoho Universytetu*, 2017, 4, pp. 81-87.
17. Wolny S. Emergency braking of a mine hoist in the context of the braking system selection. *Archives of Mining Sciences*, 2017, 62, 1, pp. 45-54. DOI: 10.1515/amsc-2017-0004
18. Dagang W., Dekun Z., Shirong G. Effect of terminal mass on fretting and fatigue parameters of a hoisting rope during a lifting cycle in coal mine. *Engineering Failure Analysis*, 2014, 36, pp. 407-422. DOI: 10.1016/j.engfailanal.2013.11.006
19. Chenming W., Jisheng W., Bo D., Iitao F., Shengli Z. The Influence to Mine Hoisting Steel Wire Rope Tension and Deformation from Velocity and Acceleration. *International Conference on Manufacturing Science and Information Engineering*, 2016, pp. 296-306. DOI: 10.12783/dtcse/icmsie2016/6345
20. Dagang W., Dekun Z., Xianbiao M., Yuxing P., Shirong G. Dynamic friction transmission and creep characteristics between hoisting rope and friction lining. *Engineering Failure Analysis*, 2015, 57, pp. 499-510. DOI: 10.1016/j.engfailanal.2015.08.010
21. Jun Z., Dagang W., Dekun Z., Shirong G., Dao'ai W. Dynamic torsional characteristics of mine hoisting rope and its internal spiral components. *Tribology International*, 2017, 109, pp. 182-191. DOI: 10.1016/j.triboint.2016.12.037
22. Chao J., Yanshu L., Bohua W., Shuangshuang Z., Xue L. Research on nonlinear dynamical behaviors of mine hoist transmission system under external excitation. *Advanced Materials Research*, 2013, 619, pp. 9-13. DOI: 10.4028/www.scientific.net/AMR.619.9
23. Yao J., Xiao X., Peng A., Jiang Y., Ma C. Assessment of safety for axial fluctuations of head sheaves in mine hoist based on coupled dynamic model.

Engineering Failure Analysis, 2015, 51, pp. 98-107. DOI: 10.1016/j.engfailanal.2015.02.011

24. Illin S.R., Samusia V.I., Ilina I.S., Ilina S.S. Influence of dynamic processes in mine hoists on safety of exploitation of shafts with broken geometry. *Naukovyi Visnyk Natsionalnoho Hirnychoho Universytetu*, 2016, 3, pp. 48-53.

25. Dai Y., Qiao S. The Design of Mine Hoist Speed Regulation System Based on Ziegler-Nichols PID Control. *Applied Mechanics and Materials*, 2014, 651-653, pp. 996-999.

26. Wu Y.X., Zhang C.J., Liu Y.Q. Design and Simulation of Fuzzy-PID Vector Control System Based on Mine Hoist. *Applied Mechanics and Materials*, 2013, 300-301, pp. 1486-1489. DOI: 10.4028/www.scientific.net/AMM.300-301.1486

27. Szymański Z. Intelligent, energy saving power supply and control system of hoisting mine machine with compact and hybrid drive system. *Archives of Mining Sciences*, 2015, 60, 1, pp. 239-251. DOI: 10.1515/amsc-2015-0016

28. Yang Z.S., Ma X.M. Synthesis of Mine Hoist Speed Curve Based on programmable logic controller. *Advanced Materials Research*, 2013, 846-847, pp. 90-93. DOI: 10.4028/www.scientific.net/AMR.846-847.90

29. Zewen W., Wei L., Baoyu C., Fan J. Design of the Remote Monitoring System for Mine Hoists. *24th Chinese Control and Decision Conference*, 2012, pp. 3540-3544. DOI: 10.1109/CCDC.2012.6244567.

30. Huaizhong C. Study on PROFIBUS-DP Field Bus in Mine Hoists Control System. *Advanced Materials Research*, 2012, 482-484, pp. 1781-1784. DOI: 10.4028/www.scientific.net/AMR.482-484.1781.

31. Gander M.J., Wanner G. From Euler, Ritz, and Galerkin to Modern Computing. *SIAM REVIEW*, 2012, 54, 4. (Published electronically. URL: <http://www.siam.org/journals/sirev/54-4/80403.html>. Last access 11.06.2018).

32. Storn R. Differential Evolution (DE) for Continuous Function Optimization (an algorithm by Kenneth Price and Rainer Storn)., 2014 (Published

electronically. URL: <http://www1.icsi.berkeley.edu/~storn/code.html>. Last access 11.06.2018).

33. Prasad H., Maity T., Babu V.R. Recent developments in mine hoists drives. *Journal of Mining Science*, 2015, 51, 6, pp. 1157–1164.

34. Loveikin V.S., Romesevych Yu. O. Regime-parametric optimization of a mine winder deceleration. *Naukovyi Visnyk Natsionalnoho Hirnychoho Universytetu*, 2018, 5, pp. 72-78. DOI: 10.29202/nvngu/2018-5/9

35. Medved M., Ristic I., Roser J., Vulic M. An Overview of Two Years of Continuous Energy Optimization at the Velenje Coal Mine. *Energies*, 2012, 5, pp. 2017-2029. DOI: 10.3390/en5062017

36. Boyko A., Volianskaya Ya. Synthesis of the system for minimizing losses in asynchronous motor with a function for current symmetrisation. *Eastern-European Journal of Enterprise Technologies*, 2017, 4, 5 (88), pp. 50-58. DOI: 10.15587/1729-4061.2017.108545

37. Mangalekar S., Bankar V., Chaphale P. A Review on Design and Optimization with Structural Behavior Analysis of Central Drum in Mine Hoist. *International Journal of Engineering Research and General Science*, 2016, 4, 2, pp. 91-96. <http://oaji.net/articles/2016/786-1461987786.pdf>

38. Zhen-liang Y., Wei-min L. CAE Optimization Design of Mine Hoist Spindle Device. *Advanced Materials Research*, 2011, 299-300, pp. 878-882. DOI: 10.4028/www.scientific.net/AMR.299-300.878

39. Hu J., Lla J.-Ch., He X., Cao J.-Ch. Large Mine Hoist Drum Topology Optimization Design. *International Conference on Energy Development and Environmental Protection (EDEP 2016)*, 2016, pp. 520-526. <http://dpi-proceedings.com/index.php/dteees/article/download/5945/5559>

40. Lu H., Peng Yx., Cao S., Zhu Zc. Parameter Sensitivity Analysis and Probabilistic Optimal Design for the Main-Shaft Device of a Mine Hoist. *Arabian Journal for Science and Engineering*, 2019, pp. 971-979. DOI: 10.1007/s13369-018-3331-y

41. Badenhorst W., Zhang J., Xia X. Optimal hoist scheduling of a deep level mine twin rock winder system for demand side management. *Electric Power Systems Research*, 2011, 81, 5, pp. 1088-1095. DOI: 10.1016/j.epsr.2010.12.011
42. Ilin S.R., Samusya V.I., Kolosov D.L., Ilina I.S., Ilina S.S. Risk-forming dynamic processes in units of mine hoists of vertical shafts. *Naukovyi Visnyk Natsionalnoho Hirnychoho Universytetu*, 2018, 5, pp. 64-71. DOI: 10.29202/nvngu/2018-5/10
43. Zabolotnyi K.S., Panchenko O.V., Zhupiiiev O.L., Polushyna M.V. Influence of parameters of a rubber-pore cable on the torsional stiffness of the body of the winding. *Naukovyi Visnyk Natsionalnoho Hirnychoho Universytetu*, 2018, 5, pp. 54-63. DOI: 10.29202/nvngu/2018-5/11
44. Pylypaka S., Klendiy M., Zaharova T. Movement of the Particle on the External Surface of the Cylinder, Which Makes the Translational Oscillations in Horizontal Planes. *Advances in Design, Simulation and Manufacturing*, 2019, pp. 336-345. DOI: 10.1007/978-3-319-93587-4\_35
45. Grigorov O., Druzhynin E., Anishchenko G., Strizhak M., Strizhak V. Analysis of Various Approaches to Modeling of Dynamics of Lifting-Transport Vehicles. *International Journal of Engineering & Technology*, 2018, 7(4.3), pp. 64-70. DOI: 10.14419/ijet.v7i4.3.19553
46. Romasevych Yu., Loveikin V. A Novel Multi-Epoch Particle Swarm Optimization Technique, *Cybernetics and Information Technologies*, 2018, 18(3), pp. 62-74. DOI: 10.2478/cait-2018-0039
47. Szymański Z. Intelligent, energy saving power supply and control system of hoisting mine machine with compact and hybrid drive system. *Archives of Mining Sciences*, 2015, 60, 1, pp. 239-251. DOI: 10.1515/amsc-2015-0016
48. Loveikin V.S., Romesevych Yu.O., Kurka V.P. Energy optimization of a hoisting engine acceleration. *Naukovyi Visnyk Natsionalnoho Hirnychoho Universytetu*, 2019, 5, pp. 107-112. DOI:10.29202/nvngu/2019-5/18

## **CHAPTER 2. AGROTRONICS AND OPTIMAL CONTROL OF TOWER CRANE MECHANISMS**

### **2.1 Dynamical analysis of the tower crane slewing mechanism (the case of the steady velocity of the crane trolley)**

Tower cranes are widely used in many areas of the modern industry. They are especially often used in the construction of civil engineering objects. The tower crane slewing mechanism is one of the main. Its effective exploitation is connected with the dynamical and energetic processes that occur during transient modes of mechanism motion. The considerable dynamic loads that take place in shafts, toothed gears, clutches, etc. harm the life duration of the mechanism. In addition, one of the important issues for research is the energy efficiency of the crane slewing drive mechanism. These and other factors cause the need to study the dynamic and energy processes in the crane slewing mechanism. Previous studies have found that they have the greatest impact during transient modes of motion.

Moreover, we specify a factor that harms the crane performance – the load oscillations on a flexible suspension. In the case of crane's slew, the load oscillations occur in the plane of trolley motion and perpendicular to it. In order to develop methods for their elimination, it is necessary to conduct the study and establish the basic laws of their origin and evolution.

In the scientific work by Vaynson A.A. [1] the calculation of dynamic loads during the operation of the crane slewing mechanism is performed on the basis of a dynamic model with reduced masses. The integration of the corresponding mathematical model under constant driving force and from zero initial conditions allowed to obtain an expression for determining the elastic torque in the crane slewing mechanism. Its analysis allowed the author to make recommendations for reducing dynamic loads in crane elements: it is necessary to increase the inertial

features of the drive and to reduce the excess torque (force) of the drive mechanism. The first method constructively lies in the insertion of the flywheel to the kinematic chains. This leads to an increasing of the duration of the start-up of the mechanisms, which affects the mechanism's energy indicators. Therefore, the rational way to ensure an acceptable level of dynamic loads at low energy consumption in the drive is to control its excessive torque.

In the research of Gaidamaka V.F. [2] the expression of determining the maximum dynamic loads is carried out in the same way: first of all, a dynamic model of the mechanisms has been built, equations of motion of the system reduced masses have been found, and then the equations have been integrated at zero initial conditions and the constant of the driving factor (torque or force). The difference in calculations with previous work lies in the torque which is created by the friction forces, the crane tilt, and wind. Aside from this, Gaydamaka V.F. did not take into account the effect of centrifugal force in the calculations.

In the work of Scheffler M., Dresig H. and Kurt F. [3] the emphasis is on establishing the magnitudes of the deviation of the load from the vertical in radial and tangential directions. This approach is approved due to the fact that in many calculation methods of the tower cranes elements it is necessary to know the values of the angles of deviation of the load from the vertical. The authors have compared the results of their researches with already known works.

In general, the approach of determining the dynamic loads at which the driving force is assumed as constant is quite simplistic. It does not reflect the features of the mechanical characteristics of the drive mechanisms, which in many cases are a significant factor in the study of the dynamics of the mechanisms of the crane's slew and the trolley movement.

Gohberg M.M. in work [4] indicated the combinations of load actions that should be used in the calculations of tower crane mechanisms: self-weight, load weight with the gripping unit, inertial loads, tilt forces, forces caused by wind loads, as well as mounting and transport loads. The author points out that in the case of the

low angular velocity of crane's slewing, it is permissible to use expressions related to the dynamics of two-mass systems described in the works [5, 6].

One of the important factors that determine the dynamic loads in tower crane elements is the load oscillations on a flexible suspension. Such oscillations are complex and occur in radial and tangential directions. In addition, they cause difficulty in load positioning. Their elimination is quite a difficult problem, which experienced crane operators cope with by constant monitoring of the crane movement. In order to establish the main factors that influence their appearance, it is necessary to synthesize mathematical models of the motion of the tower cranes mechanisms.

In [7, 8], a mathematical model of a crane's boom (jib) system with two freedom of freeness was developed. The authors examined the uniformly and uniniformly accelerated tilt of the guide link (crane's boom). Nonlinear models have also been used to study oscillations on a flexible suspension [9].

In [10], the dynamics of a tower crane under the condition of pendular load oscillations (they are modeled as linear) was investigated. The construction of the tower crane is described with the finite element method. Dynamic load analysis was performed using an author-developed approach based on the numerical method. It was established that the crane metal structure is the most responsive to the influences which have the frequencies of the first several harmonics of metal structure oscillations and load oscillations as well. In addition, dynamic loads tend to increase as the angle of pendulum (load) deviation increases.

In [11], a crane rotation simulation was performed based on the Euler-Lagrange equations. The analysis of the obtained results made it possible to trace the nature of the pendulum oscillations of the load on a flexible suspension and to compare them with the results of experimental studies in order to minimize the load oscillations, authors have come up with a method for controlling the driving torque of the crane slewing mechanism.

In the scientific work [12] the influence of pendulum load oscillations on mechanical stresses of crane metal structure for different modes of its motion was

investigated. On the basis of the analysis, the author made a recommendation for the positioning of the trolley on the boom in the conditions of wind rushes for reducing the risk of the emergency crane collapse.

The purpose of the current work is to establish the level of dynamic and energy loads of the tower crane slewing mechanism, as well as to study the load oscillations on a flexible suspension. In order to achieve this goal it is necessary to solve the following problems: 1) to develop a dynamic model of the tower crane slewing mechanism; 2) to synthesize a mathematical model, which is suitable for research, by using second-order Lagrange equations; 3) to analyze the dynamic and energy loads of the tower crane slewing mechanism; 4) to investigate the appearance and evolution of the load oscillations on a flexible suspension and to determine the main factors that affect them. The tower crane during the process of the start of the slewing mechanism in the steady-state mode of trolley movement is presented as a holonomic mechanical system (fig. 2.1), which consists of absolutely rigid bodies, except for load flexible suspension, which oscillates in the vertical plane during crane slewing. In the selected dynamic model of the crane, we have generalized coordinates. They are: angular coordinates of the crane  $\varphi$  and the load  $\psi$  slewing, as well as the linear coordinate of the load movement  $x$ .

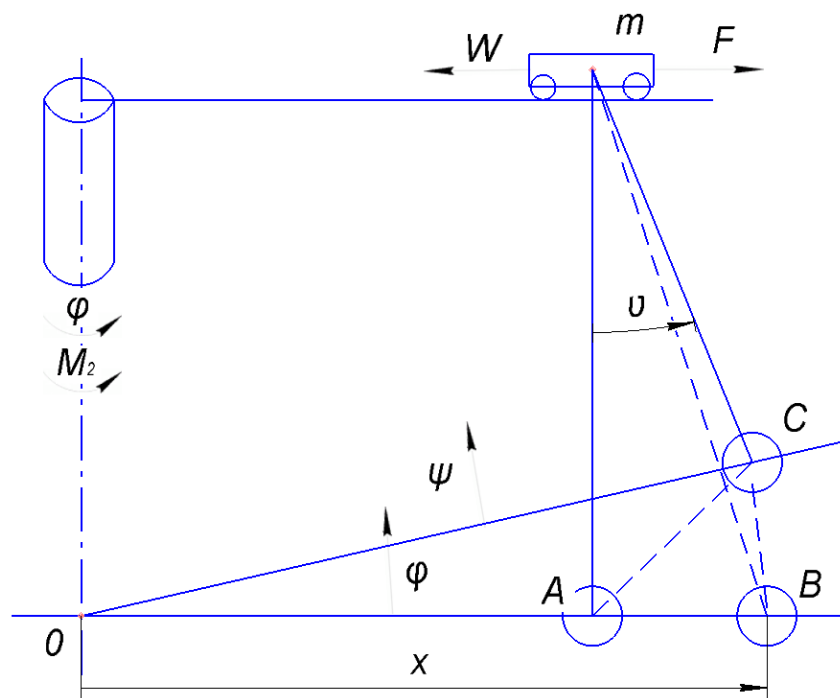


Fig. 2.1 A dynamic model of the tower crane slewing mechanism

For such a dynamic model, we have defined the deviation of the rope from the vertical. In this case, we assume that the deviation of the rope from the vertical is negligible and does not exceed  $12^\circ$ . Therefore, the arc load movement during its oscillations is replaced by straight lines. As a result, we have the next expressions:

$$AB = x - vt; \quad (2.1)$$

$$BC = x(\varphi - \psi); \quad (2.2)$$

$$AC = \sqrt{AB^2 + BC^2 - 2AB \cdot BC \cdot \cos \angle ABC}, \quad (2.3)$$

where  $t$  is time;  $v$  is the steady linear speed of the trolley movement. For expression (2.3) we found  $\angle ABC$ :

$$\angle ABC = \frac{\pi - (\psi - \varphi)}{2} = \frac{\pi}{2} - \frac{\psi - \varphi}{2}; \quad (2.4)$$

As a result of substituting dependencies (2.1), (2.2) and (2.4) into expression (2.3) we obtained:

$$\begin{aligned} AC &= \sqrt{(x - vt)^2 + x^2(\psi - \varphi)^2 - 2x(x - vt)(\psi - \varphi) \cos\left(\frac{\pi}{2} - \frac{\psi - \varphi}{2}\right)} = \\ &= \sqrt{(x - vt)^2 + x^2(\psi - \varphi)^2 - 2x(x - vt)(\psi - \varphi) \sin\left(\frac{\psi - \varphi}{2}\right)}. \end{aligned}$$

Then the angular coordinate of the deviation of the rope from the vertical is determined by the dependence:

$$\nu = \frac{AC}{L} = \frac{\sqrt{(x - vt)^2 + x^2(\psi - \varphi)^2 - 2x(x - vt)(\psi - \varphi) \sin\left(\frac{\psi - \varphi}{2}\right)}}{L}. \quad (2.5)$$

For the model represented by the dynamic model shown in fig. 2.1, we should use the Lagrange equations to find the corresponding mathematical model:

$$\begin{cases} \frac{d}{dt} \frac{\partial T}{\partial \dot{\varphi}} - \frac{\partial T}{\partial \varphi} = Q_{\varphi} - \frac{\partial \Pi}{\partial \varphi}; \\ \frac{d}{dt} \frac{\partial T}{\partial \dot{\psi}} - \frac{\partial T}{\partial \psi} = -\frac{\partial \Pi}{\partial \psi}; \\ \frac{d}{dt} \frac{\partial T}{\partial \dot{x}} - \frac{\partial T}{\partial x} = -\frac{\partial \Pi}{\partial x}, \end{cases} \quad (2.6)$$

where  $T, \Pi$  – is the kinetic and potential energy of the boom system, respectively;  $Q_{\varphi}$  is a non-potential component of the generalized force that corresponds to the generalized coordinate  $\varphi$  of the crane's slew.

The potential energy of the boom system is as follows:

$$\Pi = m_1 g L + m g L (1 - \cos \nu), \quad (2.7)$$

where  $m_1, m$  – reduced masses of the trolley and the load respectively;  $g$  – acceleration of free fall. Taking partial derivatives of expression (2.7) with respect to the dependence (2.5) of the generalized coordinates  $\varphi, \psi$ , and  $x$ , we have:

$$\frac{\partial \Pi}{\partial \varphi} = -\frac{mg}{L} xvt(x - \varphi); \quad (2.8)$$

$$\frac{\partial \Pi}{\partial \psi} = \frac{mg}{L} xvt(x - \varphi); \quad (2.9)$$

$$\frac{\partial \Pi}{\partial x} = \frac{mg}{L} (x - vt(1 - \frac{(x - \varphi)^2}{2})). \quad (2.10)$$

The kinetic energy of the system is expressed by the next dependency:

$$T = 2 \frac{I_1}{D^2} v^2 + \frac{1}{2} m_1 v^2 (1 + \dot{\varphi}^2 t^2) + \frac{1}{2} I_2 \dot{\varphi}^2 + \frac{1}{2} m (\dot{x}^2 + x^2 \dot{\psi}^2). \quad (2.11)$$

Calculating the necessary derivatives of the expression (2.11), we obtain:

$$\frac{\partial T}{\partial \varphi} = 0; \quad \frac{\partial T}{\partial \psi} = 0; \quad \frac{\partial T}{\partial x} = mx\dot{\psi}^2; \quad (2.12)$$

$$\frac{\partial T}{\partial \dot{\varphi}} = m_1 v^2 \dot{\varphi}^2 t + I_2 \dot{\varphi} = (m_1 v^2 \dot{\varphi} t + I_2) \dot{\varphi}; \quad (2.13)$$

$$\frac{\partial T}{\partial \dot{\psi}} = mx^2 \dot{\psi}; \quad (2.14)$$

$$\frac{\partial T}{\partial \dot{x}} = m\dot{x}; \quad (2.15)$$

$$\frac{d}{dt} \frac{\partial T}{\partial \dot{\varphi}} = (m_1 v^2 t + I_2) \ddot{\varphi} + 2m_1 v^2 t \dot{\varphi}; \quad (2.16)$$

$$\frac{d}{dt} \frac{\partial T}{\partial \dot{\psi}} = mx^2 \ddot{\psi} + 2mx\dot{x}\dot{\psi}; \quad (2.17)$$

$$\frac{d}{dt} \frac{\partial T}{\partial \dot{x}} = m\ddot{x}. \quad (2.18)$$

The nonpotential component of the generalized force, which corresponds to the generalized coordinate  $\varphi$  is determined by the following dependency:

$$Q_\varphi = \frac{2M_{kp}u\eta(1+as_{kp})}{1 - \frac{\dot{\varphi}u}{\omega_0}} - M_0, \quad (2.19)$$

$$\frac{s_{kp}}{1 - \frac{\dot{\varphi}u}{\omega_0}} + \frac{\omega_0}{s_{kp}} + 2as_{kp}$$

where  $M_{kp}$  – maximum (critical) torque on the electromotor's shaft of the crane slewing mechanism;  $u$  and  $\eta$  are respectively the gear ratio and the efficiency coefficient of the crane slewing mechanism;  $\omega_0$  – synchronous angular velocity of the rotor of the electromotor of the crane slewing mechanism;  $s_{kp}$  – critical slippage of the engine of the slewing mechanism, which is determined by the following dependency:

$$s_{kp} = (1 - \frac{\omega_{НОМ}}{\omega_0})(\lambda + \sqrt{\lambda^2 - 1}), \quad (2.20)$$

where  $a = R_1 / R_2'$  – dimensionless parameter, which is the ratio of the resistance of the stator  $R_1$  to the resistance of the rotor  $R_2'$  (all the values are reduced to the stator windings);  $\omega_{ном}$  – the nominal angular velocity of the motor;  $\lambda$  is a torque capacity ( $\lambda = M_{кр} / M_{ном}$ );  $M_{ном}$  – the nominal moment on the motor shaft.

After substitution of expressions (2.8)-(2.19) to a system (2.6) we obtain a system of differential equations of the start-up of the crane slewing mechanism at the steady-state mode of the load trolley motion:

$$\left\{ \begin{array}{l} (I_2 + m_1 v^2 t^2) \ddot{\varphi} + 2m_1 v^2 t \dot{\varphi} = \frac{2M_{кр} u \eta (1 + a s_{кр})}{s_{кр} (1 - \frac{\dot{\varphi} u}{\omega_0})^{-1} + (1 - \frac{\dot{\varphi} u}{\omega_0}) s_{кр}^{-1} + 2a s_{кр}} - \\ - M_0 + \frac{mg}{L} xvt(\psi - \varphi); \\ mx^2 \ddot{\psi} + 2mx \dot{x} \dot{\psi} = -\frac{mg}{L} xvt(\psi - \varphi); \\ m\ddot{x} + mx \dot{\psi}^2 = -\frac{mg}{L} (x - vt(1 - \frac{(\psi - \varphi)}{2})). \end{array} \right. \quad (2.21)$$

The mathematical model will be used in further calculations for carrying out dynamic analysis of the slewing mechanism during trolley steady motion. We will focus on the start of the system.

All calculations were made for the parameters of the crane Liebherr 140 hc [13], which are shown in Table 2.1.

Table 2.1. Parameters of the tower crane Liebherr 140 hc

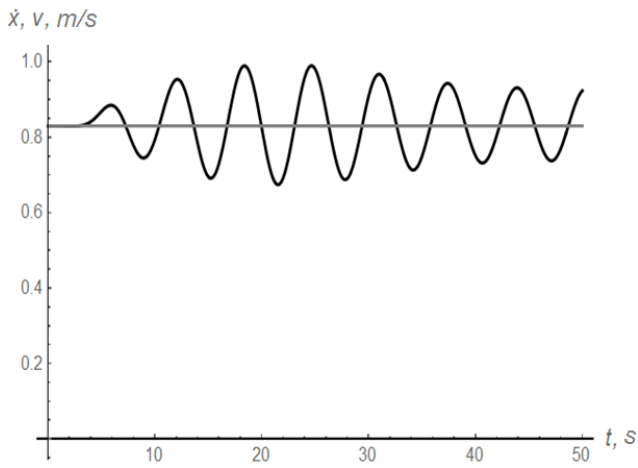
| Parameter  | Unit of measurement | Value               |
|--|---------------------|---------------------|
| 1  | 2                   | 3                   |
| Trolley reduced mass, $m_1$  | kg                  | 300                 |
| Load reduced mass, $m$   | kg                  | 5000                |
| The moment of inertia of the turnable part of the crane reduced to its slewing axis, $I_0$ | kg·m <sup>2</sup>   | 5.5·10 <sup>6</sup> |

Table 2.1 continuation

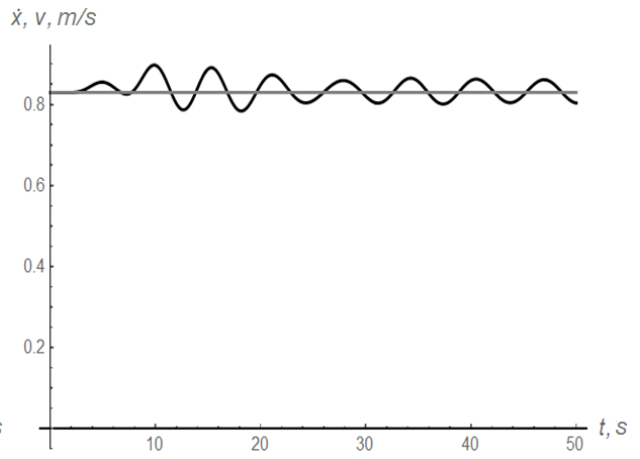
| 1   | 2                 | 3     |
|---|-------------------|-------|
| The moment of inertia of the rotor of the electromotor of the trolley movement mechanism, $I_1$ | kg·m <sup>2</sup> | 0.3   |
| The moment of inertia of the rotor of the electromotor of the crane slew mechanism, $I_2$       | kg·m <sup>2</sup> | 0.056 |
| The force of static resistance of the trolley movement, $W$                                     | N                 | 5500  |
| The torque of static resistance of the crane slew, $M_0$  | Nm                | 50100 |
| The maximum torque on the electromotor shaft of the crane slew mechanism, $M_{kp}$              | Nm                | 120   |
| The dimensionless parameter of the electromotor of the crane slew mechanism, $a_1$              | -                 | 0.2   |
| The dimensionless parameter of the electromotor of the crane slew mechanism, $a_2$              | -                 | 0.2   |
| Critical slippage of the engine of the crane slewing mechanism, $s_{kp2}$                       | -                 | 0.37  |
| The gear ratio of the crane slew mechanism, $U_2$   | -                 | 1429  |
| The synchronous angular velocity of the engine of the crane slew mechanism, $\omega_0$          | rad               | 104.7 |
| The drum diameter of the trolley movement mechanism, $D$  | m                 | 0.3   |
| The length of the load's flexible suspension, $L$   | m                 | 10    |
| Efficiency coefficient of the drive mechanism of the crane slew, $\eta_2$                       | -                 | 0.80  |

In order to analyze the tower crane slewing mode with the constant velocity of the trolley, we have built some graphical dependencies (fig. 2.2).

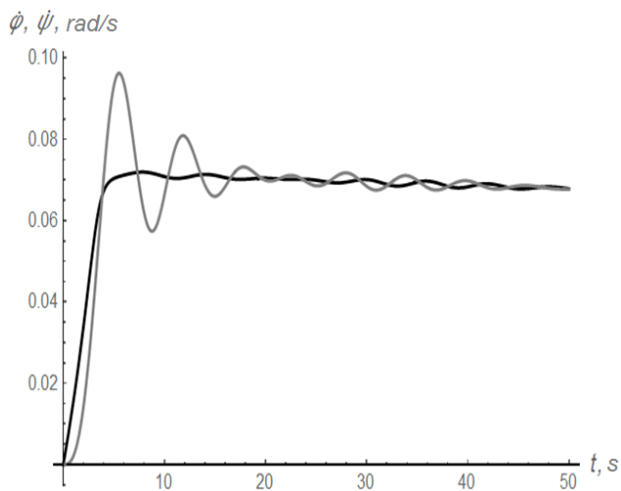
## CHAPTER 2



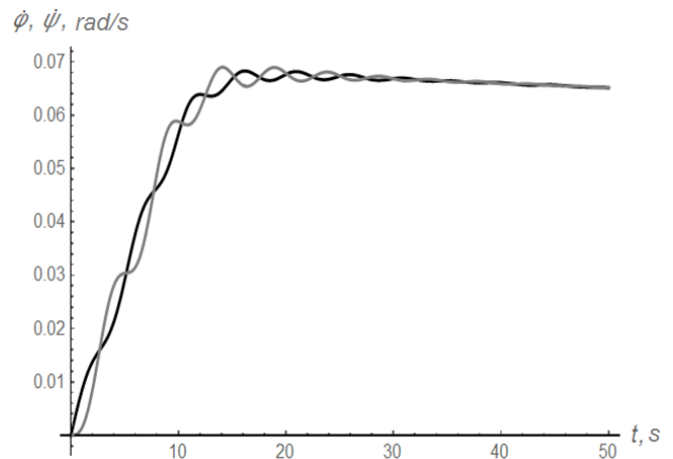
a)



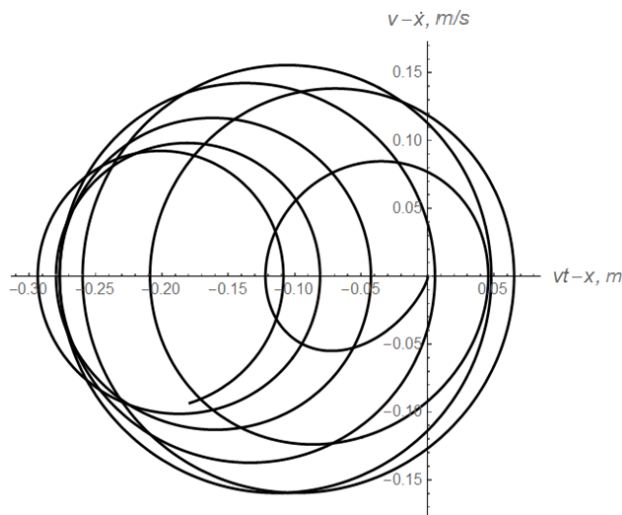
b)



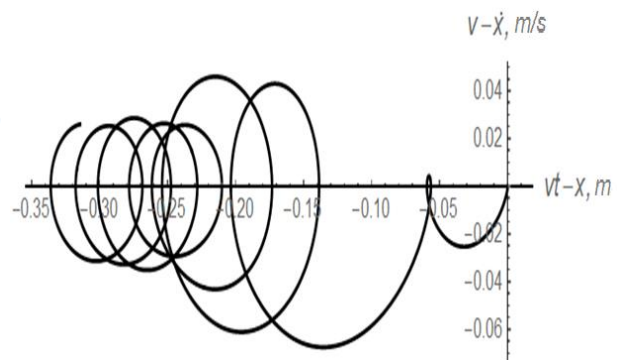
c)



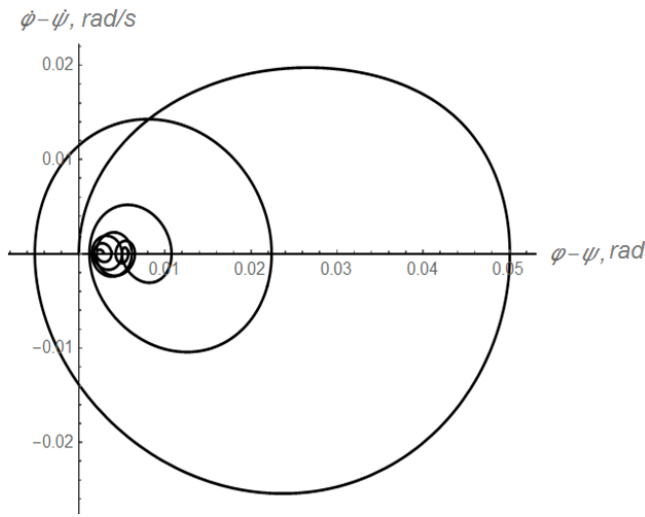
d)



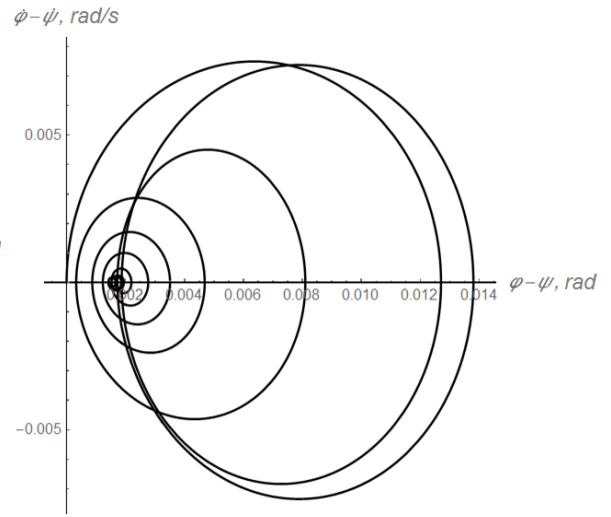
e)



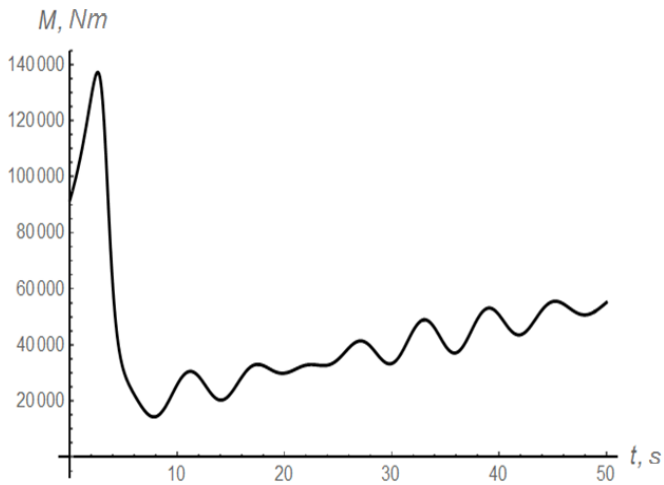
f)



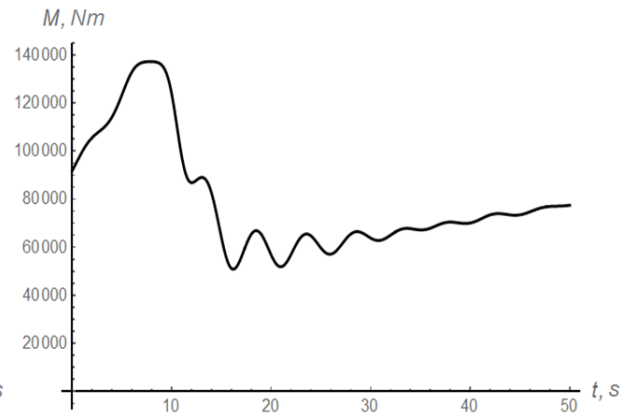
g)



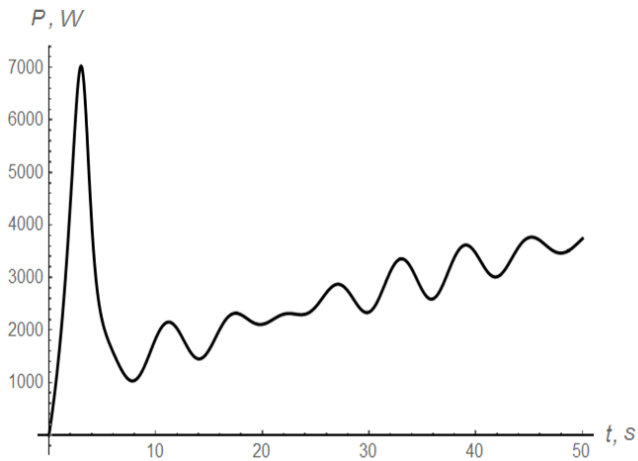
h)



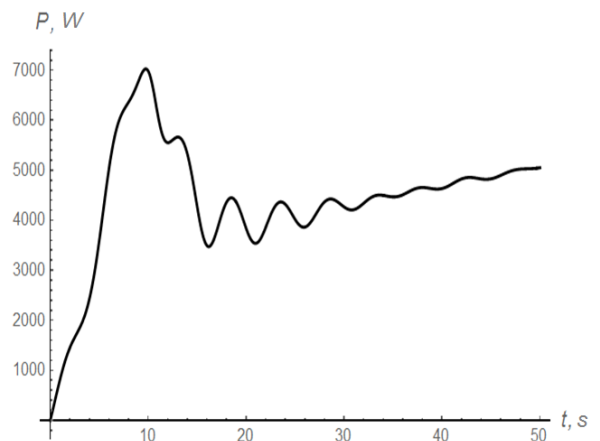
i)



j)



k)



l)

Fig. 2.2. Plots of the characteristics refer to the system direct start.

We have shown graphical dependencies on fig. 2.2 (a) velocity of the trolley (grey line) and the load (black line) in the radial direction at  $x_0=3$  m; b) the same at  $x_0=30$  m; c) angular velocity of the tower (black line) and the load (grey line) in the tangential direction  $x_0=3$  m; d) the same at  $x_0=30$  m; e) the phase portrait of radial load oscillations at  $x_0=3$  m; f) the same at  $x_0=30$  m; g) the phase portrait of the load oscillations in the tangential direction at  $x_0=3$  m; h) the same at  $x_0=30$  m; i) the torque of the drive mechanism of the tower at  $x_0=3$  m; j) the same at  $x_0=30$  m; k) the drive power of the crane slewing mechanism at  $x_0=3$  m; l) the same at  $x_0=30$  m) as follows: in the left column, the graphs correspond to the case  $x_0=3$  m, and in the right one – to the case  $x_0=30$  m.

In order to establish the quantitative characteristics of the movement of the system, the numerical data were calculated. They were set in Table 2.2.

Table 2.2 Kinematic, dynamical and energetic characteristics of the system direct start

| Parameter  | Unit of measurement | $x_0$ value |        |
|--|---------------------|-------------|--------|
|  |                     | 3 m         | 30 m   |
| 1  | 2                   | 3           | 4      |
| Maximum torque value of the drive of the crane slew mechanism              | Nm                  | 137253      |        |
| The maximum value of the drive power of the crane slew mechanism           | W                   | 6993        |        |
| The maximum amplitude of the load deviation in the radial direction        | m                   | 0.294       | 0.336  |
| Maximum amplitude of load deviation in the tangential direction            | rad                 | 0,0501      | 0,0138 |
| The root-mean-square value of the drive torque of the crane slew mechanism | Nm                  | 112213      | 111001 |
| The root-mean-square value of the power of the slew mechanism              | W                   | 4456        | 4837   |

Table 2.2 continuation

| 1  | 2   | 3       | 4       |
|--|-----|---------|---------|
| The root-mean-square deviation value of the load in the radial direction     | m   | 0.00093 | 0.10744 |
| The root-mean-square deviation value of the load in the tangential direction | rad | 0.0306  | 0.0076  |

Analysis of the graphical dependencies, which are presented on fig. 2.2, and the numerical data listed in Table 2.2, shows that the maximum torque and power values for the cases  $x_0=3$  m and  $x_0=30$  m are the same. This derives from the torque capacity of the crane slewing mechanism. In addition, practically equal root-mean-square values of these characteristics can be observed.

For the case  $x_0=30$  m, as we can see from fig. 2.2 (j) and fig. 2.2 (l), the torque and power of the slewing mechanism after the end of start are increasing. This is due to the fact that with increasing the distance from the trolley to the rotational axis, firstly, the moment of the system's inertia increases, and secondly the angular speed of the crane's slewing decreases. To compensate the speed reduction, it is necessary to provide the system with angular acceleration. The product of this acceleration at the increasing moment of inertia caused by the increasing value  $x_0$  influences the engine driving torque. Moreover, the torque increase causes a slight decrease in the angular speed of the crane's slewing (fig. 2.2 (c) and (d)).

In spite of this, a larger value of  $x_0$  causes an increase in the amplitude of the pendulum oscillations of the load in the radial direction. Here, the reason for such an increasing is the centrifugal force, is proportional to the  $x_0$  value. Indeed, as one may obtain from fig. 2.2 (f), the load in the course of time deviates more radially from the vertical due to the centrifugal force.

On the other hand, the amplitude of the load oscillations in the tangential direction is smaller. It is caused by the fact that in the case of  $x_0=30$  m, the slewing mechanism duration of the start is much longer (again, this is caused by an increased

moment of the system inertia at a larger value of  $x_0$ ). Similar tendencies are observed when analyzing the root-mean-square values of the load oscillations in both planes.

## **2.2 Optimization of the tower crane slewing (the case of the steady velocity of the crane trolley)**

Tower cranes are widespread used in many sectors of modern industry. They are especially often used in the area of civil engineering. The efficiency of their operation depends on the load oscillations at the flexible suspension. There are many ways of elimination of the load oscillations. Among them is a class of methods based on optimal control. They make it possible to use the available reserves as efficiently as possible.

Most of the works referred to optimal motion control of tower crane mechanisms used duration of movement on [13-19] and linear-quadratic criteria [16, 20, 21, 26]. All of these works are characterized by the requirement of elimination the load oscillations on a flexible suspension.

In work [13], the tower crane model is presented as a system of four nonlinear differential equations describing the tower's slew, the movement of the trolley on the boom, and the oscillation of the load on a flexible suspension in two planes (along the trolley's motion and perpendicular to its direction). In the statement of the problem, the constraints on speed and acceleration of the trolley, as well as the speed and acceleration of the tower were used. To find the quasi-optimal control (by the duration criterion), the authors have developed an algorithm that determines the parameters of the predefined (basis) piecewise motion functions of the individual system's masses. The results of theoretical studies were tested by means of execution of laboratory experiments. However, they did not allow to establish the practical applicability of the obtained results.

In the research [14], where a nonlinear model of the joint action of several crane mechanisms (crane slew, trolley movement, and hoisting) was used, constraints were imposed on the tower, trolley, and load accelerations. A gradient method was

used to find the criterion minimum. This research paper also does not contain the validation of experimental research in production conditions, although the theoretical and laboratory data have a quite close agreement.

In scientific investigation [15], authors, based on specialized software, have obtained the optimal parameters of tower crane modes movements (tower slewing, load hoisting, and trolley movement). The obtained results can be applied only in cases of small displacements since the problem is solved in the absence of a steady-state mode of mechanisms motion.

In the article [16], authors developed approaches for elimination the load oscillations of slewing (including tower) cranes, by using the linear-quadratic optimization criterion. The solution of the problem is illustrated by graphical dependencies. In addition, the issues of control implementation have been developed in this work, in particular, the structure of the controlled drive mechanism has been specified.

Article [17] is devoted to the development of the duration optimal control of the crane slewing mechanism based on the applying of the Pontryagin maximum principle. By using nonlinear equations of the system's motion, authors have found a solution of the problem. The control function has been found as the acceleration of the trolley. It complicates the practical implementation of the work results.

In the work [18], the same method was applied to optimize the duration of a tower crane slew. The linear motion model of the system is used in this scientific work.

In [19], based on the Lagrange equations, a mathematical model of a tower crane has been obtained. It is presented in a matrix form and describes the tower slew, the trolley movement, the load hoisting and its oscillations in two planes. Authors reduced the problem of linear-quadratic functional minimization to the system of Riccati equations. However, authors of the work did not explain the physics of the used criterion. The results obtained during the calculations were analyzed by using graphical dependencies.

In the dissertation of A.L. Galafshani [20] developed a mathematical model of a tower crane and solved the optimization problem of eliminating the load oscillations on a flexible suspension. He considered a condition that the integral functional, which reflects the quadratic values of the phase coordinates of the system motion, should be minimized. There were imposed constraints on the position of the individual masses of the system and their velocities. The analysis of the obtained results showed that some of them cannot be implemented on practice.

Hanafy M. Omar and other researchers in [21, 22] have developed approaches to the synthesis of motion controllers for tower crane mechanisms that would allow eliminating the load oscillations on a flexible suspension. The numerical calculations given in the papers refer only to the parameters of laboratory cranes' models and do not reflect the effect of possible external impacts (for example, wind rushes). It is advisable to use these results at the initial stage of the synthesis of optimal controllers as a first approximation.

In the research [23], an approximate solution of the optimal control problem of the slewing mechanism of a tower crane has been found. The model, which is used in the calculations, is nonlinear with variable parameters (flexible suspension length). It has complicated solving of the problem and did not allow finding its exact solution. The approaches' analysis, which was carried out in the paperwork led the authors to the conclusion that the impossibility of reducing the mathematical model of the system to the normal form did not allow the application of Pontryagin's maximum principle.

Non-classical controllers (based on fuzzy logic) of control of the tower crane slewing and trolley movement have been developed in the paperwork [24]. The simulation of the results has shown that the obtained adaptive fuzzy controllers allow eliminating the load oscillations. They are quite robust. The influence of the structure of the controller, in particular, the number of expert rules, on the control quality was also investigated. The obtained results do not allow performing the optimal movement of the mechanisms. They are rather universal theoretical developments.

In [25], different approaches to elimination of the load oscillations in the joint operation of the crane slewing and trolley movement have been analyzed. It is found that the implementation of optimal control requires more sensors than other methods: PID control, input shaping, and notch filtering. On the other hand, optimal control is less sensitive to the incorrect determination of the system parameters, such as the length of the flexible suspension of the load.

In [26], an approach was applied to determine the discrete values of the tower crane slewing mechanism control. For this purpose, a modified method of particle swarm was applied [27]. As a result, the authors developed a control that minimized the complex dynamic criterion, which reflected the root-mean-square value of the driving torque and its rate (the time derivative).

The issues of implementation of optimal tower cranes' mechanisms control, as well as the analysis of modern tendencies in this field, are given in the article [28]. Based on a wide analysis of the work, authors have identified two classes of control systems: a program control (a function of time) and closed-loop control (a function of phase coordinates). They pointed out the advantages and disadvantages of using each of the classes.

Apart from studies on optimization of the slewing control of the tower crane mechanism, there are those that reflect developments in optimization of the parameters of their mechanisms. In particular, in [29, 30], the optimal range of values of the dissipation coefficient of the elastic-damper device was determined on the basis of the numerical analysis of the trolley movement. Moreover, in [30] the system of equations that describe processes of the trolley movement mechanism by using the dynamic mechanical characteristic of the drive is obtained.

Thus, in most of the works refer to the area of optimal slewing control of tower crane mechanism used nonlinear mathematical models. Besides that, theoretical calculations and experimental studies have been performed only for the parameters of laboratory models of tower cranes. It complicates their implementation in the real conditions of operation.

The purpose of the presented work is to determine the optimal laws of motion of the slewing mechanism of the tower crane during its acceleration.

To achieve this goal it is necessary to solve the following problems: 1) to develop a mathematical model of slewing mode of the system „tower crane - load on a flexible suspension” at a constant speed of the trolley movement; 2) to state the problem of optimal control of the system movement; 3) to find a solution to the problem with ME-PSO method; 4) to analyze the obtained results. In order to optimize the movement of the tower crane slewing mechanism at the constant velocity of the trolley, we have used the dynamic model, which is shown in fig. 2.3.

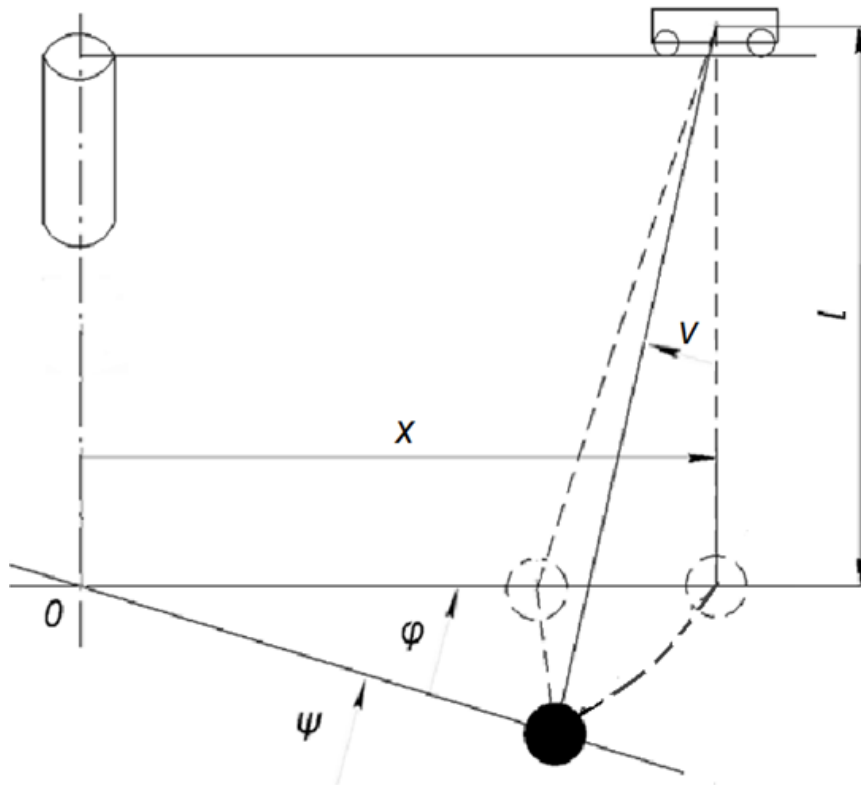


Fig 2.3 The dynamic model of the tower crane (the case of a constant velocity of the trolley)

We will assume that in this model all links of mechanisms (trolley movement and crane slewing) are absolutely rigid bodies, except the load on a flexible suspension which oscillates about a fixed point. The presented dynamic model (fig. 2.3) with the combined movement of mechanisms is presented as a holonomic mechanical system with three degrees of freedom. As the generalized coordinates, we

have taken the linear coordinate of the center of mass of the trolley  $x$ , as well as the angular coordinates of the slewing of the crane  $\varphi$  and the load  $\psi$ .

At the same time, we assume that the linear coordinate  $x$  changes according to the linear law  $x=x_0+vt$  (where  $x_0$  is the initial coordinate of the trolley position,  $t$  is the time,  $v=\text{const}$  is the constant velocity of the trolley movement along the boom). Since the law of motion of the mass of the trolley along the boom is given, the dynamic model (fig. 2.3) is represented as a mechanical system with two degrees of freedom. To compose the equations of the motion of the mechanisms, we have used the Lagrange equations:

$$\begin{cases} \frac{d}{dt} \frac{\partial T}{\partial \dot{\varphi}} - \frac{\partial T}{\partial \varphi} = Q_{\varphi} - \frac{\partial \Pi}{\partial \varphi}; \\ \frac{d}{dt} \frac{\partial T}{\partial \dot{\psi}} - \frac{\partial T}{\partial \psi} = -\frac{\partial \Pi}{\partial \psi}, \end{cases} \quad (2.22)$$

where  $T$ ,  $\Pi$  are respectively the kinetic and potential energy of the system;  $Q_{\varphi}$  is a non-potential component of the generalized crane slew force. The kinetic and non-potential energy of the dynamic system presented in fig. 2.3, are as follows:

$$T = \frac{1}{2} J_0 \dot{\varphi}^2 + \frac{1}{2} m_1 (v^2 + (x_0 + vt)^2 \dot{\varphi}^2) + \frac{1}{2} m (v^2 + (x_0 + vt)^2 \dot{\psi}^2); \quad (2.23)$$

$$\Pi = m_1 gl + mgy = m_1 gl + mgl(1 - \cos \nu) = m_1 gl + mgl(1 - \cos \frac{(\varphi - \psi)(x_0 + vt)}{l}), \quad (2.24)$$

where  $J_0$  is the moment of inertia of the slewing part of the crane reduced to the axis of its slew;  $m_1$ ,  $m$  are the masses of the trolley and the load respectively;  $l$  is the length of the flexible suspension of the load. Let's take the derivatives of expressions (2.23) and (2.24), which are necessary for the system (2.22):

$$\begin{aligned} \frac{\partial T}{\partial \varphi} &= \frac{\partial T}{\partial \psi} = 0; \\ \frac{\partial T}{\partial \dot{\varphi}} &= J_0 \dot{\varphi} + m_1 (x_0 + vt)^2 \dot{\varphi}; \\ \frac{\partial T}{\partial \dot{\psi}} &= m (x_0 + vt)^2 \dot{\psi}; \end{aligned} \quad (2.25)$$

$$\frac{d}{dt} \frac{\partial T}{\partial \dot{\varphi}} = J_0 \ddot{\varphi} + m_1(x_0 + vt)^2 \ddot{\varphi} + 2m_1(x_0 + vt)v\dot{\varphi}; \quad (2.26)$$

$$\frac{d}{dt} \frac{\partial T}{\partial \dot{\psi}} = m(x_0 + vt)^2 \ddot{\psi} + 2m(x_0 + vt)v\dot{\psi}; \quad (2.27)$$

$$\frac{\partial \Pi}{\partial \varphi} = \frac{mg}{l}(x_0 + vt)^2(\varphi - \psi); \quad (2.28)$$

$$\frac{\partial \Pi}{\partial \psi} = -\frac{mg}{l}(x_0 + vt)^2(\varphi - \psi). \quad (2.29)$$

As a result of the substitution of expressions (2.25)-(2.29) into the system (2.22) and replacement of the generalized force  $Q_\varphi$  at the driving torque of the crane slew mechanism  $M$  (reduced to the axis of the crane slewing), we will obtain differential equations of the joint motion of the slewing mechanism and the trolley movement mechanism (in a condition of movement of the trolley at a constant velocity):

$$\begin{cases} (J_0 + m_1(x_0 + vt)^2)\ddot{\varphi} + 2m_1(x_0 + vt)v\dot{\varphi} = M - \frac{mg}{l}(x_0 + vt)^2(\varphi - \psi); \\ m(x_0 + vt)^2\ddot{\psi} + 2m(x_0 + vt)v\dot{\psi} = \frac{mg}{l}(x_0 + vt)^2(\varphi - \psi). \end{cases} \quad (2.30)$$

The second equation of system (2.30) may be written in the following form:

$$(x_0 + vt)^2\ddot{\psi} + 2(x_0 + vt)v\dot{\psi} = \frac{g}{l}(x_0 + vt)^2(\varphi - \psi). \quad (2.31)$$

From equation (2.31) we may express the coordinate  $\varphi$  and find its time derivatives:

$$\varphi = \psi + 2\frac{l}{g}v\frac{\dot{\psi}}{x_0 + vt} + \frac{l}{g}\ddot{\psi}; \quad (2.32)$$

$$\dot{\varphi} = \dot{\psi} + 2\frac{l}{g}v\frac{\ddot{\psi}(x_0 + vt) - v\dot{\psi}}{(x_0 + vt)^2} + \frac{l}{g}\ddot{\psi}; \quad (2.33)$$

$$\ddot{\varphi} = \ddot{\psi} + 2\frac{l}{g}v\frac{\ddot{\psi}(x_0 + vt)^2 - 2v(\ddot{\psi}(x_0 + vt) - v\dot{\psi})}{(x_0 + vt)^3} + \frac{l}{g}IV\ddot{\psi}. \quad (2.34)$$

From the first equation of system (2.30), we might express the driving torque of the drive:

$$M = (J_0 + m_1(x_0 + vt)^2)\ddot{\varphi} + 2m_1(x_0 + vt)v\dot{\varphi} + m\frac{g}{l}(x_0 + vt)^2(\varphi - \psi). \quad (2.35)$$

As the criterion of optimization mode of the movement of the mechanisms we have chosen the RMS value of the driving torque of the slewing mechanism:

$$M_{ck} = \left[ \frac{1}{t_n} \int_0^{t_n} M^2 dt \right]^{\frac{1}{2}} \rightarrow \min, \quad (2.36)$$

where  $t_n$  is the duration of system acceleration.

The boundary conditions of the system movement are as follows:

$$\begin{cases} \varphi(0) = 0, \dot{\varphi}(0) = 0, \psi(0) = 0, \\ \dot{\psi}(0) = 0, \ddot{\psi}(0) = \ddot{\varphi}(0), \\ \psi(t_n) = \varphi(t_n) = \frac{\omega t_n}{2}, \\ \dot{\psi}(t_n) = \dot{\varphi}(t_n) = \omega, \ddot{\psi}(t_n) = \ddot{\varphi}(t_n), \end{cases} \quad (2.37)$$

where  $\omega$  – is the angular velocity of the tower slewing. With the help of dependencies (2.30)-(2.34) we reduce the angular coordinate  $\varphi$ , velocity, and acceleration to the coordinate  $\psi$  and its time derivatives. It allows us to rewrite the boundary conditions (2.37) and represent them in terms of values of function  $\psi$  and its higher time derivatives:

$$\begin{cases} \psi(0) = 0, \dot{\psi}(0) = 0, \ddot{\psi}(0) = 0, \\ \overset{IV}{\ddot{\psi}}(0) = 0, \psi(0) = 0; \\ \psi(t_n) = \frac{\omega t_n}{2}, \dot{\psi}(t_n) = \omega, \ddot{\psi}(t_n) = -\frac{2v\omega}{vt_n + x_0}, \\ \ddot{\psi}(t_n) = \frac{6v\omega}{(vt_n + x_0)^2}, \overset{IV}{\psi}(t_n) = \frac{24v\omega}{(vt_n + x_0)^3}. \end{cases} \quad (2.38)$$

The constraints in the problem statement are non-exceedance of the torque capacity of the drive and the positiveness of the angular velocity of the tower:

$$\begin{cases} \frac{M_{\max}}{M_{HOM}} \leq \lambda; \\ \omega_{\min} \geq 0, \end{cases} \quad (2.39)$$

where  $M_{HOM}$  – nominal and maximal drive torque respectively;  $\lambda$  is the torque capacity of the drive of the tower slew mechanism;  $\omega_{\min}$  – the minimum value of the angular velocity of the crane slewing during the controlled movement. The condition of the minimum of the integral criterion (2.36) is a Poisson equation, which is a nonlinear one for the case that is under consideration. The situation is complicated by the constraints (2.39). Therefore, to solve the presented optimization problem, we have used the ME-PSO method [15].

In order to take into account for the constraints (2.39), to minimize the criterion (2.36), and to determinate of such a minimum value of the duration  $t_n$ , where requirements (2.39) and (2.36) are met, a generalized criterion was developed:

$$Cr = M_{CK} + t_n \delta_t \delta_1 + (\tilde{C}r_1 + \tilde{C}r_2) \delta_2, \quad (2.40)$$

where  $\tilde{C}r_1$  and  $\tilde{C}r_2$  – criteria that take into account constraints (2.39);  $\delta_1$ ,  $\delta_2$  are weight coefficients that show the importance of minimization of the corresponding components (within the framework of this study were set  $\delta_1=10^4$  and  $\delta_2=10^6$ , which made it possible to satisfy the conditions (2.39) and to minimize the duration of the transient mode of the system movement);  $\delta_t$  is the coefficient that reduces the dimension of time to the dimension of criterion (2.26). Criteria  $\tilde{C}r_1$  and  $\tilde{C}r_2$  are defined by the expressions:

$$\begin{aligned} \tilde{C}r_1 &= \begin{cases} \frac{M_{\max}}{M_{HOM}} \delta_M, & \text{if } \frac{M_{\max}}{M_{HOM}} > \lambda; \\ 0, & \text{if } \frac{M_{\max}}{M_{HOM}} \leq \lambda; \end{cases} \\ \tilde{C}r_2 &= \begin{cases} |\omega_{\min}| \delta_\omega, & \text{if } \omega_{\min} < 0; \\ 0, & \text{if } \omega_{\min} \geq 0, \end{cases} \end{aligned} \quad (2.41)$$

where  $\delta_m$  and  $\delta_\omega$  – are the coefficients that reduce the dimension of the relevant components (drive overload, tower angular velocity) to the dimension of criterion (2.36). The essence of the criteria  $\tilde{C}r_1$  and  $\tilde{C}r_2$  is that they are quite large in the case when constraints (2.39) are not met. If constraints (2.39) are satisfied, then the criteria equal to zero. The basis function that will be used to find an approximate solution of the problem was found as the solution of the boundary problem:

$$\left\{ \begin{array}{l} \overset{XV}{\psi} = 0; \\ \left\{ \begin{array}{l} \overset{IV}{\psi}(0) = \overset{IV}{\dot{\psi}}(0) = \overset{IV}{\ddot{\psi}}(0) = \overset{IV}{\dddot{\psi}}(0) = \overset{IV}{\psi}^{(5)}(0) = 0; \\ \overset{V}{\psi}(0) = \overset{V}{\psi}_0; \\ \psi\left(\frac{t_n}{2}\right) = \psi_{t_n/2}; \dot{\psi}\left(\frac{t_n}{2}\right) = \dot{\psi}_{t_n/2}; \ddot{\psi}\left(\frac{t_n}{2}\right) = \ddot{\psi}_{t_n/2}; \\ \psi(t_n) = \frac{\omega t_n}{2}; \dot{\psi}(t_n) = \omega; \ddot{\psi}(t_n) = \ddot{\psi}_n; \\ \ddot{\psi}(t_n) = \ddot{\psi}_n; \overset{IV}{\psi}(t_n) = \overset{IV}{\psi}_n; \overset{V}{\psi}(t_n) = \overset{V}{\psi}_n, \end{array} \right. \end{array} \right. \quad (2.42)$$

where  $\ddot{\psi}_n, \dddot{\psi}_n, \overset{IV}{\psi}_n$  – acceleration, jerk, and rate of jerk of the load at the moment of the end of the controlled mode of the system;  $\psi_{t_n/2}, \dot{\psi}_{t_n/2}, \ddot{\psi}_{t_n/2}$  – position, speed and acceleration of the load at a time  $\frac{t_n}{2}$ ;  $\overset{V}{\psi}_0$  та  $\overset{V}{\psi}_n$  – the fifth derivatives of coordinate  $\psi$  at the beginning and at the end of the controlled mode of the system respectively.

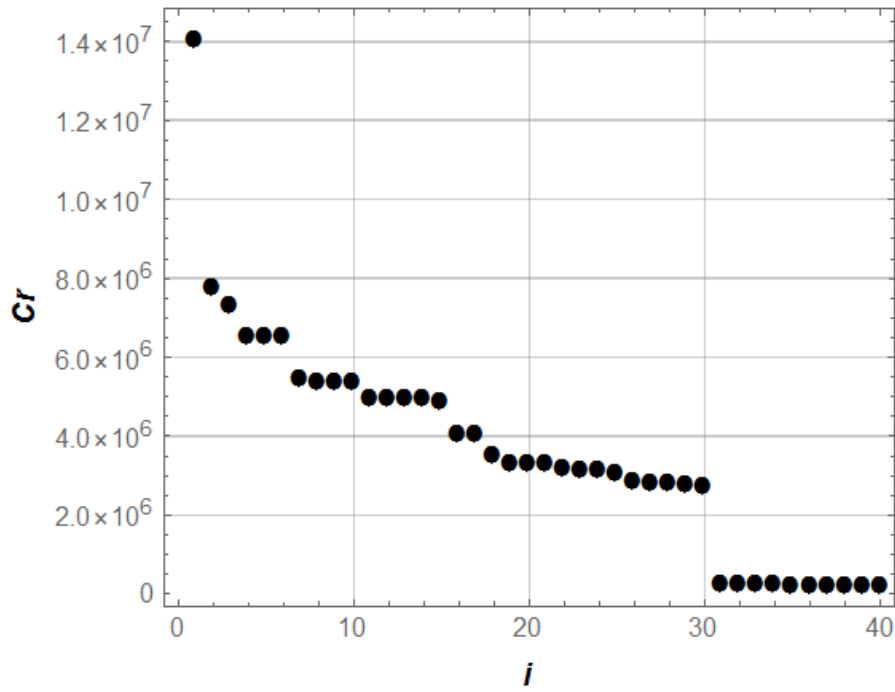
The solution of the boundary three-point problem (2.42) has a considerable volume and, therefore, is not given here. The optimization was performed with the parameters of the ME-PSO method and the search domains for the optimal values of the arguments are listed in Table 2.3.

All calculations have been made with the system parameters corresponding to the tower crane Liebherr 140 HC [12]:  $l=10$  m;  $m_1=300$  kg;  $m=5000$  kg;  $v=0.84$  m/s;  $\omega=0.066$  rad/s;  $J_0=5.5 \cdot 10^6$  kgm<sup>2</sup>.

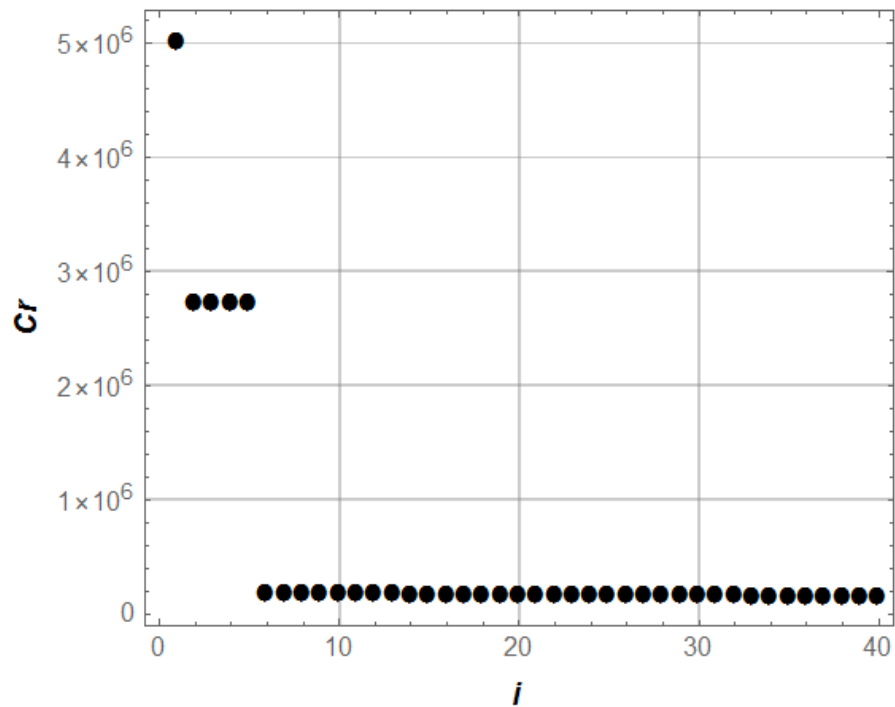
Table 2.3. Parameters of the ME-PSO method, which is used for minimization of criterion (2.40) and the argument search domains

| Parameter                       | Value                         |
|---------------------------------|-------------------------------|
| Parameters of the ME-PSO method |                               |
| Number of iterations            | 40                            |
| Swarm population                | 30                            |
| Acceptable rate value           | 0.05                          |
| The argument search domains     |                               |
| $\overset{V}{\psi}_0$           | 0...1                         |
| $\psi_{t_n/2}$                  | 0...5 $\omega$                |
| $\dot{\psi}_{t_n/2}$            | 0... $\omega$                 |
| $\ddot{\psi}_{t_n/2}$           | -2.5 $\omega$ ...2.5 $\omega$ |
| $\overset{V}{\psi}_n$           | -1...1                        |
| $t_n$                           | 2...10                        |

As a result of the method applying, values were obtained:  $\overset{V}{\psi}_0=0.1111$  rad/s<sup>5</sup>,  $\psi_{t_n/2}=0.0632$  rad,  $\dot{\psi}_{t_n/2}=0.0243$  rad/s,  $\ddot{\psi}_{t_n/2}=-0.0003$  rad/s<sup>2</sup>,  $\overset{V}{\psi}_n=-0.1961$  rad/s<sup>5</sup> and the duration of the controlled mode  $t_n=9.99$  s for the trolley movement from the initial position  $x_0=1.5$  m from the tower. For the second case (the movement of the trolley from the initial position  $x_0=30$  m towards the tower) the following values are obtained:  $\overset{V}{\psi}_0=0.0$  rad/s<sup>5</sup>,  $\psi_{t_n/2}=0.0475$ rad,  $\dot{\psi}_{t_n/2}=0.0395$  rad/s,  $\ddot{\psi}_{t_n/2}=0.0165$  rad/s<sup>2</sup>,  $\overset{V}{\psi}_n=-0.1609$  rad/s<sup>5</sup> and the duration of the controlled mode  $t_n=8,94$  s. To illustrate the efficiency of the algorithm, we present plots of decreasing the criterion (2.40) values during performing ME-PSO algorithm (fig. 2.4).



a)



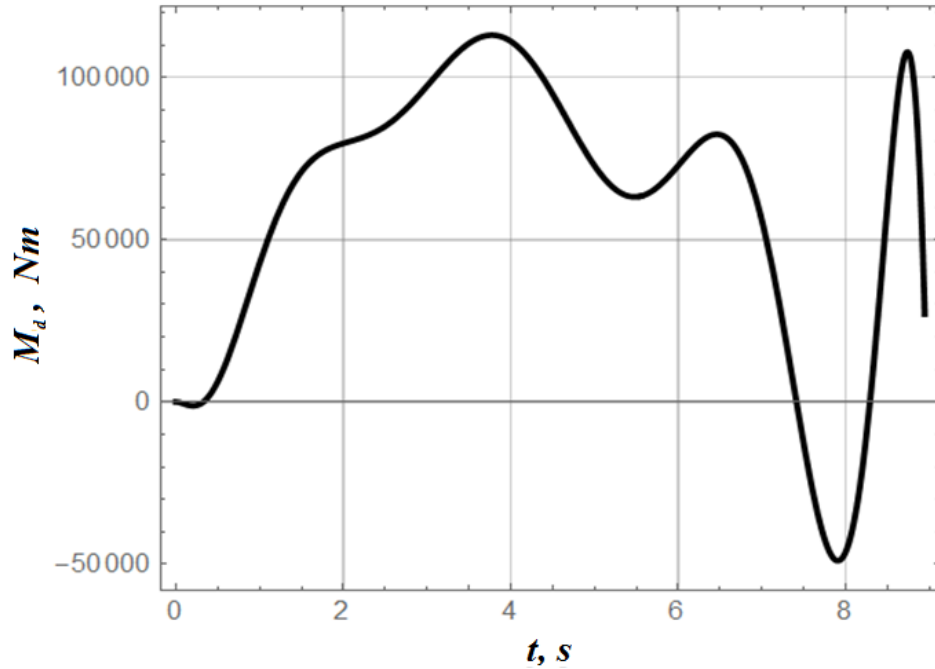
b)

Fig. 2.4 Plots of reducing the value of criterion (2.40): a) the case of the trolley movement from the tower; b) the case of trolley movement towards the tower

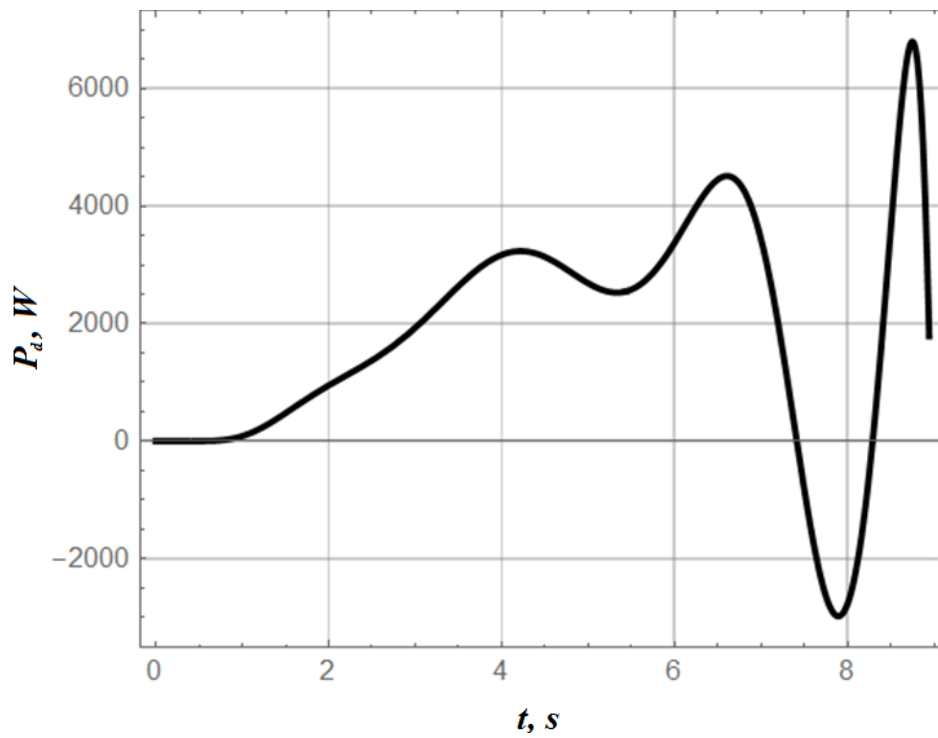
Graphical dependencies' analysis shows that determining the optimal values of function arguments is performed quite effectively.

For the first case, 30 iterations were enough, and for the second one, only 6 were enough.

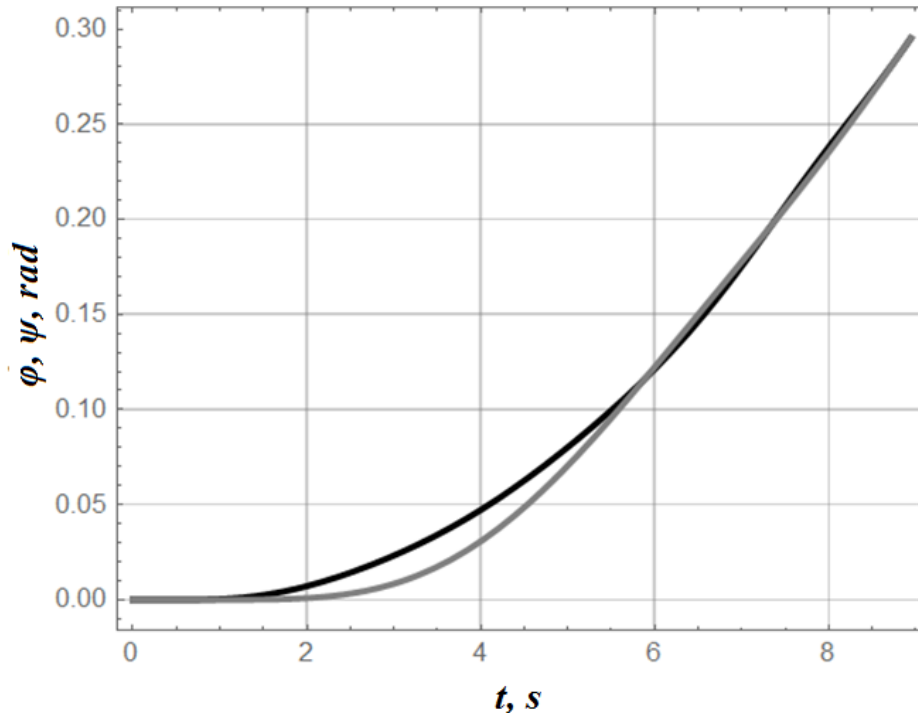
In order to estimate the dynamical features of the found approximate optimal laws of the system movement, plots (fig. 2.4) for the second case are built.



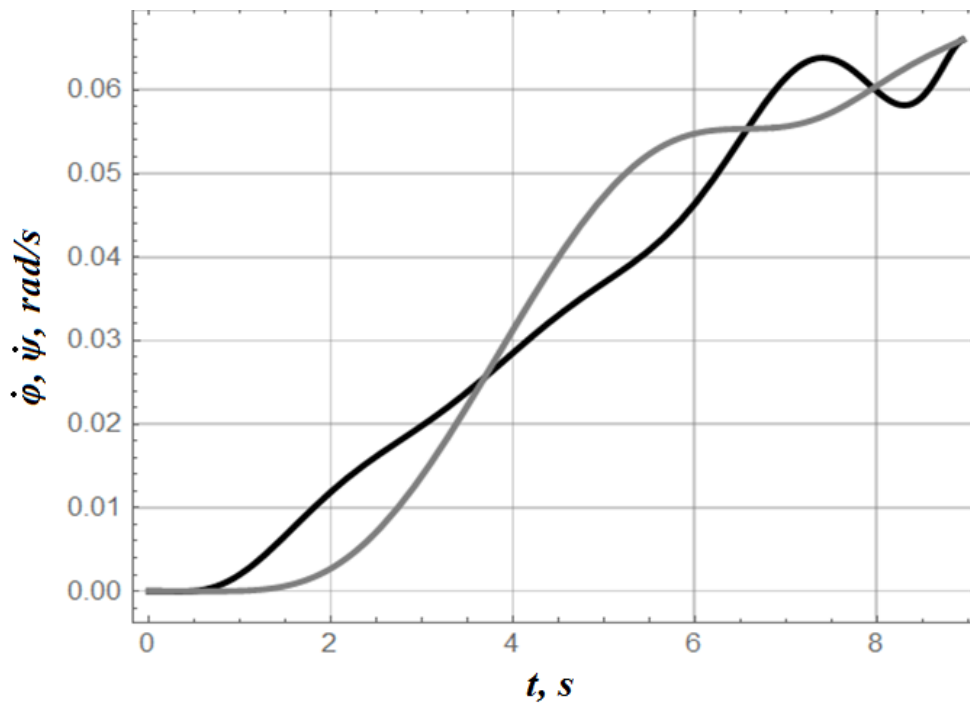
a)



b)



c)



d)

Fig. 2.5 Plots of kinematic, dynamical and energetic characteristics of system motion for the second case: a) dynamic component of the driving torque; b) the required drive power to overcome the dynamic component of the driving torque; c) trolley (black line) and load (gray line) positions; d) trolley (black line) and load (gray line) velocities

Analysis of the plots given in fig. 2.5, shows that they are smooth, which is a consequence of the selection of a basis function from a class of continuously differentiated functions. All boundary conditions of the system movement, as well as constraints (2.39) are satisfied.

Some numerical characteristics of the optimal laws of motion were calculated. They are listed in Table 2.4 (hereinafter all the numerical values of the approximate optimal laws of motion of the tower crane slew mechanisms refer to the dynamical power components and energetic characteristics).

Analyzing the values of dynamic, energetic, and kinematic indicators of optimal modes (Table 2.4), we may determine that the maximum driving torque, the maximum drive power, and the root-mean-square of the drive power for both of the cases differ slightly.

When the trolley is moving from the tower, the load deviations (maximum and root-mean-square values) are larger than those that occur when the trolley is moving toward the tower. On the other hand, when the trolley is moving to the tower, the root-mean-square value of the driving torque is 32% bigger.

Table 2.4 Numerical values of the optimal laws of motion of the system

| Parameter   | Trolley movement |               |
|---|------------------|---------------|
|   | from tower       | towards tower |
| 1   | 2                | 3             |
| The maximum value of the driving torque, Nm                       | 118572           | 113004        |
| The minimum value of the driving torque, Nm                       | -61055           | -48909        |
| The maximum value of the driving power, W                         | 6283             | 6798          |
| The minimum value of the driving power, W                         | -4030            | -2978         |
| Maximum difference in the position of the trolley and the load, m | 0,036            | 0,017         |
| RMS value of the driving torque, Nm                               | 55944            | 73859         |
| RMS driving power, W  | 2218             | 2669          |

Table 2.4 continuation

| 1  | 2      | 3      |
|--|--------|--------|
| RMS value of the difference in the position of the trolley and the load, m | 0.0182 | 0.0084 |
| The value of the optimization criterion                                    | 255755 | 163318 |

Thus, changing the direction of the trolley movement causes an increase in some indicators and a decrease in others.

### **2.3 Optimization of the slewing of the boom crane upon a complex integral criterion**

The operation of the slewing mechanism results in load oscillations on a flexible suspension and large dynamic forces on the elements of the drive mechanism and the metal structures of the crane [31-39]. These loads are especially dangerous during the transient processes of the slewing mechanism (starting and braking). It is proposed that in order to eliminate the load oscillations and to reduce the dynamical forces, the starting process should be optimized [40-51].

It is reasonable to use a complex integral criterion, which takes into account the effect of the dynamic forces in the crane slewing drive mechanism and their rate. The latter has a significant influence on the occurrence of oscillations in the drive mechanism and the load on a flexible suspension. While solving the optimization problem, the problem of minimizing the complex nonlinear integral criterion (functional) arises that cannot be solved using the existing analytical and numerical methods. One of the ways to solve the above-mentioned problem is to use a metaheuristic algorithm [52, 53], in particular, the ME-PSO method [55] or other similar methods. The solution of this problem will make it possible to apply the optimization methods for the motion modes of nonlinear mechanical systems.

The expansion of the scope of activities and the emergence of new lines of research and new, more difficult problems contribute to the need for other methods to solve problems of increased complexity and dimensionality. This requires further improvement of optimization methods and the development of new mathematical optimization models which may be applied in present-day information technologies [52].

Studies [52, 53] provide the findings of recent research on the development and implementation of applied combinatorial optimization methods, the issues of formalization, classification, and assessment of the computing complexity of combinatorial optimization problems, and state-of-the-art approaches to the solution of the above problems. The main focus is on metaheuristic methods. It has been confirmed that combinatorial optimization methods can be used to solve a wide range of applied problems arising in science, technology, biology, economics, production, etc. Optimization by means of natural (biological) methods is becoming widely spread in the various domains of human activities [54].

One of the methods applied for the solution of this problem is the particle swarm optimization (PSO) method, which simulates the swarm behavior when it is moving in some environment (water, air, etc.) [55].

The authors of [56] have analyzed the genetic algorithm, the PSO algorithm, and the neuron-genetic method for the solution of the problem.

The PSO method is used to calculate various control problems, develop artificial neural networks, process signals, etc. [55, 57-60].

Authors in [61] propose a new technology based on the particle swarm optimization technology. The basic idea consists in the re-initiation of the stagnation swarm with low intelligence efficiency.

The use of swarm-based technologies, the PSO method or other similar methods and their modifications [52-61] makes it possible to use the optimization methods of the motion modes of nonlinear mechanical systems.

The purpose of this study is to optimize the slewing mode of the boom crane upon a complex integral criterion. To achieve this purpose, the following problems

should be solved: 1) to choose the model of the boom crane slewing dynamics; 2) to justify the optimization criterion of the crane slewing mode and to determine its extreme values; 3) to determine the optimal mode of the slewing mechanism motion; 4) to analyze the obtained results.

While developing the dynamic model of the boom crane slewing mechanism, we suppose that the basic elements of the crane are absolutely solid objects, except for the drive mechanism, whose elements have elastic properties, and the load on a flexible suspension, which is represented in the form of a moveable mathematical pendulum. Besides, we ignore the rope's radial vertical deviations that do not depend on the slewing mode and are determined by the centrifugal force, so we only take into account the rope's deviation in the direction that is tangential to the circular load motion. Thus, the dynamic model of the boom crane slewing mechanism may be represented as a holonomic mechanical system with three degrees of freedom, as shown in fig. 2.6 [34].

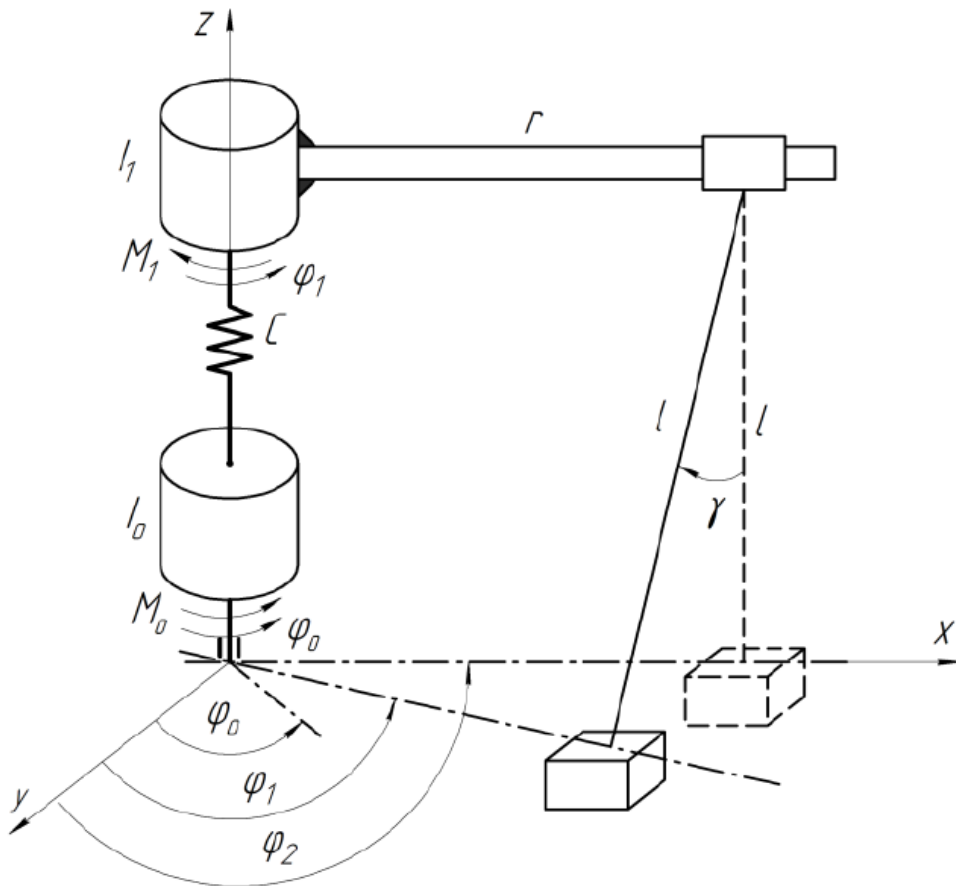


Fig. 2.6 A dynamic model of the slewing mechanism

The angular coordinates of the rotation angle of the electric motor rotor  $\varphi_0$ , the revolving part of the boom crane  $\varphi_1$ , and the load  $\varphi_2$  reduced to the axis of rotation of the crane are taken as generalized coordinates.

The presented dynamic model of the crane slewing mechanism is matched with the mathematical model in the form of a system of three differential second-order equations [34]:

$$\begin{cases} I_0 \ddot{\varphi}_0 = M_0 - C(\varphi_0 - \varphi_1), \\ I_1 \ddot{\varphi}_1 = C(\varphi_0 - \varphi_1) - mr^2 \frac{g}{l} (\varphi_1 - \varphi_2) - M_1 \\ \ddot{\varphi}_2 = \frac{g}{l} (\varphi_1 - \varphi_2), \end{cases} \quad (2.43)$$

where  $m$  – is the mass of the load on a flexible suspension;  $I_0$  – is the inertia moment of the drive mechanism reduced to the axis of the crane slewing;  $I_1$  – is the inertia moment of the revolving part of the crane relative to its revolution axis;  $M_0$  – is the breakaway torque on the electric motor shaft reduced to the revolution axis of the crane;  $M_1$  – is the resistance torque in the revolving part of the crane relative to its revolution axis;  $C$  – is the rigidity factor of the drive mechanism, reduced to the revolution axis of the crane;  $r$  – is the length of the boom from the revolution axis of the crane to the trolley position;  $l$  – is the length of the flexible load suspension;  $g$  – is the free-fall acceleration.

Loads emerging during the starting process in the transmission mechanism are significant for the crane slewing mechanism. In addition, the nature of the change in these loads has a considerable influence on the oscillatory processes that take place in the transmission mechanism and the flexible load suspension. Therefore, a complex dimensionless integral dynamic criterion, which takes into account the relative root-mean-square value of elastic torque in the drive mechanism, and its rate have been chosen as the optimization criterion and is represented by the following dependence:

$$K = \left\{ \frac{1}{t_1} \int_0^{t_1} \left[ \delta \left( \frac{M_{01}}{M_H} \right)^2 + (1 - \delta) \left( \frac{\dot{M}_{01}}{M_H} t_1 \right)^2 \right] dt \right\}^{1/2}, \quad (2.44)$$

where  $t$  – is the time;  $t_1$  – is the duration of a transient process (starting, braking);  $M_{01}, \dot{M}_{01}$  – are the elastic torque in the drive mechanism and its rate, respectively, reduced to the crane revolution axis;  $M_n$  – is the nominal torque on the drive motor shaft reduced to the crane revolution axis;  $\delta$  – is the dimensionless weighting factor that takes into account the proportion of the elastic torque and may vary from 0 to 1.

Let us determine the constituents of the criterion (2.44). First, the dependence of the elastic torque in the drive mechanism is found from the second equation of the system (2.43):

$$M_{01} = C(\varphi_0 - \varphi_1) = I_1 \ddot{\varphi}_1 + mr^2 \ddot{\varphi}_2 + M_1. \quad (2.45)$$

Dependence (2.45) may be reduced only to the generalized coordinate  $\varphi_2$  and its time derivatives. For this purpose, let us express the coordinate  $\varphi_1$  from the last equation (2.43) through coordinate  $\varphi_2$  and its derivative; as a result, we obtain:

$$\varphi_1 = \varphi_2 + \frac{l}{g} \ddot{\varphi}_2. \quad (2.46)$$

Having taken time derivatives from expression (2.46), we shall have:

$$\dot{\varphi}_1 = \dot{\varphi}_2 + \frac{l}{g} \ddot{\varphi}_2, \quad (2.47)$$

$$\ddot{\varphi}_1 = \ddot{\varphi}_2 + \frac{l}{g} \overset{IV}{\varphi}_2, \quad (2.48)$$

Having put expression (2.48) into dependence (2.45), we shall find:

$$M_{01} = I_1 \frac{l}{g} \overset{IV}{\varphi}_2 + \left( I_1 + mr^2 \right) \ddot{\varphi}_2 + M_1. \quad (2.49)$$

Having taken a time derivative from expression (2.49), we shall find the rate of the elastic torque change in the drive mechanism:

$$\dot{M}_{01} = I_1 \frac{l}{g} \varphi_2 + (I_1 + mr^2) \ddot{\varphi}_2. \quad (2.50)$$

Having put expressions (2.49) and (2.50) into criterion (2.44) and made some transformations, we shall have:

$$K = \left\{ \left\{ \frac{1}{M_H^2 t_1} \int_0^{t_1} \left\{ \delta \left[ I_1 \frac{l}{g} \varphi_2 + (I_1 + mr^2) \ddot{\varphi}_2 \right]^2 + (1-\delta) t_1^2 \left[ I_1 \frac{l}{g} \varphi_2 + (I_1 + mr^2) \ddot{\varphi}_2 \right]^2 \right\} dt \right\} \right\}^{1/2} \quad (2.51)$$

Let us determine the boundary conditions of the starting process for the dynamic model of the boom system, as shown on fig. 2.6:

$$\begin{cases} t=0: & \varphi_0 = \varphi_1 = \varphi_2 = 0, \quad \dot{\varphi}_0 = \dot{\varphi}_1 = \dot{\varphi}_2 = 0; \\ t=t_1: & \varphi_0 = \varphi_1 = \varphi_2 = \omega_y t_1 / 2, \quad \dot{\varphi}_0 = \dot{\varphi}_1 = \dot{\varphi}_2 = \omega_y, \end{cases} \quad (2.52)$$

where  $\omega_y$  – is the set angular velocity of the crane slewing;  $t_0$  and  $t_n$  – are the initial and the end points of the motion interval.

Let us reduce the system's boundary conditions (2.52) to coordinate  $\varphi_2$  and its time derivatives. For this purpose, let us express the motor rotor angle coordinate  $\varphi_0$ :

$$\varphi_0 = \varphi_1 + \frac{I_1}{C} \dot{\varphi}_1 + \frac{mr^2}{C} \ddot{\varphi}_2. \quad (2.53)$$

Using dependencies (2.46) and (2.48), expression (2.53) takes the following form

$$\varphi_0 = \varphi_2 + \left( \frac{l}{g} + \frac{I_1 + mr^2}{C} \right) \ddot{\varphi}_2 + \frac{I_1}{C} \frac{l}{g} \varphi_2 + \frac{M_1}{C}. \quad (2.54)$$

Having taken time derivatives from expression (2.54), we shall have:

$$\dot{\varphi}_0 = \dot{\varphi}_2 + \left( \frac{l}{g} + \frac{I_1 + mr^2}{C} \right) \ddot{\varphi}_2 + \frac{I_1}{C} \frac{l}{g} \varphi_2; \quad (2.55)$$

$$\ddot{\varphi}_0 = \ddot{\varphi}_2 + \left( \frac{l}{g} + \frac{I_1 + mr^2}{C} \right) \ddot{\varphi}_2 + \frac{I_1}{C} \frac{l}{g} \varphi_2. \quad (2.56)$$

Having put expressions (2.46), (2.47), (2.52) and (2.54) into conditions (2.52), we have the extreme conditions of the boom system starting process expressed through the coordinate  $\varphi_2$  and its time derivatives:

$$\begin{cases} t=0: \varphi_2=0, \dot{\varphi}_2=0, \ddot{\varphi}_2=0, \overset{IV}{\ddot{\varphi}}_2=0, \overset{IV}{\varphi}_2=-\frac{M_1g}{I_1l}, \overset{V}{\varphi}_2=0; \\ t=t_1: \varphi_2=\frac{\omega_y t_1}{2}, \dot{\varphi}_2=\omega_y, \ddot{\varphi}_2=0, \overset{IV}{\ddot{\varphi}}_2=0, \overset{IV}{\varphi}_2=-\frac{M_1g}{I_1l}, \overset{V}{\varphi}_2=0. \end{cases} \quad (2.57)$$

The condition for the minimum of criterion (2.51) under boundary conditions (2.57) is Poisson's equations that cannot be solved analytically. Therefore, in order to solve such a complicated problem, we shall use the approximation methods of swarm-based technologies, in particular, the PSO method. For this purpose, let us break the motion interval of the boom system  $[0, t_1]$  into discrete points with an interval  $\Delta t=(t_n-t_0)/n$ , where  $n$  – is the number of intervals.

Let us replace  $\varphi_2 = \varphi$ ,  $\dot{\varphi}_2 = \dot{\varphi}$ ,  $\ddot{\varphi}_2 = \ddot{\varphi}$ ,  $\overset{IV}{\ddot{\varphi}}_2 = \overset{IV}{\ddot{\varphi}}$ ,  $\overset{IV}{\varphi}_2 = \overset{IV}{\varphi}$ ,  $\overset{V}{\varphi}_2 = \overset{V}{\varphi}$  independences (2.43), ..., (2.57) and replace the continuity of these functions with the approximate discrete values. For example, the continuous coordinate  $\varphi$  shall be represented in discrete values  $\varphi_0, \varphi_1, \varphi_2, \dots, \varphi_{n-1}, \varphi_n$ .

Here,  $\varphi_0$  – is the initial value of a function  $\varphi$ , and  $\varphi_n$  is its end value. Similarly, functions  $\dot{\varphi}$ ,  $\ddot{\varphi}$ ,  $\overset{IV}{\ddot{\varphi}}$ ,  $\overset{IV}{\varphi}$ ,  $\overset{V}{\varphi}$  shall be replaced with discrete values.

Then extreme conditions (2.57) are formulated as follows:

$$\begin{cases} t=t_0=0: \varphi=\varphi_0=0, \dot{\varphi}=\dot{\varphi}_0=0, \ddot{\varphi}=\ddot{\varphi}_0=0, \overset{IV}{\ddot{\varphi}}=\overset{IV}{\ddot{\varphi}}_0=0, \overset{IV}{\varphi}=\overset{IV}{\varphi}_0=-\frac{M_1g}{I_1l}, \overset{V}{\varphi}=\overset{V}{\varphi}_0=0; \\ t=t_n: \varphi=\varphi_n=\frac{\omega_y t_n}{2}, \dot{\varphi}=\dot{\varphi}_n=\omega_y, \ddot{\varphi}=\ddot{\varphi}_n=0, \overset{IV}{\ddot{\varphi}}=\overset{IV}{\ddot{\varphi}}_n=0, \overset{IV}{\varphi}=\overset{IV}{\varphi}_n=-\frac{M_1g}{I_1l}, \overset{V}{\varphi}=\overset{V}{\varphi}_n=0. \end{cases} \quad (2.58)$$

In the middle of the interval  $[t_0, t_n]$  without extreme values, let us set the discrete values of a function  $\varphi$  from  $\varphi_1, \varphi_2$ , etc. to  $\varphi_{n-1}$ , as shown in fig. 2.7.

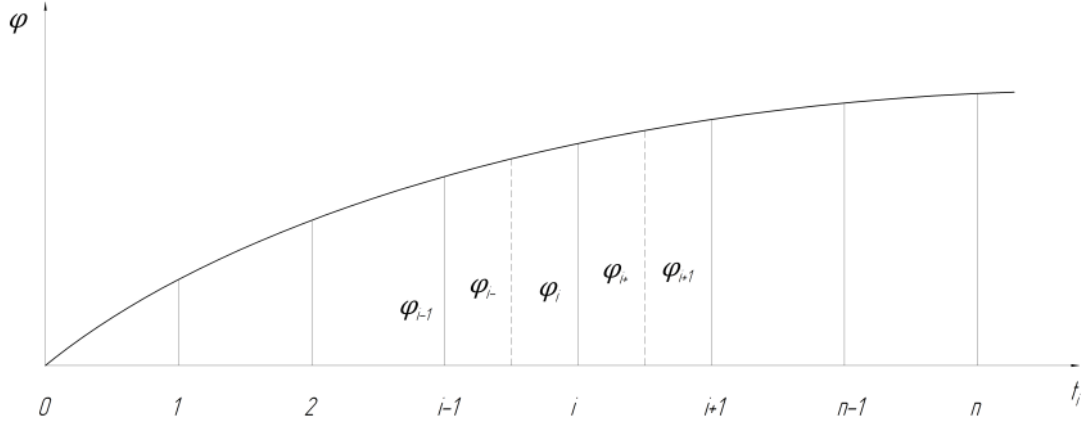


Fig. 2.7 Function representation with discrete values

In the middle of the interval, the discrete values of the function are determined by dependencies:

$$\begin{cases} \varphi_{i-} = (\varphi_{i-1} + \varphi_i)/2; \\ \varphi_{i+} = (\varphi_i + \varphi_{i+1})/2. \end{cases} \quad (2.59)$$

For discrete values of the function  $\varphi_{i-1}$ ,  $\varphi_{i-}$ ,  $\varphi_i$ ,  $\varphi_{i+}$ ,  $\varphi_{i+1}$ , when  $i$  changes from 1 to  $n-1$ , discrete values of time derivatives of this function are calculated and used for the criterion:

$$\begin{cases} \dot{\varphi}_{i-} = \frac{\varphi_i - \varphi_{i-1}}{\Delta t}; \\ \dot{\varphi}_{i+} = \frac{\varphi_{i+1} - \varphi_i}{\Delta t}; \\ \dot{\varphi}_i = \frac{\dot{\varphi}_{i-} + \dot{\varphi}_{i+}}{2}; \end{cases} \quad (2.60)$$

$$\ddot{\varphi}_i = \frac{\dot{\varphi}_{i+} - \dot{\varphi}_{i-}}{\Delta t}; \quad (2.61)$$

$$\begin{cases} \ddot{\varphi}_{i-} = \frac{\ddot{\varphi}_i - \ddot{\varphi}_{i-1}}{\Delta t}; \\ \ddot{\varphi}_{i+} = \frac{\ddot{\varphi}_{i+1} - \ddot{\varphi}_i}{\Delta t}; \\ \ddot{\varphi}_i = \frac{\ddot{\varphi}_{i-} + \ddot{\varphi}_{i+}}{2}; \end{cases} \quad (2.62)$$

$$IV \quad \varphi_i = \frac{\ddot{\varphi}_{i+} - \ddot{\varphi}_{i-}}{\Delta t};$$

(2.63)

$$\left\{ \begin{array}{l} V \\ \varphi_{i-} = \frac{IV}{\Delta t} \varphi_{i-1}; \\ V \\ \varphi_{i+} = \frac{IV}{\Delta t} \varphi_i; \\ V \\ \varphi_i = \frac{V}{2} (\varphi_{i-} + \varphi_{i+}). \end{array} \right. \quad (2.64)$$

By using the boundary conditions (2.58) and the discrete values of the function  $\varphi_1, \varphi_2, \dots, \varphi_{n-1}$  as well as dependencies (2.59), ..., (2.64), the value of the optimization criterion may be determined:

$$K = \frac{1}{M_H \sqrt{t_n}} \left\{ \left\{ \sum_{i=0}^{n-1} \left[ \delta \left[ (I_1 + mr^2) \ddot{\varphi}_i + I_1 \frac{l}{g} \frac{IV}{\Delta t} \varphi_i \right]^2 + (1-\delta) \Delta t^2 \left[ (I_1 + mr^2) \ddot{\varphi}_i + I_1 \frac{l}{g} \frac{V}{\Delta t} \varphi_i \right]^2 \right] \Delta t_i \right\} \right\}^{1/2} \quad (2.65)$$

By using the PSO method, the determination of new values  $\varphi_1, \varphi_2, \dots, \varphi_{n-1}$  is carried out until the criterion (2.65) reaches its minimum value. The end discrete values of the function will signify the optimal mode of the boom system slewing during the starting process.

The calculations have been made for the slewing mechanism of a crane QTZ-80 with parameters  $I_0=71626.12 \text{ kg}\cdot\text{m}^2$ ;  $I_1=4920738 \text{ kg}\cdot\text{m}^2$ ;  $C=6626669 \text{ N}\cdot\text{m}/\text{rad}$ ;  $m=2000 \text{ kg}$ ;  $r=40 \text{ m}$ ;  $l=30 \text{ m}$ ;  $M_H=36.8 \text{ N}\cdot\text{m}$ ;  $u=1355.2$ ;  $\eta=0.86$ ;  $\omega_y=0.07 \text{ rad/s}$ ;  $t_1=6 \text{ s}$ ;  $\omega_0=95 \text{ rad/s}$ ;  $\omega_H=95.04 \text{ rad/s}$ ;  $\lambda=2.8$ ;  $g=9.81 \text{ m/s}^2$  and provided that  $M_1=0$ . As a result of the solution, the optimal motion mode has been found, which is represented graphically (fig. 2.8-2.10).

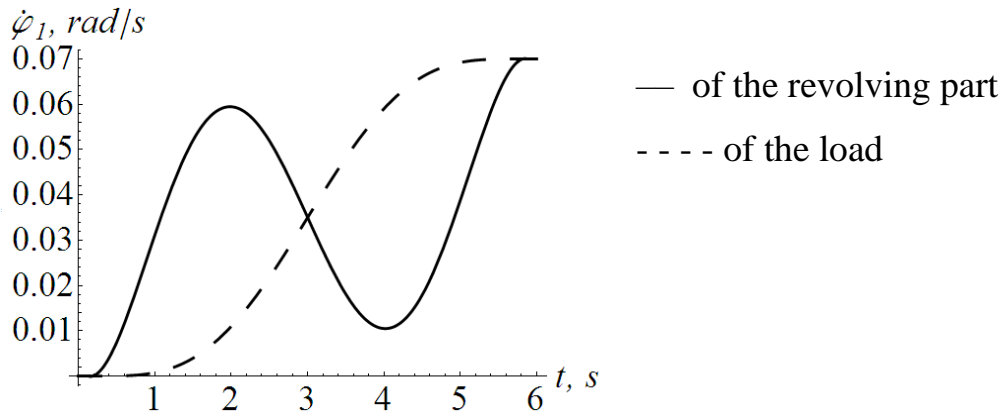


Fig. 2.8 Dependences of the crane revolving part and the load angular velocities

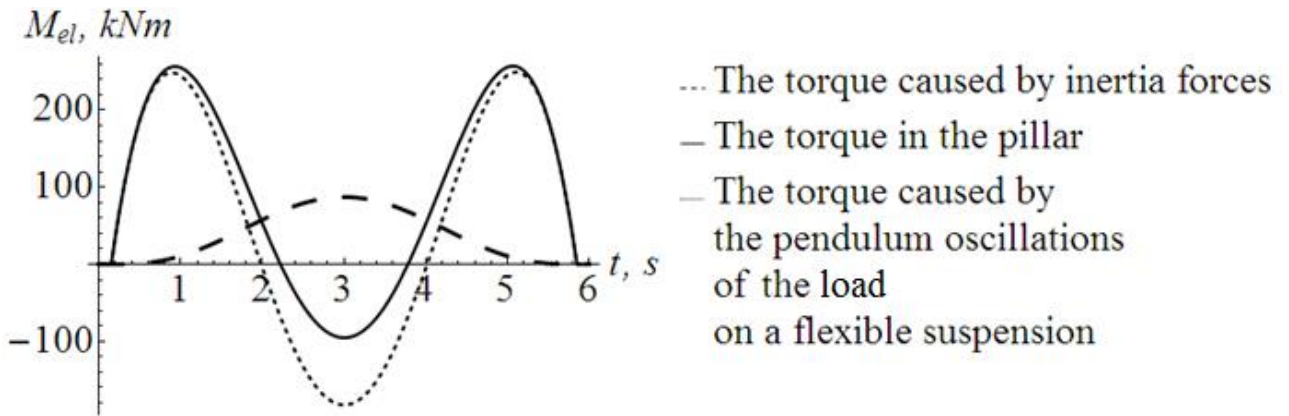


Fig. 2.9 Dependences of torques changes

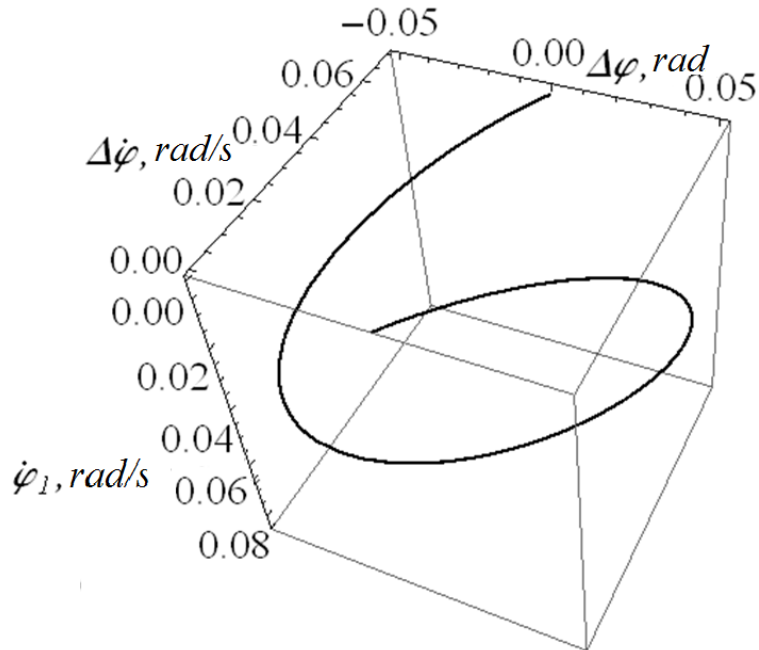


Fig. 2.10 3D phase portrait

We can see from the graphical dependences of changes in the angular velocity of the revolving part of the crane and the load (fig. 2.8) obtained after solving the optimization problem using a complex dimensionless integral dynamic criterion, which takes into account the relative root-mean-square value of the elastic torque in the drive mechanism and its rate, it reaches its set-value at 6-th second. The transient mode is smooth, without any oscillations in the system as contrasted to the direct start characteristic, as shown in [33, 34]. It allows achieving a considerable reduction in both the forces in the pillar (fig. 2.9) during the transient processes and the oscillations of the load (fig. 2.10).

## **2.4 Optimization of tower crane luffing and slewing**

The tower cranes are widely used in many sectors of the economy, including machinery construction and civil engineering. Their performance, durability, and energy efficiency, as well as operational safety depend on the modes of movement of their mechanisms.

The rational or optimal modes of crane movement allow realizing to a considerable extent the growth potential of the basic technical and operational indicators of the crane.

The perfection of modern drive systems makes it possible to implement the optimal laws of motion of tower crane mechanisms qualitatively. Therefore, the relevance of scientific and applied works on the optimization of modes of movement of tower cranes is an extremely relevant area of research.

The purpose of the presented work is to synthesize optimal modes of simultaneous movement of crane's slewing and luffing mechanisms, which eliminate load oscillations and minimize energy consumption during the start-up. In order to achieve this goal it is necessary to execute the following tasks: 1) to develop a mathematical model of the simultaneous movement of the crane's slewing and luffing mechanisms, suitable for the study of the optimal control problems; 2) to perform the statement of the problem of optimal control of the mechanisms; 3) to apply

numerical optimization methods and find an approximate solution to the problem; 4) to analyze the obtained results.

In this investigation, the compatible movement of luffing and slewing of the crane is represented by the dynamic model with four degrees of freedom (fig. 2.11).

We have chosen as generalized coordinates: linear coordinates of the centers of mass of the trolley  $x_1$  and the load  $x$  in the plane of a crane luffing, as well as the angular coordinates of the boom slewing  $\varphi$  and the load  $\psi$  in the horizontal plane. We assume that the length of the flexible suspension  $l$  is a constant value.

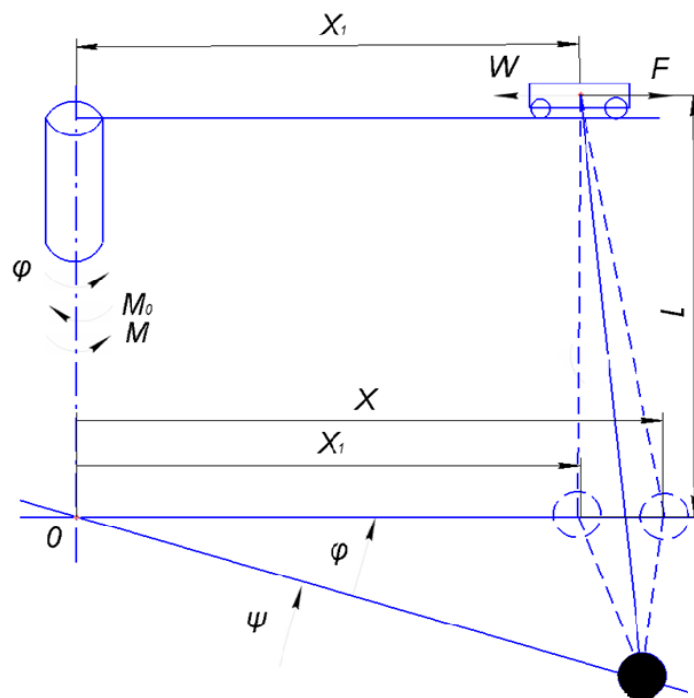


Fig. 2.11 A dynamic model of simultaneous operation of crane luffing and slewing

The accepted dynamic model (fig. 2.11) corresponds to the system of differential equations:

$$\begin{cases} m_1 \ddot{x}_1 - m_1 x_1 \dot{\varphi}^2 = F - W - \frac{mg}{l}(x - x_1); \\ \ddot{x} - \dot{\psi}^2 x = \frac{g}{l}(x - x_1 + x(\psi - \varphi)^2); \\ (J + m_1 x_1^2) \ddot{\varphi} + 2m_1 x_1 \dot{x}_1 \dot{\varphi} = M - M_0 - \frac{mg}{l} x^2 (\psi - \varphi); \\ \ddot{\psi} x - 2\dot{x} \dot{\psi} = \frac{g}{l} ((\psi - \varphi)), \end{cases} \quad (2.66)$$

where  $m_1$  and  $m$  – are masses of the trolley and the load respectively;  $F$  – is the driving force of the trolley drive (reduced to the center of the trolley mass);  $W$  – is the resistance of trolley movement;  $g$  – is free-fall acceleration;  $l$  – is the length of flexible load suspension;  $J$  – is a moment of inertia of the slewing unit and crane pillar reduced to the axis of its rotation;  $M$  and  $M_0$  – are the torque of the slewing unit drive and the torque made by resistance forces respectively (all the values are reduced to the axis of the crane slewing).

From the last equation of the system (2.66) we find the difference of angular coordinates and the difference of linear coordinates:

$$\psi - \varphi = \frac{l}{g} (\ddot{\psi} - 2 \frac{\dot{x}\dot{\psi}}{x}); \quad (2.67)$$

$$x - x_1 = \frac{l}{g} \left( \ddot{x} - x \left( \frac{l}{g} (\ddot{\psi} - 2 \frac{\dot{x}\dot{\psi}}{x})^2 + \dot{\psi}^2 \right) \right). \quad (2.68)$$

From the formula (2.67) we express the angular coordinate of a crane slewing unit and find its first and second derivatives, as a result of which we have:

$$\varphi = \psi - \frac{l}{g} (\ddot{\psi} - 2 \frac{\dot{x}\dot{\psi}}{x}); \quad (2.69)$$

$$\dot{\varphi} = \dot{\psi} - \frac{l}{g} (\ddot{\psi} - 2 \frac{\ddot{x}\dot{\psi} + \dot{x}\ddot{\psi}}{x} - 2 \frac{\dot{x}^2\dot{\psi}}{x^2}); \quad (2.70)$$

$$\ddot{\varphi} = \ddot{\psi} - \frac{l}{g} (\overset{IV}{\psi} + 2 \frac{\ddot{x}\dot{\psi} + 2\ddot{x}\ddot{\psi} + \dot{x}\ddot{\psi}}{x} - 2 \frac{2\dot{x}^2\dot{\psi} + 3\dot{x}\ddot{x}\dot{\psi}}{x^2} + 4 \frac{2\dot{x}^3\dot{\psi}}{x^3}). \quad (2.71)$$

From math equation (2.68), we express the linear coordinate  $x_1$  and find its first and second derivatives:

$$x_1 = x + \frac{l}{g} \left( x \left( \frac{l}{g} (\ddot{\psi} + 2 \frac{\dot{x}\dot{\psi}}{x})^2 + \dot{\psi}^2 \right) - \ddot{x} \right); \quad (2.72)$$

$$\dot{x}_1 = \dot{x} + \frac{l}{g} \left( \dot{x} \left( \frac{l}{g} (\ddot{\psi} + 2 \frac{\dot{x}\dot{\psi}}{x})^2 + \dot{\psi}^2 \right) + 2x \left( \frac{l}{g} (\ddot{\psi} + 2 \frac{\dot{x}\dot{\psi}}{x}) (\ddot{\psi} + 2 \frac{\ddot{x}\dot{\psi} + \dot{x}\ddot{\psi}}{x} - 2 \frac{\dot{x}^2\dot{\psi}}{x^2} + \dot{\psi}\ddot{\psi}) \right) - \ddot{x} \right); \quad (2.73)$$

$$\begin{aligned}
 \ddot{x}_1 = \ddot{x} + \frac{l}{g} & \left( \ddot{x} \left( \frac{l}{g} (\ddot{\psi} + 2 \frac{\dot{x}\dot{\psi}}{x})^2 + \dot{\psi}^2 \right) + 4\dot{x} \left( \frac{l}{g} (\ddot{\psi} + 2 \frac{\dot{x}\dot{\psi}}{x}) (\ddot{\psi} + 2 \frac{\ddot{x}\dot{\psi} + \dot{x}\ddot{\psi}}{x} - 2 \frac{\dot{x}^2\dot{\psi}}{x^2} + \dot{\psi}\ddot{\psi}) \right) + \right. \\
 + 2x & \left( \frac{l}{g} (\ddot{\psi} + 2 \frac{\ddot{x}\dot{\psi} + \dot{x}\ddot{\psi}}{x} - 2 \frac{\dot{x}^2\dot{\psi}}{x^2})^2 + \frac{l}{g} (\ddot{\psi} + 2 \frac{\dot{x}\dot{\psi}}{x}) \left( x + 2 \frac{\ddot{x}\dot{\psi} + 2\dot{x}\ddot{\psi} + \dot{x}\ddot{\psi}}{x} - 2 \frac{2\dot{x}^2\dot{\psi} + 3\dot{x}^3\dot{\psi}}{x^2} + \right. \right. \\
 + 4 & \left. \left. \frac{\dot{x}^3\dot{\psi}}{x^3} \right) + \dot{\psi}^2 + \dot{\psi}\ddot{\psi} \right) - \frac{IV}{x} \Bigg); \tag{2.74}
 \end{aligned}$$

Taking into account the expression (2.68) from the first equation of the system (2.66), we express the driving force of the trolley drive, resulting in:

$$F = m_1(\ddot{x}_1 - \dot{\phi}^2 x_1) + m \left( x \left( 1 + \frac{l}{g} \left( \ddot{\psi} + 2 \frac{\dot{x}\dot{\psi}}{x} \right)^2 + \dot{\psi}^2 \right) - \ddot{x} \right) + W. \tag{2.75}$$

Taking into account expression (2.67) from the third equation of the system (2.66), we express the driving torque of the slewing mechanism:

$$M = (J + m_1 x_1^2) \ddot{\phi} + 2m_1 x_1 \dot{x}_1 \dot{\phi} + m x^2 \left( \ddot{\psi} + 2 \frac{\dot{x}\dot{\psi}}{x} \right) + M_1. \tag{2.76}$$

In the process of starting the mechanisms (the trolley movement and the crane slewing), we should choose a mode that provides the least energy losses. Therefore, as the optimization criterion, we have chosen the root mean square of the power of the driving mechanisms of the trolley movement and the crane slewing, which is determined by the following dependence:

$$P_{CK} = \sqrt{\frac{1}{t_n} \int_0^{t_n} (F\dot{x}_1)^2 + (M\dot{\phi}_1)^2 dt}, \tag{2.77}$$

where  $t_n$  – is the duration of the start mode of both mechanisms.

After substituting (2.75) and (2.76) into criterion (2.77), it takes the next form:

$$\begin{aligned}
 P_{CK} = & \left( \frac{1}{t_n} \int_0^{t_n} \left( m_1(\ddot{x}_1 - \dot{\phi}^2 x_1) + m \left( x \left( 1 + \frac{l}{g} \left( \ddot{\psi} + 2 \frac{\dot{x}\dot{\psi}}{x} \right)^2 + \dot{\psi}^2 \right) - \ddot{x} \right) + W \right) \dot{x}_1 \right)^2 + \\
 + & \left( \left( (J + m_1 x_1^2) \ddot{\phi} + 2m_1 x_1 \dot{x}_1 \dot{\phi} + m x^2 \left( \ddot{\psi} + 2 \frac{\dot{x}\dot{\psi}}{x} \right) + M_1 \right) \dot{\phi}_1 \right)^2 dt \Bigg)^{\frac{1}{2}}. \tag{2.78}
 \end{aligned}$$

Taking into account expressions (2.75) and (2.76), the integral functional (2.78) is nonlinear concerning the unknown functions  $x=x(t)$  and  $\psi=\psi(t)$  and their derivatives.

The minimum of the criterion (2.78) should be determined concerning the boundary conditions:

$$\begin{cases} x_1(0) = x(0) = x_0; \varphi(0) = \psi(0) = 0; \\ \dot{x}_1(0) = \dot{x}(0) = 0; \dot{\varphi}(0) = \dot{\psi}(0) = 0; \\ x_1(t_n) = x(t_n) = x_{t_n}; \varphi(t_n) = \psi(t_n) = \psi_{t_n}; \\ \dot{x}_1(t_n) = \dot{x}(t_n) = v; \dot{\varphi}(t_n) = \dot{\psi}(t_n) = \omega, \end{cases} \quad (2.79)$$

where  $x_{t_n}$  and  $\psi_{t_n}$  – are linear and angular positions, respectively, of the the trolley and the load (in the radial direction), the crane tower and the load (in the tangential direction) at the end of crane acceleration.

We reduce the boundary conditions (2.79) to the functions  $x=x(t)$  and  $\psi=\psi(t)$  and their derivatives:

$$\begin{cases} x(0) = x_0; \dot{x}(0) = \ddot{x}(0) = \ddot{\ddot{x}}(0) = 0; \\ \psi(0) = \dot{\psi}(0) = \ddot{\psi}(0) = \ddot{\ddot{\psi}}(0) = 0; \\ x(t_n) = x_{t_n}; \dot{x}(t_n) = v; \ddot{x}(t_n) = (x_0 + \Delta x)\omega^2; \ddot{\ddot{x}}(t_n) = -3v\omega^2; \\ \psi(t_n) = \psi_{t_n}; \dot{\psi}(t_n) = \omega; \ddot{\psi}(t_n) = -\frac{2v\omega}{x_0 + \Delta x}; \ddot{\ddot{\psi}}(t_n) = \frac{6v^2\omega}{(x_0 + \Delta x)^2} - 2\omega^3, \end{cases} \quad (2.80)$$

where  $\Delta x$  – is the distance that the trolley passes during time  $t_n$ .

In addition, in the problem statement of optimal motion control of both mechanisms, we should use constraints that are connected with the torque capacities of the engines:

$$\begin{cases} \frac{M_{\max}}{M_n} \leq \lambda_1; \\ \frac{F_{\max}}{F_n} \leq \lambda_2. \end{cases} \quad (2.81)$$

where  $M_{\max}$  and  $M_n$  – is maximum and rated-load torques of the mechanism;  $F_{\max}$  and  $F_n$  – is maximum and nominal driving force of the engine of the luffing mechanism;

$\lambda_1$  and  $\lambda_2$  – is the torque capacities of the crane engines of the slewing and the luffing mechanisms respectively.

Taking into account the constraints (2.81) and the requirement of minimizing criterion (2.78), a generalized criterion was formulated:

$$Cr = P_{CK} + t_n \delta_1 \delta_1 + (\tilde{C}r_1 + \tilde{C}r_2) \delta_2, \quad (2.82)$$

where  $\delta_1, \delta_2$  – is weighting coefficients that show the importance of minimizing the relevant components (this study assumes that  $\delta_1=10^4$  and  $\delta_2=10^6$ , which made it possible to meet the conditions (2.81) and minimize the duration of the transient mode of the system motion);  $\tilde{C}r_1$  and  $\tilde{C}r_2$  – are criteria that take into consideration the first and the second constraints (2.81). They are determined by the following dependencies:

$$\tilde{C}r_1 = \begin{cases} \frac{M_{\max}}{M_n} & \text{if } \frac{M_{\max}}{M_n} > \lambda_1; \\ 0, & \text{if } \frac{M_{\max}}{M_n} \leq \lambda_1; \end{cases} \quad (2.83)$$

$$\tilde{C}r_2 = \begin{cases} \frac{F_{\max}}{F_n} & \text{if } \frac{F_{\max}}{F_n} > \lambda_2; \\ 0, & \text{if } \frac{F_{\max}}{F_n} \leq \lambda_2. \end{cases}$$

The essence of the criteria  $\tilde{C}r_1$  and  $\tilde{C}r_2$  is that they are quite big when conditions (2.81) are not met.

If constraints (2.81) are met, then the criteria become zero. Thus, the topology of criterion (2.82) is quite complex. To solve this optimization problem, we use the ME-PSO method [27].

To do this, first, we set out the basis functions that will be used later to find an approximate solution to the optimization problem.

We have found the basis function for the luffing mechanism as the solution of the boundary problem:

$$\left\{ \begin{array}{l} IX \\ x = 0; \\ \left\{ \begin{array}{l} x(0) = x_0; \dot{x}(0) = \ddot{x}(0) = \ddot{\ddot{x}}(0) = 0; \\ x(\frac{t_n}{2}) = x_{t_n/2}; \\ \left\{ \begin{array}{l} x(t_n) = x_0 + \Delta x; \dot{x}(t_n) = v; \ddot{x}(t_n) = (x_0 + \Delta x)\omega^2; \ddot{\ddot{x}}(t_n) = -3v\omega^2, \end{array} \right. \end{array} \right. \end{array} \right. \quad (2.84)$$

where  $x_{t_n/2}$  – is the radial position of the load at the moment  $\frac{t_n}{2}$ .

The basis function for the coordinate  $\psi$  is the solution of the boundary problem:

$$\left\{ \begin{array}{l} IX \\ \psi = 0; \\ \left\{ \begin{array}{l} \psi(0) = 0; \dot{\psi}(0) = \ddot{\psi}(0) = \ddot{\ddot{\psi}}(0) = 0; \\ \psi(\frac{t_n}{2}) = \psi_{t_n/2}; \\ \left\{ \begin{array}{l} \psi(t_n) = \psi_{t_n}; \dot{\psi}(t_n) = v; \ddot{\psi}(t_n) = -\frac{2v\omega}{x_0 + \Delta x}; \ddot{\ddot{\psi}}(t_n) = \frac{6v^2\omega}{(x_0 + \Delta x)^2} - 2\omega^3, \end{array} \right. \end{array} \right. \end{array} \right. \quad (2.85)$$

where  $\psi_{t_n/2}$  – the tangential position of the load at the moment  $\frac{t_n}{2}$ . The final conditions of the load movement (in both boundary problems) are set in such a manner that its oscillations on the flexible suspension at the time  $t_n$  are absent.

The ME-PSO method parameters for solving the problem and argument search domains for both basis functions are: number of iterations – 40; swarm population – 30; criterion's minimization acceptable rate – 0.05;  $\Delta\psi=4\omega\dots10\omega$ ;  $\psi_{t_n/2}=0\dots5\omega$ ;  $\Delta x=(4\dots10)v$ ;  $x_{t_n/2}=0\dots5v$ ;  $t_n = 2\dots10$  s.

Approximate solutions have been obtained for two variants: trolley movement from tower and trolley movement to the tower. All calculations were conducted on the basis of system parameters:  $l=3$  m;  $J=5.5\cdot10^6$  kg·m<sup>2</sup>;  $m_1=300$  kg;  $m=5000$  kg;  $v=0.84$  m/s (in case of the trolley movement towards the tower  $v=-0.84$  m/s);  $\omega=0.066$  rad/s; the starting position of the trolley: for the first case  $x_0=3$  m, for the

second case  $x_0=30$  m. The parameters correspond to the Liebherr 140 hc tower crane [12].

As a result of ME-PSO method application for the first variant the next parameters were obtained:  $\Delta x=1.68$  m;  $x_{t_n/2}=1.61$  m;  $\Delta\psi=0.322$  rad;  $\psi_{t_n/2}=0.04$  rad and the acceleration duration  $t_n=6.49$  s. For the second case, the following values of the basic functions parameters were obtained:  $\Delta x=-6.15$  m;  $x_{t_n/2}=25.80$  m;  $\Delta\psi=0.219$  rad;  $\psi_{t_n/2}=0.04$  rad and the acceleration duration  $t_n=6.56$  s.

The efficiency of the algorithm is confirmed by graphs showing the decrease of the  $Cr$  criterion when using the ME-PSO algorithm (fig. 2.12).

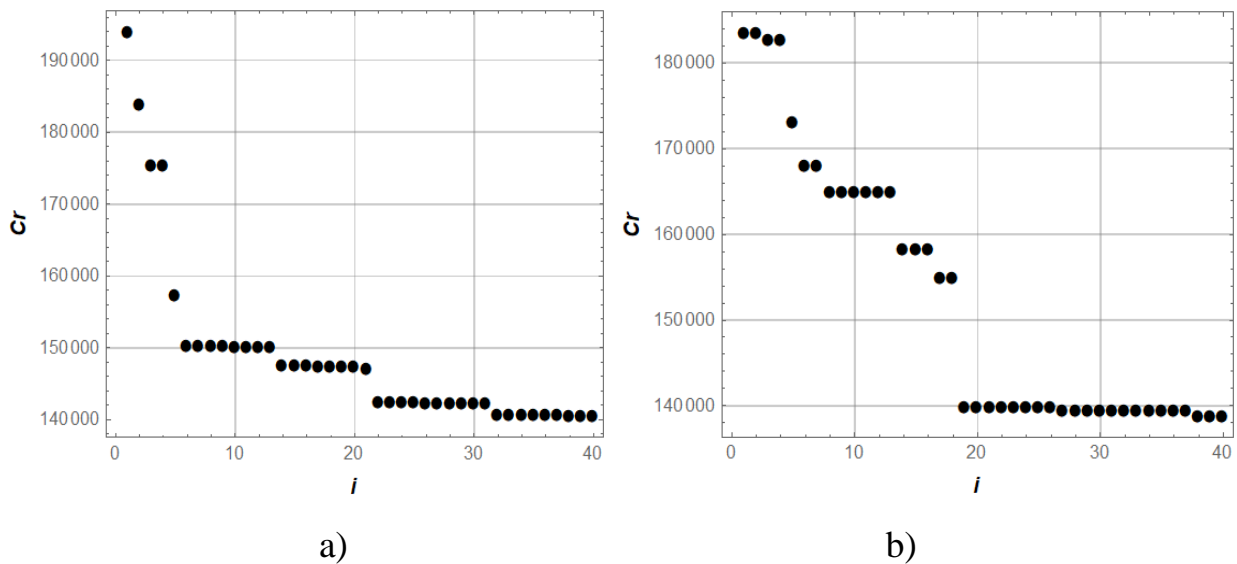
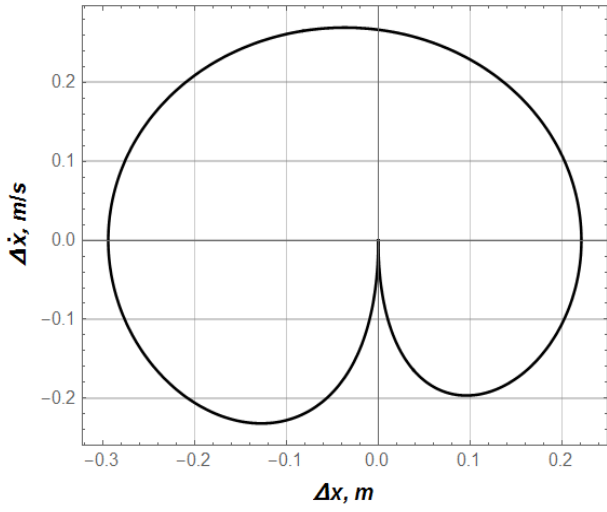


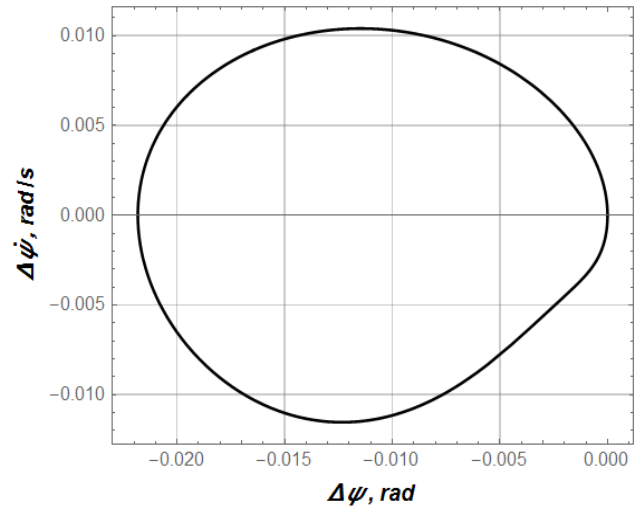
Fig. 2.12 Graphs of reducing the  $Cr$  criterion for the first (a) and second cases (b)

It can be seen from fig. 2.12 that at the early iterations of the algorithm, a rapid minimization of the  $Cr$  criterion value is performed.

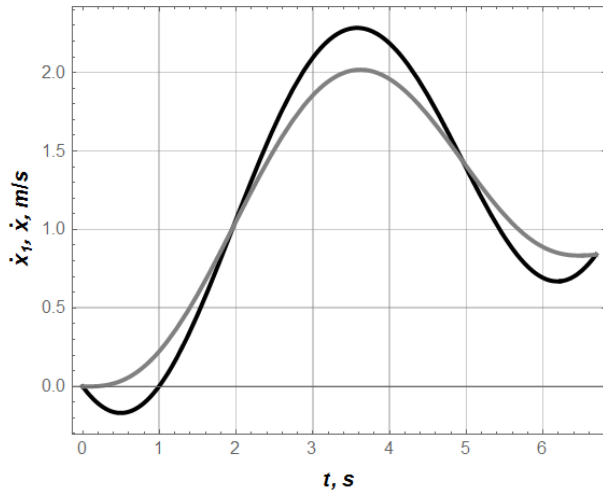
In order to illustrate the obtained results on fig. 2.13 and 2.14, the graphical dependencies of the kinematic, dynamic, and energetic characteristics of the movements of luffing and slewing mechanisms of the Liebherr 140 hc tower crane are shown.



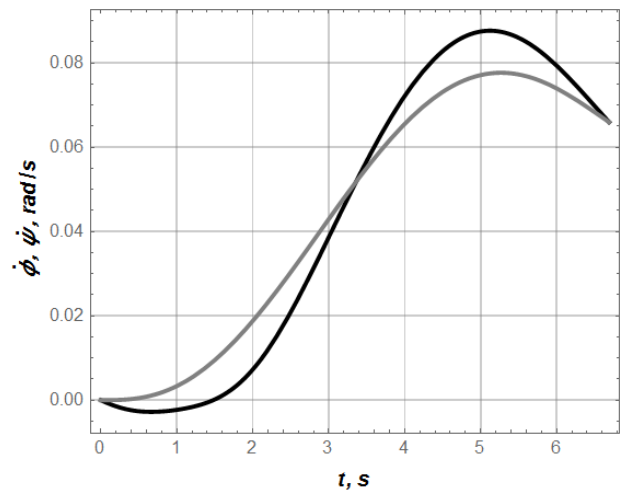
a)



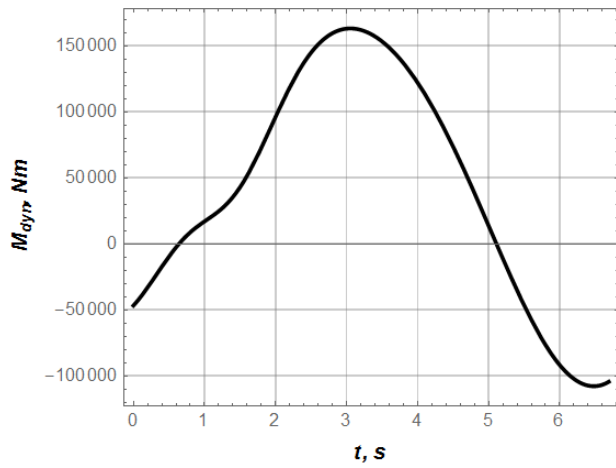
b)



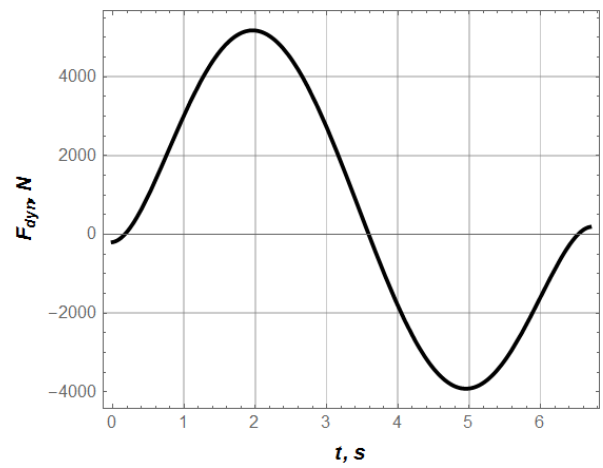
c)



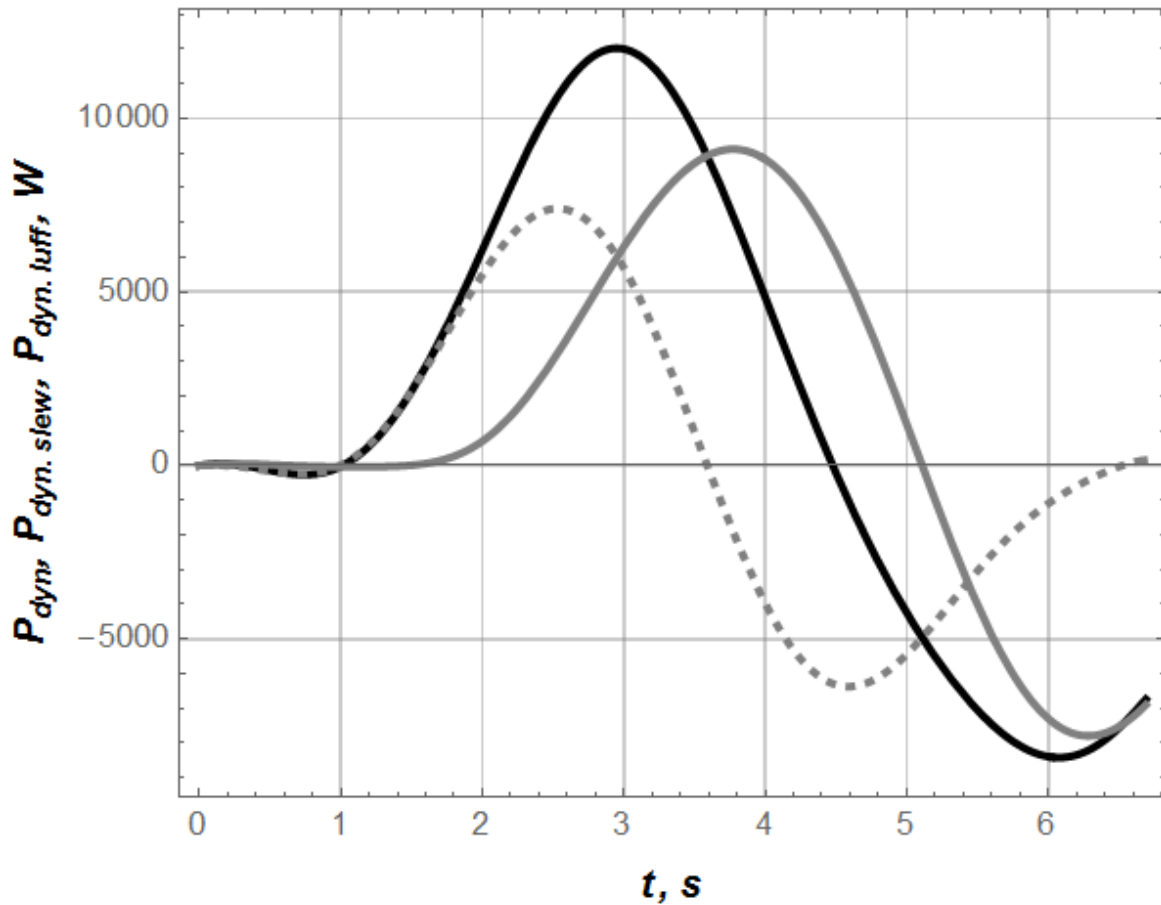
d)



e)

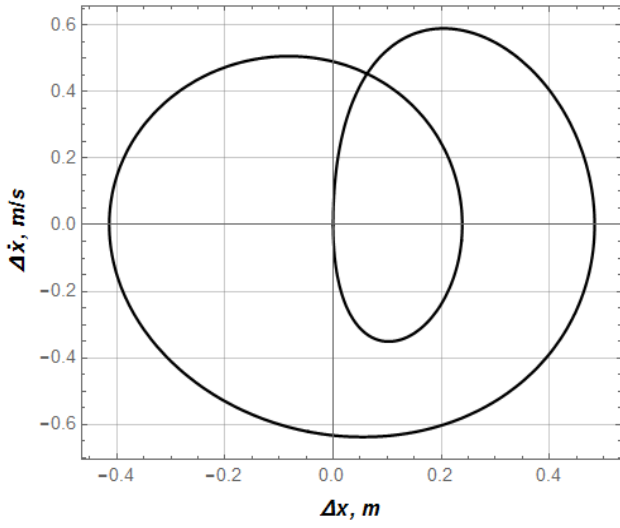


f)

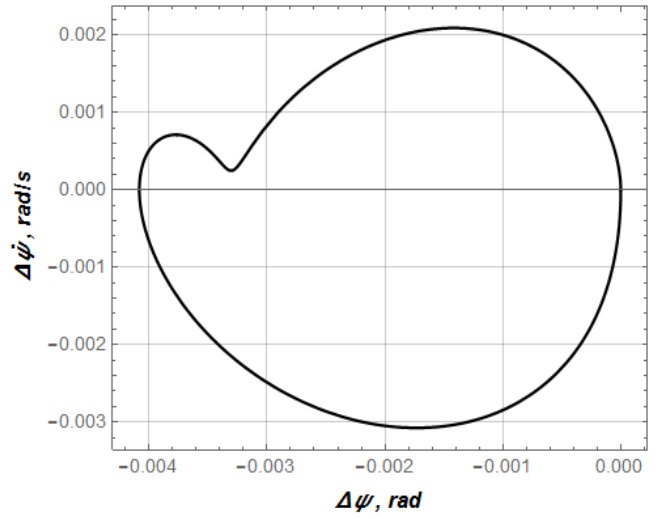


g)

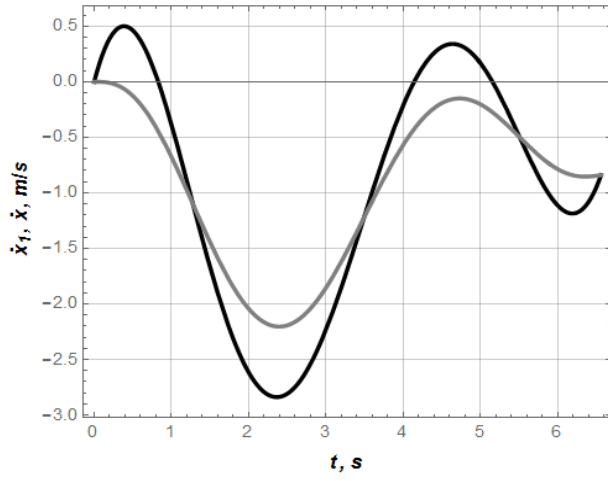
Fig. 2.13 Plots of kinematic, dynamic and energetic characteristics of luffing and slewing mechanisms for the case of trolley movement from the tower: a) the phase trajectory of the load oscillation in the radial direction; b) the phase trajectory of the load oscillation in the tangential direction; c) the speed of trolley movement (black line) and the load speed in the radial direction (gray line); d) the speed of crane slewing (black line) and the load slewing in the tangential direction (gray line); e) the dynamic component of the driving torque of the crane slewing mechanism; f) the dynamic component of the driving force of the luffing mechanism; g) the dynamic component of the drive power of the luffing mechanism, (gray dashed line), the dynamic component of the drive power of the crane slewing mechanism (gray line) and the sum of these powers (black line)



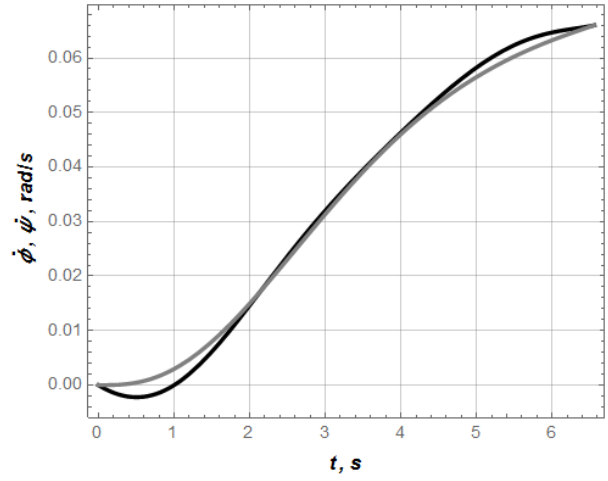
a)



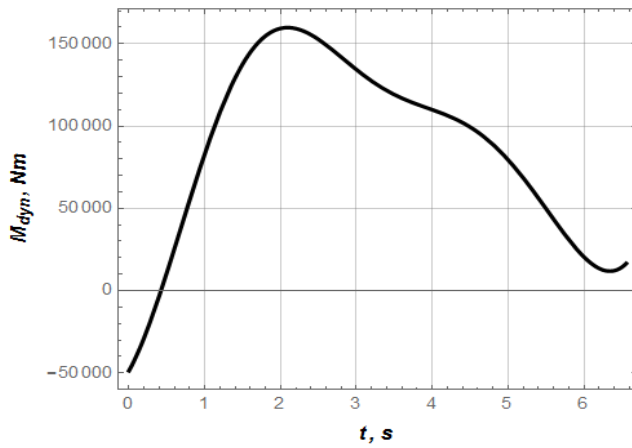
b)



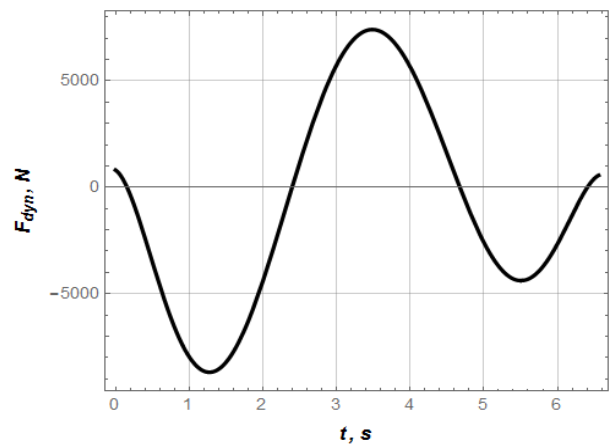
c)



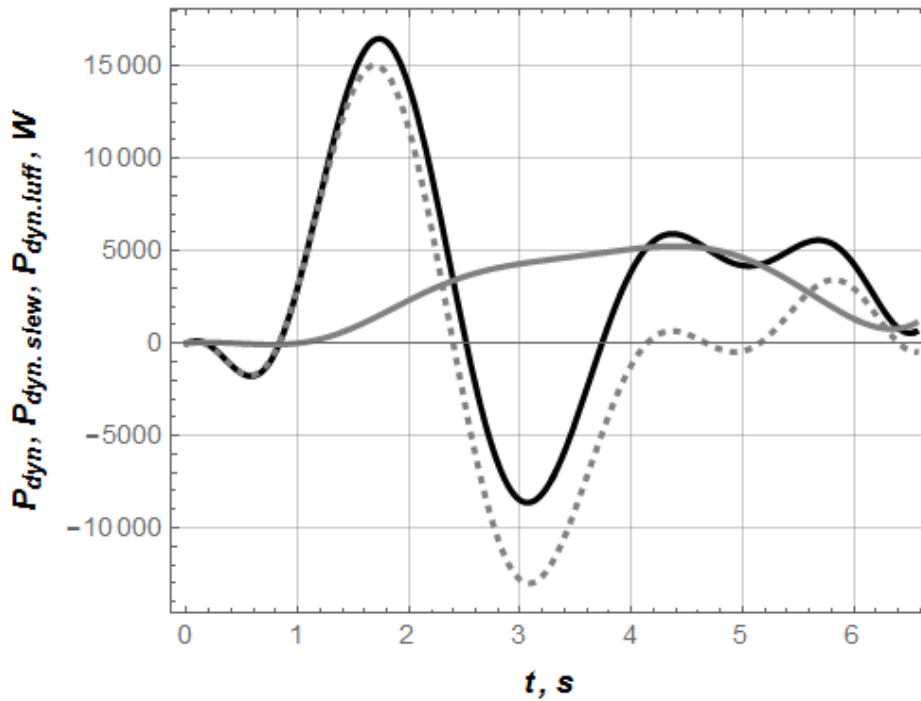
d)



e)



f)



g)

Fig. 2.14 Graphs of kinematic, dynamic and energetic characteristics of the luffing and the slewing mechanisms for the case of the trolley movement toward the tower:

- a) the phase trajectory of the load oscillation in the radial direction;
- b) the phase trajectory of the load oscillation in the tangential direction;
- c) the speed of the trolley movement (black line) and the load speed in the radial direction (gray line);
- d) the speed of the crane slewing (black line) and load slewing in the tangential direction (gray line);
- e) the dynamic component of the driving torque of the crane slewing mechanism;
- f) the dynamic component of the driving force of the luffing mechanism;
- g) the dynamic component of the drive power of luffing mechanism (gray dashed line), the dynamic component of the drive power of the crane slewing mechanism (gray line) and the sum of these powers (black line)

The analysis of the data given in Table 2.5, as well as the plots on fig. 2.13 and fig. 2.14 allows to state that the applied technique makes it possible to find the approximate solutions to the optimization problem of the simultaneous work of both mechanisms (slewing and luffing), taking into account the constraints caused by their drives.

Table 2.5 Numerical values of the optimal movement of the slewing and the luffing mechanisms

| Parameter   | Trolley movement |                  |
|---|------------------|------------------|
|   | from the tower   | toward the tower |
| The maximum torque of the slewing mechanism, Nm   | 163193           | 159790           |
| The minimum torque of the slewing mechanism, Nm   | -107844          | -47848           |
| The maximum force of the luffing mechanism, N   | 5177             | 7410             |
| The minimum force of the luffing mechanism, N   | -3917            | -8690            |
| The maximum of the total power of both mechanisms, W  | 11351            | 13633            |
| The minimum of the total power of both mechanisms, W  | -8701            | -6668            |
| The maximum deviation in positions of the trolley and the load in the radial direction, m       | 0.2941           | 0.4842           |
| The maximum deviation in positions of the trolley and the load in the tangential direction, rad | 0.0218           | 0.0041           |
| The RMS value of the driving torque of the crane slewing mechanism, Nm                          | 96529            | 102942           |
| The RMS value of the driving force of the luffing mechanism, N                                  | 3103             | 4934             |
| The RMS of the total power of both mechanisms, W  | 6643             | 6010             |
| The RMS value of the deviation in the position of the trolley and the load, m                   | 0.0128           | 0.0028           |
| The RMS value of the deviation in the position of the boom and the load, rad                    | 0.1760           | 0.2752           |

The difference in the values of the evaluation indexes (Table 2.5) is due to the action of centrifugal force acting on the trolley and the load in the radial direction. The energetic, dynamic, and kinematic parameters of the found laws of the

mechanisms motion are smooth, which confirms the possibility of their practical implementation utilizing of controlled asynchronous electric drive.

### **Conclusions to chapter 2**

1. A dynamic model and mathematical model for the movement of the crane slewing mechanism with a constant velocity of the trolley movement have been developed. The torque (force) of the drive is modeled with the Kloss equation.

2. The analysis of the modes of movement of slewing and luffing mechanisms has been carried out and it is established that the drive of the slew mechanism during the transitional mode of movement is overloaded by torque and power. The steady power of the slewing mechanism is proportional to the distance from the trolley to the axis of rotation. The maximum value of the total power of the mechanisms at different values of the trolley initial position  $x_0$  is approximately the same, although the moment of occurrence of the maximum depends on the value  $x_0$ .

3. The optimization problem of the boom crane slewing mode has been solved by minimizing the integral functional. In order to solve the, an approximate method ME-PSO has been used. This method has made it possible to optimize the motion modes of mechanical system.

4. The optimal slewing mode of the crane boom system has made it possible to minimize the dynamical forces in the drive mechanism and the metal structures of the crane and eliminate oscillations of the load on a flexible suspension during the transient process, which improves the performance in terms of reliability and efficiency of the crane.

5. The problem of the mechanism movement optimal control has been stated. It includes the criterion of energy consumption during the start-up of the mechanisms; the requirement to ensure the torque capacity of the mechanism drives; boundary conditions corresponding to the elimination of the load oscillations in the radial and tangential directions at the end of the mechanisms acceleration. A generalized

criterion was developed to ensure that the constraints are met. It includes the penalty coefficients required to ensure that the system's movement is constrained. In addition, the basis functions were selected to search for approximate solutions to the optimization problem.

6. Using the ME-PSO metaheuristic method, the parameters of the basic functions, and the duration of the transition mode were found. These parameters minimize the value of the generalized criterion. All the calculations were made for the cases of the trolley movement from the tower and toward it. There has been established the smoothness of the change of system motion characteristics. It improves the reliability of the mechanisms. In addition, eliminating of the load oscillations in radial and tangential directions allows increasing the crane productivity, reduces the hoistman's workload, and provides the possibility of automating load movement operations.

### **Reference to chapter 2**

1. Vaynson A.A. Hoisting mashines. M. Mashinostroenie, 1989, p. 536 (in Russian).
2. Gaydamaka V.F. Hoisting mashines, K.: Vishcha shkola, 1989, p. 328 (in Russian).
3. Hoisting cranes. Book 2 / Sheffler M., Dresig Kh., Kurt F.; [transl. from german by M.M. Runov, V.N. Fedoseev]; edited by. M.P. Aleksandrova. – M.: Mashinostoenie, 1981, p. 287 (in Russian).
4. Gohberg M.M. Metal structures of hoisting machines. M.: Mashinostroenie, 1969, p. 520 (in Russian).
5. Kazak S.A. Bridge cranes dynamics. M.: Mashinostroenie, 1968, p. 331 (in Russian).
6. Lobov N.A. Hoisting cranes dynamics, M.: Mashinostroenie, 1987, p.160 (in Russian).

7. Priymakov O.G., Gradis`kii Yu.O. Moathematical model of load oscolations during crane slewing. Agrarian machimery. 2013, Vol 25, pp. 111-117 (in Ukrainian).

8. Kuz`min A.N., Suglobov V.V., Fedun V.I. Study of oscillations of the load on the flexible suspension during crane slewing. Protecton of metarurgical machimes from the breakdowns: collection of scientific works. PDTU. Mariupol, 2011, Vol. 13, pp. 141-147 (in Russian).

9. Loveykin V.S., Boyko A.V., Chovnyuk Yu.V. Nonlinear pendulum oscillations of a load under different modes og slewing. Herald of TNTU., 2010, Tom 15, № 3, pp. 41-48 (in Ukrainian).

10. Bulatov Zh.L., Sinel`shhikov A.V. The state of issue of tower cranes dynamics under big movements. Herald of Astrakhansk State Technical University. 2014, #1 (57), pp. 23-29 (in Russian).

11. Hamid Nalbandian Abhar Dynamic Analysis of the Tower Crane / Dissertation submitted to the faculty of engineering, university of malaya in partial fulfillment of the requirement for the degree of master of mechanical engineering, p. 125.

12. Tower crane Liebherr 140 HC / URL: <https://cranemarket.com/specs/liebherr/140-hc> (date of access 07.02.2020)

13. Zhuoqing L., Tong Y., Ning S., Yongchun F. An Antiswing Trajectory Planning Method with State Constraints for 4-DOF Tower Cranes: Design and Experiments. IEEE Access. 2019, Vol. 7, pp. 62142-62151. DOI: 10.1109/ACCESS.2019.2915999

14. Böck M., Kugi A. Real-time Nonlinear Model Predictive Path-Following Control of a Laboratory Tower Crane. IEEE Transactions on control system technology. 2016, Vol. 22, №4, pp. 1461-1473.

15. Makarevych E.V., Shamardina V.N., Palis F., Palis S. Development of optimal control of tower crane movements. Electrotechnical and computer systems, 2011, № 3, pp. 170-171. (in Ukrainian).

16. Palis S., Palis F., Lahner M. System of damping of oscillations for rotating cranes URL: <http://masters.donntu.org/2009/eltf/zyuzin/library/translate.htm>. (date of access доступу 25.02.2020) (in Russian).

17. Devesse W., Ramteen M., Feng L., Wikander J. A real-time optimal control method for swing-free tower crane motions. 2013 IEEE International Conference on Automation Science and Engineering (CASE). Madison, WI. 2013, pp. 336-341.

18. Gerasimiak R.P., Leschev V.A. Analysis and synthesis of crane electromechanical systems. 2008. Odessa. SMIL, 192 p. (in Russian).

19. Carmona I.G., Collado J. Control of a two-wired hammerhead tower crane. *Nonlinear Dynamics*. 2016, № 84, pp. 2137-2148. DOI: 10.1007/s11071-016-2634-3

20. Galafshani A.L. Modeling and Optimal Control of Tower Crane Motions. A thesis of Doctor of Philosophy in Electrical Engineering, 1999, p. 133.

21. Hanafy M.O., Ali H.N. Gain Scheduling Feedback Control for Tower Cranes. *Journal of Vibration and Control*, 2003, № 9, pp. 399–418. DOI: 10.1177/107754603030778

22. Hanafy M.O., Ali H.N. Gain Scheduling Feedback Control of Tower Cranes with Friction Compensation *Journal of Vibration and Control*, 2004, № 10, pp. 269–289. DOI: 10.1177/1077546304035610.

23. Kostikov A.A., Perig A.V., Larichkin O.V., Stadnik A.N., Gribkov E.P. Research into Payload Swaying Reduction Through Cable Length Manipulation During Boom Crane Motion. *FME Transactions*, 2019, № 47, pp. 464-476. DOI: 10.5937/fmet1903464K.

24. Phuong D.N., Yung C.Sh. Gain estimation of nonlinear dynamic systems modeled by an FBFN and the maximum outputs scaling factor of a self-tuning PI fuzzy controller. *Engineering Applications of Artificial Intelligence*, 2015, № 42, pp. 1–15.

25. Devesse W. Slew Control Methods for Tower Cranes. Performance comparison of different methods with a focus on optimal control. Master of Science

Thesis. 2012. MMK 2012:44 MDA 432 KTH Industrial Engineering and Management Machine Design SE-100 44 STOCKHOLM.

26. Loveikin V., Romasevych Y., Kadykalo I., Liashko A. Optimization of the swinging mode of the boom crane upon a complex integral criterion. *Journal of Theoretical and Applied Mechanics*, 2019, Vol. 49, pp. 285-296 (in Ukrainian)

27. Romasevych Y., Loveikin V. A Novel Multi-Epoch Particle Swarm Optimization Technique. *Cybernetics and information technologies*, 2018, Vol. 18, No. 3, pp. 62–74.

28. Loveikin V.S., Aftandiliants E.G., Shevshuk O.G. Analysis of system of control of tower cranes mechanisms for load oscillations elimination. *Mashinobuduvania*, 2015, № 15, pp. 39-45 (in Ukrainian).

29. Loveikin V.S., Romasevych Y.A., Stechno A.V. Parametric optimization of tower crane mechanism of trolley movement with beam boom. *Synergy*, 2017, № 2, pp. 116-124 (in Russian).

30. Loveikin V.S., Romasevych Y.A., Stechno A.V. Optimization of movement of trolley modes TsP „COMPRINT”, 2017, 172 p. (in Ukrainian).

31. Grigorov O.V., Petrenko N.O. Hoisting machines: tutorial, NTU „HPI”. 2006, p. 304 (in Ukrainian).

32. Loveikin V.S., Romasevych Yu. O. Analysis and synthesis of modes of movement of mechanisms of load-lifting machines. Kiev, CP «KOMPRÍNT», 2012, p. 299 (in Ukrainian).

33. Loveikin V.S., Chovnyuk Yu.V., Mel'nichenko V.V. Analysis of the fluctuations of cargo on a flexible suspension when turning the boom of a load-lifting crane. *Hoisting and transport equipment*, 2013, 4(40), pp. 4-16 (in Ukrainian).

34. Loveikin V.S., Pylypaka S.F., Kadykalo I.O. Dynamic analysis of the mechanism of rotation of the jib crane. *Scientific Herald of National University of Life and Environmental Science of Ukraine. Series: Technique and energy of APK*, Kiev, 2017, Vol. 258, pp. 192-202 (in Ukrainian).

35. Loveikin V.S., Romasevych Yu.O. Dynamics and optimization of modes of movement of bridge cranes, Kiev, CP «KOMPRÍNT», 2016, p. 314. (in Ukrainian).

36. Loveykin V.S., Romasevich Yu.O. Dynamic analysis of the acceleration of the trolley on the natural mechanical characterization. Scientific Herald of National University of Life and Enviromental Science of Ukraine. Series: Technique and energy of APK, Kiev, 2011, Vol. 166 (1), pp. 46–49 (in Ukrainian).

37. Shengchun Wang, Rongsheng Shen, Tonghong Jin, Shijun Song. Dynamic behavior analysis and its application in tower crane structure damage identification. Advanced Materials Research. Trans tech publications, Switzerland, 2012, Vols 368-373, pp. 2478-2482.

38. Loveykin V.S., Romasevich Yu.O. Dynamics of machines. «KOMPRINT». 2013, p. 227 (in Ukrainian).

39. Rong Gao, Jing Yang, Gang Luo, Congxun Yan. The Simulation of rotary motion of the flexible multi-body dynamics of tower crane. Advanced Materials Research. Trans tech publications, Switzerland, 2013, Vols 655-567, pp. 281-286.

40. Gerasimyak R.P., Naydenko O.V. Features of the electric drive control of the boom mechanism during the rotation of the crane with suspended load. Electrical machinery and electrical equipment, 2007, 68, pp. 11–15 (in Ukrainian).

41. Loveikin V.S., Romasevych Yu.O. Optimization of the transition modes of the mechanical systems of the direct variation method, Kiev, Nizhyn, Publisher of P.P. Lysenko M.M, 2010, p. 184 (in Ukrainian).

42. Loveikin V.S., Romasevych Yu.O. Optimization of regimes of crane mechanisms, Kiev, Nizhyn, Publisher of PP Lysenko M.M., 2011, p. 307 (in Ukrainian).

43. Romasevych Yu.A., Shumilov G.V. Optimization behavior of variation boom of hoisting crane for singular kinematical criterions, Motrol, 2011, Vol. 13b, pp. 167-173 (in Ukrainian).

44. Loveikin V.S., Mel'nichenko V.A. Optimization of the dynamic rotation mode of the boom, Motrol, 2013, Vol. 15 (3), pp. 70-75 (in Ukrainian).

45. Loveykin V.S., Romasevich Yu.O. Analysis and synthesis of optimal control movement lifting crane direct variational method. Scientific Herald of National University of Life and Environmental Science of Ukraine. Series: Technique and energy of APK, Kiev, 2014, Vol. 196 (1), pp. 129–139 (in Ukrainian)

46. Loveykin V.S., Chovniuk YU.V., Liashko A.P. The crane's vibrating systems controlled by mechatronic devices with magnetorheological fluid: the nonlinear mathematical model of behavior and optimization of work regimes. Scientific bulletin of National Mining University Scientific and technical journal, Dnipro, 2014, Vol. 6, pp. 97-102.

47. Loveykin V.S., Palamarchuk D.A. Optimization of motion hinge-articulated jib crane system, TsP «KOMPRINT», 2015, p. 224 (in Ukrainian).

48. Loveykin V.S., Chovnyuk Yu.V., Kadykalo I.O. Optimization of modes of movement of rotating mechanism of cranes. Scientific Herald of National University of Life and Environmental Science of Ukraine. Series: Technique and energy of APK, Kiev, 2017, Vol. 262, pp. 177-190 (in Ukrainian).

49. Loveykin V.S., Loveykin Yu.V., Kadykalo I.O. Optimization of mode of movement of rotation mechanism of illicit small tap on criterion of RMS value of rate of change of elastic torque in drive. Scientific Herald of National University of Life and Environmental Science of Ukraine. Series: Technique and energy of APK, Kiev, 2017, Vol. 275, pp. 10-22 (in Ukrainian).

50. Loveykin V.S., Romasevych Yu.O. Dynamic optimization of a mine winder acceleration mode. Scientific bulletin of National Mining University Scientific and technical journal, Dnipro, 2017, Vol. 4, pp. 55-61.

51. Loveykin V.S., Loveykin Ju.V., Kadykalo I.O. Analysis of Modes of Motion of Rotation Mechanism of Jib Crane. TEKA. An International Quarterly Journal on Motorization, Vehicle Operation, Energy Efficiency and Mechanical Engineering, Lublin-Rzeszow, 2018, Vol. 18, No 1, pp. 15-25 (in Ukrainian).

52. Gulianitsky L.F., Mulessa O.Yu. Applied methods of combinatorial optimization: teach. manual Kiev, Publishing and printing center "Kyiv University", 2016, p. 142.

53. Vasilenko D.O. Modern methods of analysis, synthesis and optimization of ultra high frequency devices and antennas, Kiev, NTUU "KPI", PTF 61, 2015.
54. Bozorg-Haddad O., Solgi M., Loáiciga H.A. Meta-Heuristic and Evolutionary Algorithms for Engineering Optimization. Hoboken, USA, John Wiley & Sons Inc, 2017.
55. Kennedy J., Eberhart R. Particle swarm optimization. IEEE International Conference on Neural Networks, 1995, pp. 1942-1948.
56. Dubrovka F.F., Vasilenko D.O. Constructive synthesis of planar antennas using natural optimization algorithms. Izvestiya high schools, Radio electronics, 2009, No, 4, pp. 3-22.
57. Kiranyaz S., Ince T., Yildirim A., Gabbouj M. Evolutionary Artificial Neural Networks by Multi-Dimensional Particle Swarm Optimization, Neural Networks, 2009, Vol. 22, Issue 10, pp. 1448-1462.
58. Heo J.S., Lee K.Y., Garduno-Ramirez R. Multiobjective Control of Power Plants Using Particle Swarm Optimization Techniques. IEEE Transactions on Energy Conversion, 2006, Vol. 21, Issue 10, pp. 552-561.
59. Zamani M., Karimi-Ghartemani M., Sadati N., Parniani M. Design of a Fractional Order PID Controller for an AVR Using Particle Swarm Optimization. Control Engineering Practice, 2009, Vol. 17, Issue 12, pp. 1380-1387.
60. Chander A., Chatterjee A., Siarry P. A New Social and Momentum Component Adaptive PSO Algorithm for Image Segmentation. Expert Systems with Applications, 2011, Vol. 38, Issue 5, pp. 4998-5004.
61. Loveikin V.S., Romasevich Y.A., Khoroshun A.S., Shevchuk A.G. Time-Optimal Control of a Simple Pendulum with a Movable Pivot, Part 1, International Applied Mechanics, 2018, 54(3), pp. 358-365.

## **CHAPTER 3. MANAGEMENT AND OPTIMAL CONTROL OF OVERHEAD CRANES**

### **3.1 Optimization of bridge crane movement control**

Bridge cranes are used in many processing of modern industries. The performance of the bridge cranes influences the efficiency of the technological processes. In order to state the ways to increase crane efficiency the study of dynamical and energetic processes, that take place in the crane mechanisms, should be carried out.

In the early scientific researches of bridge cranes dynamics, the simple models of the systems and external forces were used [1-4]. The two- and three-mass models have been used. The driving force was assumed a constant value. The results of these works allowed to calculate dynamical loads with analytical expressions at the first approximation. In works [5-8] assumed that driving force is a function of time or speed of the crane drive.

The new approaches to dynamic loads calculation comprise the dynamic mechanical characteristic of the system's drive [5, 9], non-linear effects [10-15], etc.

The problems of rationalization of the bridge crane movement were studied in the works [16, 17]. Another approach to increasing bridge crane efficiency is to obtain the optimal law of its movement. One of the major conditions that have been studied in many works is the elimination of load oscillations. The major factor in such an approach is the optimization criterion. The minimization of transition regimes duration [18-25] is connected with increasing the overall level of dynamical loads. Dynamical processes in the crane depend on the external forces and system parameters [26, 27]. That is why solutions of optimal problems should be found in domains of movement modes and system parameters.

Despite rigorous researches in the area of the crane dynamics and optimal control, the unsolved scientific problems are still remain: 1) optimization of the bridge crane regimes has done only in relation to one criterion (time, energy, force, etc.). This problem statement is limited; 2) the implementation of the optimal laws of crane motion with frequency-controlled drive have not been studied properly; 3) the capability of using particular techniques in optimizations problems have studied improperly; 4) the analysis of the solved optimal problem carried out upon not all important indications and so on.

For this reason, the goal of the current research is to obtain optimal mode of movement of the bridge crane and its dynamical parameters which allow increasing the efficiency of the crane exploitation upon indications: productivity, reliability, energy efficiency, etc.

In order to achieve the goal the following tasks should be solved: 1) to state the optimization regimes problem for the bridge crane; 2) to find the solution of the stated problem; 3) to carry out a comparative study of the obtained results and to estimate the effect of optimization. In order to provide research, we choose a dynamic model of bridge crane and scheme of its asynchronous drive (fig. 3.1) [9, 17].

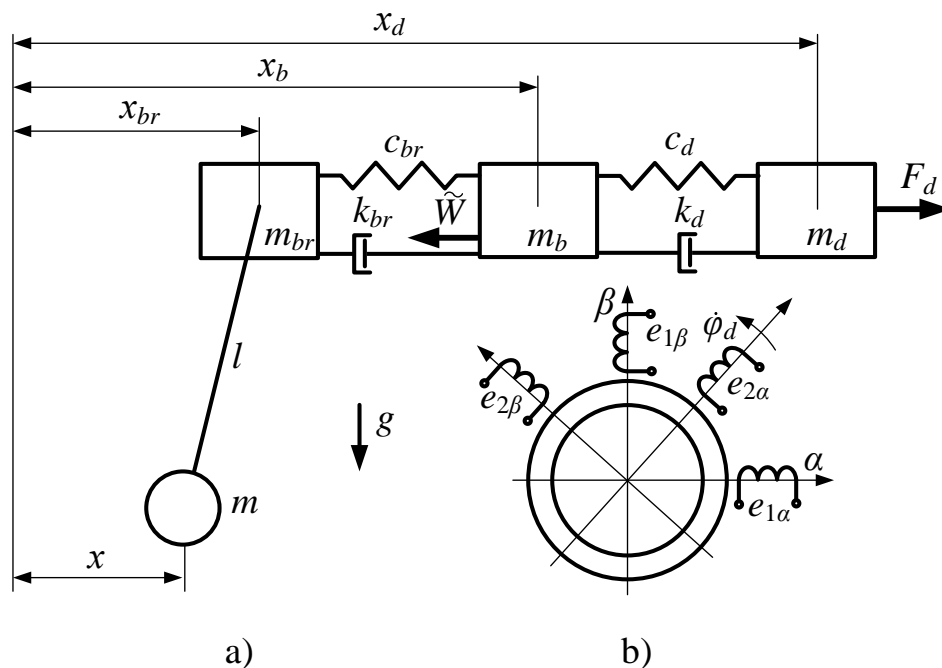


Fig. 3.1 Four-mass dynamic model of the bridge crane (a) and scheme of the bridge crane asynchronous drive (b)

Mathematical model of the crane is a system of the second order non-linear homogeneous differential equations:

$$\left\{ \begin{array}{l} \frac{di_{1\alpha}}{dt} = \frac{1}{\delta L_1} (u_{1\alpha} - i_{1\alpha} R_1 + k_r e_{2\alpha}); \\ \frac{di_{1\beta}}{dt} = \frac{1}{\delta L_1} (u_{1\beta} - i_{1\beta} R_1 - k_r e_{2\beta}); \\ \frac{di_{2\alpha}}{dt} = -\frac{1}{\delta L_2} ((u_{1\alpha} - i_{1\alpha} R_1) k_s + e_{2\alpha}); \\ \frac{di_{2\beta}}{dt} = -\frac{1}{\delta L_2} ((u_{1\beta} - i_{1\beta} R_1) k_s - e_{2\beta}); \\ 3pL_{12} (i_{1\beta} i_{2\alpha} - i_{1\alpha} i_{2\beta}) \frac{u \eta_{dr}}{r_w} = m_d \frac{d^2 x_d}{dt^2} + c_d (x_d - x_b) + k_d \left( \frac{dx_d}{dt} - \frac{dx_b}{dt} \right); \\ m_b \frac{d^2 x_b}{dt^2} = c_d (x_d - x_b) + k_d \left( \frac{dx_d}{dt} - \frac{dx_b}{dt} \right) - c_b (x_b - x_{br}) - k_b \left( \frac{dx_b}{dt} - \frac{dx_{br}}{dt} \right) - \tilde{W}; \\ m_{br} \frac{d^2 x_{br}}{dt^2} = c_b (x_b - x_{br}) + k_b \left( \frac{dx_b}{dt} - \frac{dx_{br}}{dt} \right) - \frac{mg}{l} (x_{br} - x); \\ \frac{d^2 x}{dt^2} = \frac{g}{l} (x_{br} - x), \end{array} \right. \quad (3.1)$$

where  $\tilde{W}$  – variable resistance of the bridge crane movement;  $l$  – length of flexible suspension of the load;  $g$  – acceleration of gravity;  $x, x_b, x_{br}, x_d$  – generalized coordinates of the load, end beams, crane bridge and drive respectively;  $m, m_b, m_{br}, m_d$  – reduced masses of the load, end beams, crane bridge and drive respectively;  $c_{br}, c_d$  – reduced coefficients of stiffness of the crane bridge and the drive transmission respectively;  $k_{br}, k_d$  – reduced dissipation factor of the crane bridge and transmission respectively;  $F_d$  – drive force which is reduced to the linear movement (it depends on electromagnetic torque of the crane drive);  $u_{1\alpha}, u_{1\beta}$  – projections of generalized vector

voltage stator to the coordinate axes  $\alpha$  and  $\beta$  ( $u_{1\alpha} = U_{\max} \cos(2\pi \int_0^t f dt)$ ,

$u_{1\beta} = U_{\max} \sin(2\pi \int_0^t f dt)$ );  $U_{\max}$  – phase voltage amplitude of the drive;  $f$  – frequency

of drive voltage;  $e_{2\beta}, e_{2\alpha}$  – EMF, which are being induced by flux linkage of rotor to axes  $\alpha$  and  $\beta$  respectively; ( $e_{2\alpha} = p\omega_{dr}(L_2 i_{2\beta} + L_{12} i_{1\beta}) + i_{2\alpha} R_2$ ),

$e_{2\beta} = p\omega_{dr}(L_2 i_{2\alpha} + L_{12} i_{1\alpha}) + i_{2\beta} R_2$ );  $p$  – number of crane electric drive pairs of poles;  $R_1$  – active resistance of the stator winding;  $R_2$  – reduced to the stator active resistance of the rotor winding;  $\delta$  – dispersion coefficient ( $\delta = 1 - (1 + X_1(2\pi f L_{12})^{-1})(1 + X_2(2\pi f L_{12})^{-1})^{-1}$ );  $X_1$  – inductive reactance of the stator winding;  $X_2$  – reduced to the stator inductive reactance of the rotor winding;  $L_1, L_2$  – inductance of stator and rotor windings respectively;  $L_{12}$  – coefficient of mutual induction;  $k_r$  and  $k_s$  – magnetic coupling ratio of rotor and stator respectively ( $k_r = L_{12} L_2^{-1}$ ;  $k_s = L_{12} L_1^{-1}$ );  $\omega_{dr}$  – angular speed of the drive;  $i_{1\alpha}, i_{1\beta}$  and  $i_{2\alpha}, i_{2\beta}$  – projections of generalized vector of current of stator and rotor to the coordinates axes  $\alpha$  and  $\beta$ ;  $u$  – gear ratio of the drive;  $\eta_{dr}$  – efficiency of transmission;  $r_w$  – radius of a wheel of the crane movement mechanism. The variable resistance of the bridge crane movement  $\tilde{W}$  determined as follows:

$$\tilde{W} = \begin{cases} c_d x_d + k_d \frac{dx_d}{dt}, & \text{if } c_d x_d + k_d \frac{dx_d}{dt} < (0,012\dots 0,02)(m_b + m_{br} + m)g; \\ (0,012\dots 0,02)(m_b + m_{br} + m)g, & \text{if } c_d x_d + k_d \frac{dx_d}{dt} \geq (0,012\dots 0,02)(m_b + m_{br} + m)g. \end{cases} \quad (3.2)$$

The chosen mathematical model includes mechanical and electrical values. Thus, in the research, we have taken into account complicate electrical-mechanical processes and their interinfluence.

One of the ways to increase a crane operation efficiency is to optimize its transition modes of motion and its parameters. In the framework of the study, a complex (terminal-integral) criterion has been chosen. It may be presented as follows:

$$Cr = Ter + Int = \left( \delta_1^{Ter} F_d^2(0) + \delta_2^{Ter} F_d^2(T) \right)^{0,5} + \left( T^{-1} \int_0^T (\delta_1^{Int} F_d^2 + \delta_2^{Int} R_d^2 + \delta_3^{Int} R_{br}^2 + \delta_4^{Int} \Omega_0^4 m^2 \Delta x^2) dt \right)^{0,5} \rightarrow \min, \quad (3.3)$$

where  $Ter$  and  $Int$  – terminal and integral parts of the complex criterion  $Cr$  respectively;  $T$  – duration of the transition process (acceleration or deceleration of the crane);  $R_{br}$  and  $R_d$  – dynamical loads in the crane bridge and drive (transmission) respectively;  $\Delta x$  – deviation of the load from the vertical, which determines low-

frequency dynamic loads in the crane bridge;  $\Omega_0$  – free frequency of the load on the flexible suspension ( $\Omega_0 = \sqrt{\frac{g}{l}}$ );  $\delta_1^{Ter}$  and  $\delta_2^{Ter}$  – weight coefficients for terminal part of  $Cr$ ;  $\delta_1^{Int}$ ,  $\delta_2^{Int}$ ,  $\delta_3^{Int}$  and  $\delta_4^{Int}$  – weight coefficients of the integral part of  $Cr$ . Weight coefficients for both parts of criterion (3.3) are dimensionless, their sum is equal to one. The values of weight coefficients correspond to the importance of respective factors, i.e. how important to decrease one or the other factors.

Minimization of criterion  $Cr$  (3.3) allows increasing the life duration of the crane elements (bridge, couplings, gears, shafts, etc.), crane's productivity, and energy efficiency.

Without consideration of electromagnetic transition processes in the crane drive and dissipation of energy in mechanical elements the criterion  $Cr$  (3.3) may be presented in the following form:

$$\begin{aligned}
 Cr = & \left( \delta_1^{Ter} \left( \tilde{W}(0) + \sum_{u=1}^4 A_u \frac{d^{2u} x}{dt^{2u}}(0) \right)^2 + \delta_2^{Ter} \left( \tilde{W}(T) + \sum_{h=1}^4 A_h \frac{d^{2h} x}{dt^{2h}}(T) \right)^2 \right)^{0,5} = \\
 = & \left( T^{-1} \int_0^T \left( \delta_1^{Int} \left( \tilde{W} + \sum_{i=1}^4 A_i \frac{d^{2i} x}{dt^{2i}} \right)^2 + \delta_2^{Int} \left( \tilde{W} + \sum_{j=1}^3 B_j \frac{d^{2j} x}{dt^{2j}} \right) + \delta_3^{Int} \left( \sum_{q=1}^2 C_q \frac{d^{2q} x}{dt^{2q}} \right)^2 + \right. \right. \\
 & \left. \left. + \delta_4^{Int} m^2 \left( \frac{d^2 x}{dt^2} \right)^2 \right) dt \right)^{0,5} \rightarrow \min, \tag{3.4}
 \end{aligned}$$

where  $A_i$ ,  $B_j$  and  $C_q$  – coefficients, which is determined by the following expressions:

$$A_1 = m + m_{br} + m_b + m_d ;$$

$$A_2 = \frac{(m_{br} + m)(m_d + m_b)}{c_{br}} + \frac{m_d(m_{br} + m + m_b)}{c_d} + (m_{br} + m_b + m_d)\Omega_0^{-2} ;$$

$$A_3 = \frac{(m_{br} + m)m_d m_b}{c_d c_{br}} + \left( \frac{m_d(m_{br} + m_b)}{c_d} + \frac{m_{br}(m_d + m_b)}{c_{br}} \right) \Omega_0^{-2} ;$$

$$A_4 = \frac{m_{br} m_d m_b}{c_d c_{br}} \Omega_0^{-2} ;$$

$$B_1 = m + m_{br} + m_b;$$

$$B_2 = (m_{br} + m_b)\Omega_0^{-2} + \frac{m_b}{c_{br}}(m_{br} + m);$$

$$B_3 = \frac{m_b m_{br}}{c_{br}} \Omega_0^{-2};$$

$$C_1 = m + m_{br};$$

$$C_2 = m_{br} \Omega_0^{-2}.$$

The boundary conditions for the reduced masses are as follows:

$$\left\{ \begin{array}{l} x(0) = \frac{dx}{dt}(0) = 0; \\ x_{br}(0) = \frac{dx_{br}}{dt}(0) = 0; \\ x_b(0) = \frac{dx_b}{dt}(0) = 0; \\ x_d(0) = \frac{dx_d}{dt}(0) = 0 \\ \\ x(T) = s; \quad \frac{dx}{dt}(T) = v; \\ x(T) - x_{br}(T) = x_{br}(T) - x_b(T) = x_b(T) - x_d(T) = 0; \\ \frac{dx}{dt}(T) - \frac{dx_{br}}{dt}(T) = \frac{dx_{br}}{dt}(T) - \frac{dx_b}{dt}(T) = \frac{dx_b}{dt}(T) - \frac{dx_d}{dt}(T) = 0, \end{array} \right. \quad (3.5)$$

Boundary conditions (3.9) may be rewritten in the following form:

$$\left\{ \begin{array}{l} \frac{d^i x}{dt^i}(0) = 0, \quad i = \overline{(0, 7)}; \\ x(T) = s, \quad \frac{dx}{dt}(T) = v, \quad \frac{d^j x}{dt^j}(T) = 0, \quad j = \overline{(2, 7)}. \end{array} \right. \quad (3.6)$$

Note, that adding to boundary conditions (3.6) extra conditions:

$$\left\{ \begin{array}{l} \frac{d^8 x}{dt^8}(0) = 0; \\ \frac{d^8 x}{dt^8}(T) = 0 \end{array} \right. \quad (3.7)$$

provides reaching the global minimum of the terminal criteria  $Ter$  (3.3).

The study of the integral criterion  $Int$  with Legendre condition [30] shows that it may be minimized. Indeed, the aggravated Legendre condition is met:

$$\frac{\partial^2 I}{\partial \left( \frac{d^8 x}{dt^8} \right)^2} = 2\delta_1^{Int} A_4^2 > 0, \quad (3.8)$$

where  $I$  – integrand of the functional  $Int$ .

The first part of the expression (3.3) does not cause a significant effect. So, during optimal control problem solving, let us assume  $\tilde{W}$  is constant and equal to  $0,015(m_b+m_{br}+m)g$ . This assumption greatly simplifies the solving of the problem.

Let us try to use the variation calculus [28] to find the solution of the problem. For this purpose, we should obtain the extremum necessary of the  $Cr$  criterion – the Euler-Poisson equation. It may be presented as follows:

$$L(x) = \sum_{z=0}^n (-1)^z \frac{d^z}{dt^z} \frac{\partial I}{\partial x} = 0, \quad (3.9)$$

where  $L$  – the linear operator, which forms the Euler-Poisson equation. The expanded form of the expression (3.23) has the following form:

$$L(x) = \sum_{z=2}^8 D_z \frac{d^{2z} x}{dt^{2z}} = 0, \quad (3.10)$$

where  $D_z$  – coefficients, which depend on known coefficients  $A_i$ ,  $B_j$  and  $C_q$ . In order to solve the differential equation (3.10) we should consider a characteristic equation:

$$\sum_{z=2}^8 D_z r^{2z} = 0. \quad (3.11)$$

Taking out a factor  $r^4$  and substituting  $r^2$  to  $y$  we obtain next equation:

$$y^2 \sum_{z=0}^6 D_{z+2} y^z = 0. \quad (3.12)$$

It is impossible to find the solution of the sixth-degree algebraic equation. So, find the solution of the optimal control problem is impossible. It may be shown, that the analytical solution is impossible to find with Pontryagin's maximum principle or dynamic programming method neither.

Hence, we should use an approximate approach. In order to find the approximate solution of the problem let use the direct variation method [29]. The proposed for that purpose basis function is a polynomial of the  $n$ -th order:

$$\tilde{\alpha} = \sum_{b=0}^{17} G_b t^b + \sum_{e=18}^n G_e t^e, \quad (3.13)$$

where  $G_e$  – unknown coefficients;  $n$  – the highest degree of extra members of the polynomial (they should be used in order to minimize integral criterion  $Int$ ). The unknown coefficients  $G_b$  must be found in such a way that function  $\tilde{\alpha}$  met boundary conditions:

$$\begin{cases} \frac{d^i \tilde{\alpha}}{dt^i}(0) = 0, \quad i = \overline{(0, 8)}; \\ \tilde{\alpha}(T) = s, \quad \frac{d\tilde{\alpha}}{dt}(T) = v, \quad \frac{d^j \tilde{\alpha}}{dt^j}(T) = 0, \quad j = \overline{(2, 8)}. \end{cases} \quad (3.14)$$

Thus, the polynomial expression  $\tilde{\alpha}$  is the function of  $n-18$  unknown coefficients  $G_e$ . The next step – is finding the expression:

$$\begin{aligned} & \left( T^{-1} \int_0^T \left( \delta_1^{Int} \left( \tilde{W} + \sum_{i=1}^4 A_i \frac{d^{2i} \tilde{\alpha}}{dt^{2i}} \right)^2 + \delta_2^{Int} \left( \tilde{W} + \sum_{j=1}^3 B_j \frac{d^{2j} \tilde{\alpha}}{dt^{2j}} \right) + \delta_3^{Int} \left( \sum_{q=1}^2 C_q \frac{d^{2q} \tilde{\alpha}}{dt^{2q}} \right)^2 + \right. \right. \\ & \left. \left. + \delta_4^{Int} m^2 \left( \frac{d^2 \tilde{\alpha}}{dt^2} \right)^2 \right) dt \right)^{0,5} = f(G_e, A_i, B_j, C_q, s, T). \end{aligned} \quad (3.15)$$

Note, the system parameters  $m_d, m_b, m_{br}, m$  are unchangeable (based on the meeting of the crane design conditions). Parameters  $T, v$  may be changed, but they defined by technological conditions of the crane processing. Accept that they are unchangeable. Parameters  $c_{br}, l$  are changeable, but only in limited domains. We

might obtain the values of  $c_{br}$ ,  $l$ , in their limited domains in such a manner, that expression (3.15) attains the minimum. The same is true for the mode parameter  $s$ .

In order to minimize the expression (3.15) the stated optimal control problem has been reduced to the linear programming problem [30]:

$$\begin{aligned} f(G_e, c_d, l, s) &\rightarrow \min; \\ c_{d.\min} &\leq c_d \leq c_{d.\max}; \\ l_{\min} &\leq l \leq l_{\max}, \end{aligned} \tag{3.16}$$

where  $c_{d.\min}$  and  $c_{d.\max}$  – lower and higher boundaries of parameter  $c_d$  domain respectively;  $l_{\min}$  and  $l_{\max}$  – lower and higher boundaries of parameter  $l$  domain respectively. In the context of the used approach  $n$  has been chosen equal to 5. It is the rational value – the compromise between a computational compilation and an accuracy of the problem solution. The stated linear programming problem has been solved with differential evolution method [31] for parameters' values presented in Table 3.1.

Table 3.1. Values of system parameters, which have been used in calculations

| Parameter    | Unit of measurement | Value                      |
|--------------|---------------------|----------------------------|
| $m_d$        | kg                  | $3.50 \cdot 10^3$          |
| $m_b$        |                     | $2.05 \cdot 10^4$          |
| $m_{br}$     |                     | $2.60 \cdot 10^4$          |
| $m$          |                     | $2.00 \cdot 10^4$          |
| $T$          | s                   | $4.00 \cdot 10^0$          |
| $P_{d.nom}$  | W                   | $2 \times 1.50 \cdot 10^4$ |
| $l_{\min}$   | m                   | $1.50 \cdot 10^0$          |
| $l_{\min}$   |                     | $8.00 \cdot 10^0$          |
| $v$          | m/s                 | $2.10 \cdot 10^0$          |
| $c_{br}$     | N/m                 | $6.90 \cdot 10^6$          |
| $c_{d.\min}$ |                     | $4.80 \cdot 10^6$          |
| $c_{d.\max}$ |                     | $1.92 \cdot 10^7$          |

The optimal value parameter  $c_d$  is the domain boundary  $c_{d.min}$ . The best values for parameters  $l$  and  $s$  are 2,15 m and 4,2 m respectively.

In order to show the advantages of obtained suboptimal mode of the bridge crane movement, the comparative analysis has been carried out. The suboptimal mode of the crane movement was comparing with the S-curved law of the crane motion. It is a standard curve in the variable-frequency crane drive [32].

The comparison was carried out with indicators: maximum of load's deviation angle  $\varphi_{max}$  during crane movement; maximum of load's deviation angle  $\varphi_{max.T}$  after crane stop; maximum of the force in the crane bridge  $R_{br.max}$ ; maximum of the force in the crane transmission  $R_{d.max}$ ; maximum of the crane driving torque  $M_{d.max}$ ; root-mean-square force in the crane bridge  $R_{br.RMS}$ ; root-mean-square force in the crane transmission  $R_{d.RMS}$ ; root-mean-square of the crane drive torque  $M_{d.RMS}$ ; relative maximum of the crane drive power  $\tilde{P}_{max}$  (in fractions of nominal value); relative maximum of the crane drive current  $\tilde{I}_{max}$  (in fractions of nominal value).

The indicators that been calculated for all cycles of motion „acceleration-steady movement-deceleration” are presented in Table 3.2.

Table 3.2. Values of indicators

| Indicators        | Unit of measurement | Regime of motion  |                      | Reduction |
|-------------------|---------------------|-------------------|----------------------|-----------|
|                   |                     | S-curved          | Suboptimal           |           |
| 1                 | 2                   | 3                 | 4                    | 5         |
| $\varphi_{max}$   | grad                | $1.10 \cdot 10^1$ | $7.56 \cdot 10^0$    | 45.5%     |
| $\varphi_{max.T}$ |                     | $1.10 \cdot 10^1$ | $2.50 \cdot 10^{-1}$ | 44 times  |
| $R_{br.max}$      | N                   | $4.67 \cdot 10^4$ | $4.88 \cdot 10^4$    | -4.3%     |
| $R_{d.max}$       |                     | $1.49 \cdot 10^3$ | $1.75 \cdot 10^3$    | -14.8%    |
| $R_{br.RMS}$      |                     | $1.25 \cdot 10^4$ | $1.06 \cdot 10^4$    | 17.9%     |
| $R_{d.RMS}$       |                     | $3.53 \cdot 10^2$ | $3.36 \cdot 10^2$    | 5.1%      |
| $M_{d.max}$       | N m                 | $9.77 \cdot 10^2$ | $9.98 \cdot 10^2$    | -2.1%     |
| $M_{d.RMS}$       |                     | $2.24 \cdot 10^2$ | $2.16 \cdot 10^2$    | 3.7%      |

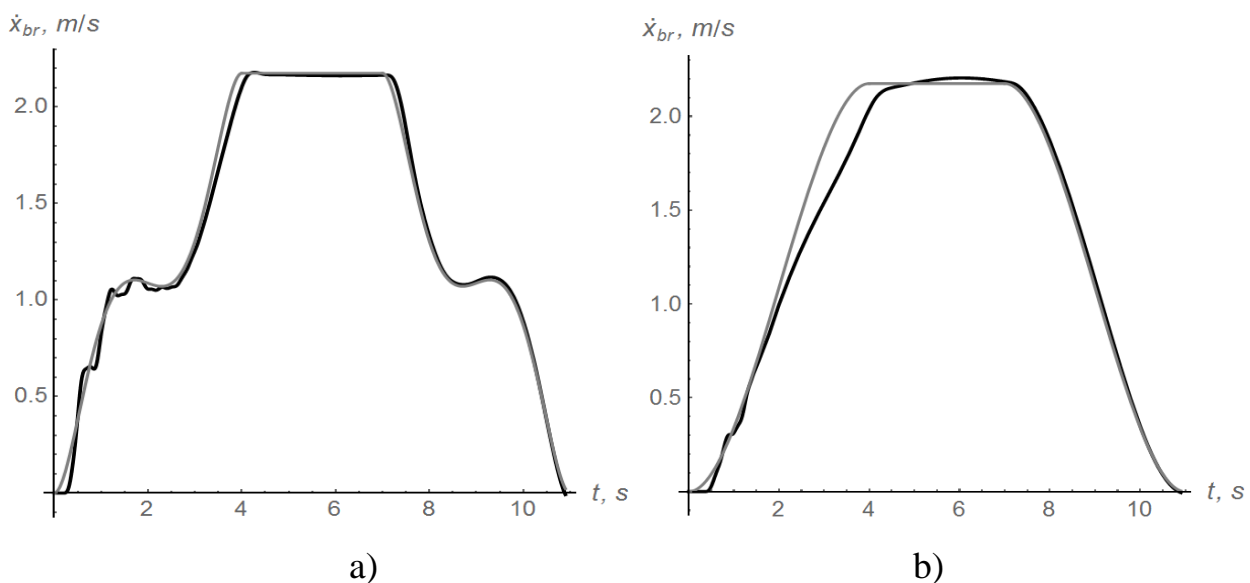
Table 3.2 continuation

| 1                  | 2 | 3                 | 4                 | 5     |
|--------------------|---|-------------------|-------------------|-------|
| $\tilde{P}_{\max}$ | - | $3.70 \cdot 10^0$ | $3.52 \cdot 10^0$ | 5.1%  |
| $\tilde{I}_{\max}$ | - | $4.47 \cdot 10^0$ | $3.91 \cdot 10^0$ | 14.3% |

The duration of the steady movement of the crane is equal to 3 s. Analysis of the data placed in Table 3.2 shows that suboptimal control of the crane movement reduced root-mean-square forces and torques, but the maximums of the dynamical loads are slightly increased. The reason why root-mean-square forces and torques have decreased is the oscillations of load on flexible suspension became much lesser and dynamical loads, which are caused by oscillations, have decreased.

The residual oscillation (after crane stop) of the load during suboptimal control practically is absent. It allows increasing crane productivity. Also, the intensity of the crane operator's work is much lesser. In order to show the quality of implementation the plots have been built (fig. 3.2).

The black plots on fig. 3.2 (a and b) present the speed of the crane; the gray ones refer to the set speed. Analysis of the plots shows that frequency-controlled crane drive able to implement the suboptimal law at high quality. Plots, which are presented in fig. 3.2, show, that the determining factor of the crane working process is the shape of the acceleration and deceleration functions [33].



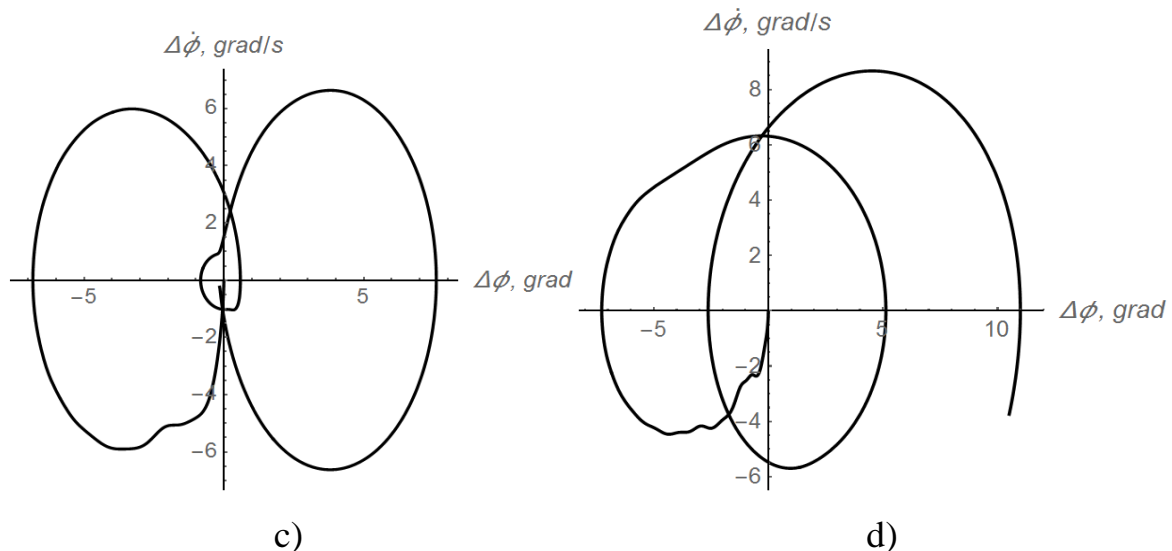


Fig. 3.2 Plots of the crane speed during suboptimal (a) and S-curved (b) control; phase trajectory of the load oscillations during suboptimal (c) and S-curved (d) control

### 3.2 Management and closed-loop optimal control of the system „crane-load” (minimum time control)

The problem of optimal control of the system „crane-load” is very important both for practical and theoretical purposes. The case when the criterion is the duration of a system’s movement is called the time-optimal control problem. The solution of the problem allows for advancing the control systems of overhead, bridge and tower cranes [16, 25, 33, 34].

A wide range of methods was used for solving the time-optimal control problem: principle maximum [16, 25, 33], variational calculus and dynamical programming [25], controllability function method [35] and others. In the theoretical context, the time-optimal control problem investigations lead to the improvement of optimization methods and their applications.

In the article [34] the non-symmetrical constraints have been used. It allowed to obtain the soft-control mode of the system motion. The same constraints will be used in the following research. In addition to that, the problem solution has to be found in the closed-loop form [25]. On the practical sense, it provides a significant

advantage: closed-loop control eliminates all the impacts of *a priori* unknown external disturbances. A combination of these two characteristics in the problem statement makes it difficult to solve.

The used in the study approaches may be applied to other optimal control problems, the theory of stability [37], synthesis of optimal automatics systems [38], etc.

The system „crane-load” is presented on fig. 3.3. Such a dynamic model is widely known in problems of optimal control of overhead, bridge [14, 26, 34, 35] and tower [16] cranes.

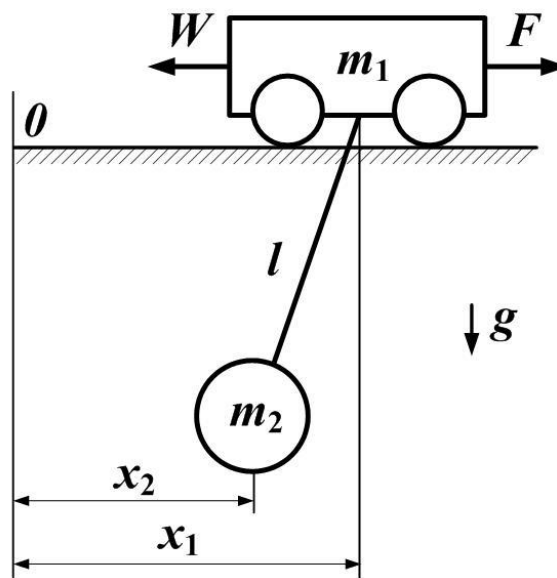


Fig. 3.3 The dynamic model of the system „crane-load”

The equations of the system’s motion for the current research are the linearized differential equations:

$$\begin{cases} m_1 \frac{d^2 x_1}{dt^2} + m_2 \frac{d^2 x_2}{dt^2} = F - W \cdot \text{sign}\left(\frac{dx_1}{dt}\right); \\ \frac{d^2 x_2}{dt^2} + \frac{g}{l}(x_2 - x_1) = 0, \end{cases} \quad (3.17)$$

where  $m_1$  is the reduced mass of the crane;  $m_2$  is the mass of the load;  $x_1$  and  $x_2$  are the coordinates of the centers of masses  $m_1$  and  $m_2$ , respectively;  $g$  is the acceleration of

gravity;  $l$  is the length of the flexible suspension;  $F$  is the driving or braking force acting on the crane;  $W$  is the reduced force resisting the motion of the crane.

The equations of the system's motion for the current research are the linearized differential equations (3.17). The reason why we have used linearized differential equations (3.3) is connected with the angle of the load deviation. In practice, the real angle of the load deviation is not bigger than 10...15 degrees. For that range of angles, the error of calculation (in terms of load position) is equal to 0.5...2.0% (these values are obtained as an expansion of the  $\sin$  and  $\cos$  functions in series in the nonlinear equations of the system (fig. 3.3) motion).

In the current investigation, the crane acceleration has been considered. Assume that the velocity of the crane during that mode does not change its sign. That

is why  $\text{sign}\left(\frac{dx_1}{dt}\right) = 1$ . Let us denote:  $x_2 - s_T = y_1$  and  $u = \frac{F - W}{m_1} \cdot \Omega_0^2$ . These

denotations allow us to rewrite the motion equations (3.17) in the following form:

$$\begin{cases} \frac{dy_j}{dt} = y_{j+1}; & j = \overline{(1, 3)}; \\ y_4 = u - \Omega^2 y_3, \end{cases} \quad (3.18)$$

where  $s_T$  is the final position of the crane;  $u$  is a control function (or just control);  $y_j$  is the  $j$ -th phase coordinate of the system;  $\Omega$  is the natural frequency of the load about

the moving crane,  $\Omega = \Omega_0 \sqrt{\frac{(m_1 + m_2)}{m_1}}$ . The initial and the final conditions of the

system motion are:

$$\begin{cases} y_1(0) = -s_T; & y_2(0) = y_3(0) = y_4(0) = 0; \\ y_1(T) = 0; & y_2(T) = v_T; & y_3(T) = y_4(T) = 0, \end{cases} \quad (3.19)$$

where  $v_T$  is the final velocity of the crane (steady velocity of the crane);  $T$  is the duration of the system's acceleration which is unknown.

Initial conditions (3.19) mean the state of rest; the final conditions (3.19) refer to the elimination of the load oscillations at the moment  $T$ .

In the frame of the current study the criterion to minimize is the duration of the crane acceleration:

$$\int_0^T dt = T \rightarrow \min. \quad (3.20)$$

Minimizing of the duration  $T$  provides increasing of crane productivity, which is desirable for the tower and overhead cranes in the sea and river ports.

Practical necessity demands to take into account the control  $u$  constraints, which is connected with the torque capacity of the crane drive. Thus, the optimal control  $u$  must satisfy the following constraints:

$$\begin{aligned} u_{\min} &\leq u \leq u_{\max}; \\ u_{\max} &= \frac{F_{\max} - W}{m_1} \Omega_0^2; \\ u_{\min} &= \frac{-W}{m_1} \Omega_0^2, \end{aligned} \quad (3.21)$$

where  $u_{\max}$  and  $u_{\min}$  are the upper and the lower boundary of the control domain;  $F_{\max}$  is the maximum drive force acting on the mass  $m_1$  during its acceleration.

It should be noted that the duration of the acceleration  $T$  will be found by solving the optimal control problem (3.18)-(3.21). In order to solve the problem (3.18)-(3.21) the general form of the solution should be developed. Since the closed-loop control problem is under consideration, the appropriate form of  $u$  is as follows:

$$u = u(y, A), \quad (3.22)$$

where  $y$  is the vector-function ( $y=(y_1, y_2, y_3, y_4)^T$ );  $A$  is a vector of some parameters.

From the previous investigation [16, 26, 34, 35] it is known that the time-optimal control  $u$  switches between  $u_{\max}$  and  $u_{\min}$ . This information allows us to specify the function (3.22). We may suggest that the time-optimal control  $u$  is described with the following formula:

$$u = \begin{cases} u_{\max} & \text{if } \sum_{i=1}^4 A_i y_i > 0; \\ u_{\min} & \text{if } \sum_{i=1}^4 A_i y_i \leq 0, \end{cases} \quad (3.23)$$

where  $A_i$  is the  $i$ -th element of the vector  $A$ .

The final position of the crane  $s_T$  may be set for practical reasons. But in the research, we considered parameter  $s_T$  as a so far unknown argument. That value should minimize criterion (3.20) as well.

Thus, the problem (3.18)-(3.21) has been reduced to the finding of the vector  $A$  and the parameter  $s_T$ . All the calculations were carried out for the parameters of the system that are set in Table 3.3.

Table 3.3. Parameters of the system „crane-load”

| Parameter  | Unit | Value |
|--|------|-------|
| Reduced mass of the crane, $m_1$                     | kg   | 300*  |
| Reduced mass of the load, $m_2$                      |      | 500   |
| Length of the flexible suspension, $l$               | m    | 5     |
| Steady-state velocity of the crane, $v_T$            | m/s  | 0.96  |
| Reduced force resisting the motion of the crane, $W$ | N    | 156   |
| Maximum drive force, $F_{\max}$                      |      | 1180  |

\* here we have used the reduced mass of the crane’s trolley

In order to meet the final conditions (3.19) a terminal criterion was developed:

$$Ter = \|\Delta\| = \sqrt{y_1(T)^2 + (y_2(T) - v_T)^2 + y_3(T)^2 + y_4(T)^2}, \quad (3.24)$$

where  $\Delta$  is a vector of phase coordinates deviation from their final (desirable) values (3.19).

Hence, the complex criterion to minimize is as follows:

$$Cr = \psi \cdot Ter + T \rightarrow \min, \quad (3.25)$$

where  $\psi$  is the weight coefficient which reflects the necessity to meet the final conditions (3.19). In the conducted calculations  $\psi=5 \cdot 10^5$ . Such a big value of  $\psi$ , which has been established empirically, allows us to find control  $u$  that transmits the system to the final state (3.19) very accurately. It means that the system phase coordinates at the end of the acceleration will be almost equal to its final values (3.19). In other words, the value of  $\psi$  is a good compromise between the accuracy of final conditions (3.19) meeting and the requirement of criterion (3.20) minimization.

Now we may consider the system as some MISO system (multiple input, single output). The inputs are elements of the vector  $A$  and the value of  $s_T$ ; the output is a value of criterion (3.25).

Note, that there is only one set of numerical values of  $A_1, A_2, A_3, A_4$ , and  $s_T$  which minimize criterion (3.25). Let us suppose that we have found the optimal set of these values. In that case  $Cr=T$  since  $Ter=0$ . Indeed, criterion  $Ter$  has a global minimum which is equal to zero. It is achieved when the final conditions (3.25) are completely met. As the final position of the crane  $x_2(T)$  verges towards optimal crane position the value of criterion (3.25) reduces. That is why the optimal value of  $s_T$  corresponds to the stable movement of the system. Otherwise, it causes the criterion (3.25) increasing.

In order to minimize the criterion (3.25) a modification of particle swarm optimization method (ME-PSO) has been used. That optimization technique has been developed and investigated in the article [50]. The parameters of the used method are set in Table 3.4 (the numerical values of parameters are crucial for algorithm performance. That is why we have shown them in Table 3.4).

Table 3.4. Parameters of the used optimization technique (ME-PSO)

| Parameter                          | Value |
|------------------------------------|-------|
| Number of particles in a swarm     | 30    |
| Acceleration constants $c_1 = c_2$ | 1.19  |
| Acceptable rate ( $AR$ )           | 0.001 |
| Number of iterations               | 500   |

By algorithm performance, we mean optimal problem (3.25) solution accuracy and duration of calculation. In the study, we have used previously tested values of ME-PSO parameters (Table 3.4), which are related to the high algorithm performance.

The components of the vector  $A$  and the value  $s_T$  have been obtained as a result of the optimization problem (3.25) solving. With ME-PSO algorithm we have calculated such values of  $A_1, A_2, A_3, A_4$ , and  $s_T$  which minimize the value of criterion (3.25). All the results are set in Table 3.5.

Table 3.5. Values of the elements of the vector  $A$  and the value  $s_T$

| Parameter | Value |
|-----------|-------|
| $A_1$     | -4122 |
| $A_2$     | 1005  |
| $A_3$     | -4953 |
| $A_4$     | -197  |
| $s_T$     | 1.00  |

The duration of the system's acceleration under time-optimal control equals 2.1 s. Thus, the closed-loop time-optimal control problem is solved. Note, that the problem has been solved in the numerical form. Variations of the system parameters lead to the necessity of the vector  $A$  and the parameter  $s_T$  correction. It requires a new solution of the problem (3.25). Finding the problem (3.25) solution does not require much calculation resources. In practice, it may be found by mean of a crane control system (microcontroller with custom-built software).

In order to investigate obtained results the graphs have been plotted (fig. 3.5). The curve in the fig. 3.4 (a) has been built as a parametric plot [40] in 3D-space. It allows for observation of the main system phase coordinates. In fig. 3.4 (a) gray points denote the initial and final states of the system. Plots in fig. 3.5 show that all the boundary conditions (3.19) are met. Hence, further system movement will continue with no load oscillations. The maximum deviation of coordinates  $x_1$  and  $x_2$  equals 0.5 m, the maximum deviation of their velocities is equal to 0.76 m/s.

A similar effect may be achieved for the deceleration mode of the crane. The obtained result may be exploited for increasing crane productivity. Indeed, there is no need to control the system's movement in manual mode. It reduces the crane operator utilization and provides the opportunity to design the completely automated crane. A curve of the trolley velocity is denoted by a gray line on the fig. 3.4 (b). It shows that at the end of the acceleration the crane velocity equals  $v_T$  (0.96 m/s). It also confirms that the previous assumption about the constancy of the trolley velocity sign is right: at the moment  $t=1.3$  s the crane stops but it has not changed its direction.

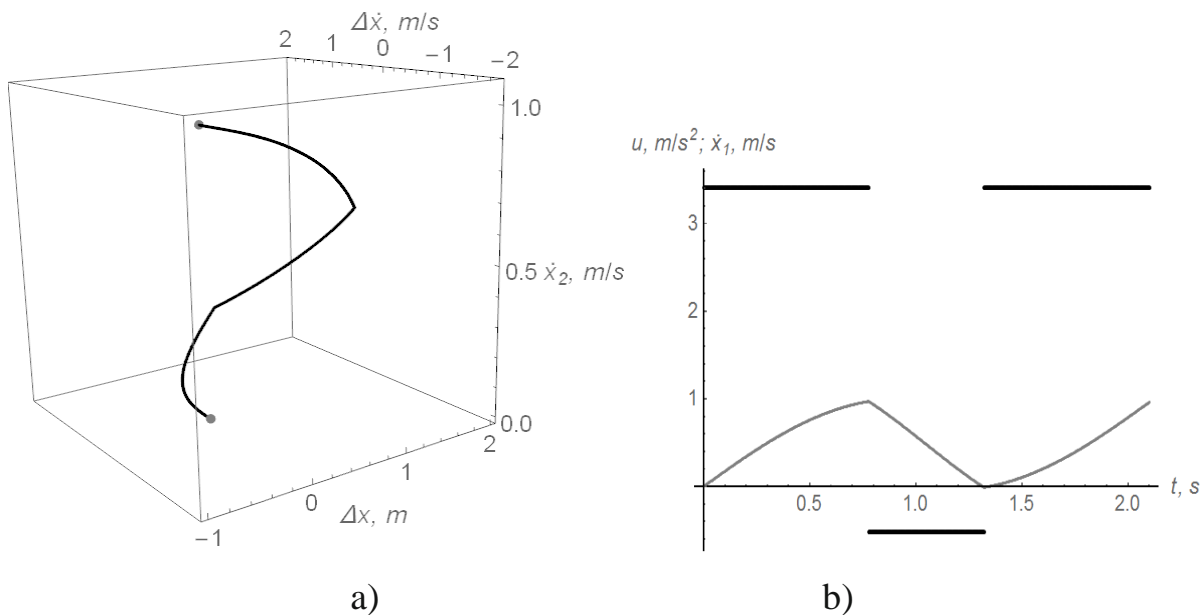


Fig. 3.4 The graphical interpretations of the problem (3.1), (3.32)-(3.34) solution:  
 a) 3D phase portrait of the system; b) control function and the crane velocity

A curve of the control function  $u$  (fig. 3.4, b) has a switching form. It leads to some undesirable consequences, for instance, high-frequency oscillations of the crane metal construction. Another negative factor is high energy losses in the drive. In order to avoid these undesirable features the constraints to control rate should be taken into consideration.

The root-mean-square value of the driving force is equal to 882 N or 74.7% of the full drive load. It reveals that during crane acceleration the drive mechanism does not work with full power.

During the second period of acceleration (from 0.8 to 1.3 s) the crane moves with turned off motor (fig. 3.5, b). During that period the motor does not consume any power (fig. 3.5).

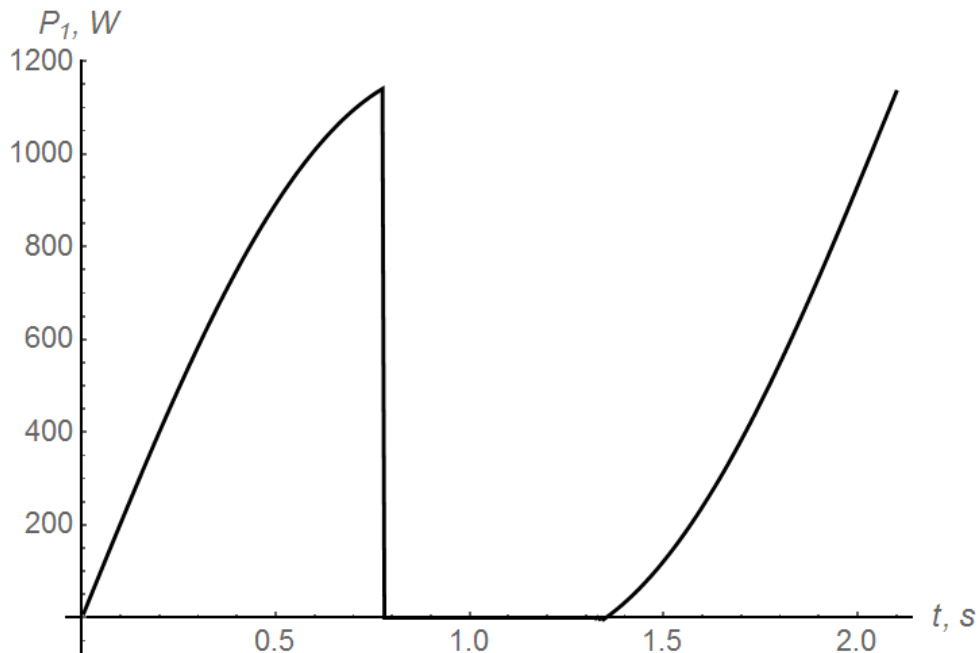


Fig. 3.5 The curve of the consumed power of the crane drive

Observing the plot which is shown on fig. 3.5, one can note two peaks of power. The values of these maximums are approximately equal to each other (1140 W – at the end of the first period and 1133 W – at the end of the third one). The drive maximum power is 7.5 times as steady-state power. Power overload acts during very short periods and does not dramatically affect the motor work.

In order to illustrate one of the advantages of the calculated optimal closed-loop control, we have considered the external stochastic disturbance – a wind rush. It influences both the crane and the load, but for the latter, the impact is much bigger. In the calculation, we have used the model of the wind rush, which includes: the speed of the wind, middle transverse section of the load and air density. The wind rush model (formula) was inserted into the equations (3.19).

Results of numerical integration of the modified mathematical model we have presented on fig. 3.6 (it should be noted, we investigate the optimal control we obtained with no consideration of the external forces).

$u, m/s^2; \dot{x}_1, m/s; F_{w,2} \times 10^2, N; (x_1 - x_2) \times 5, m$

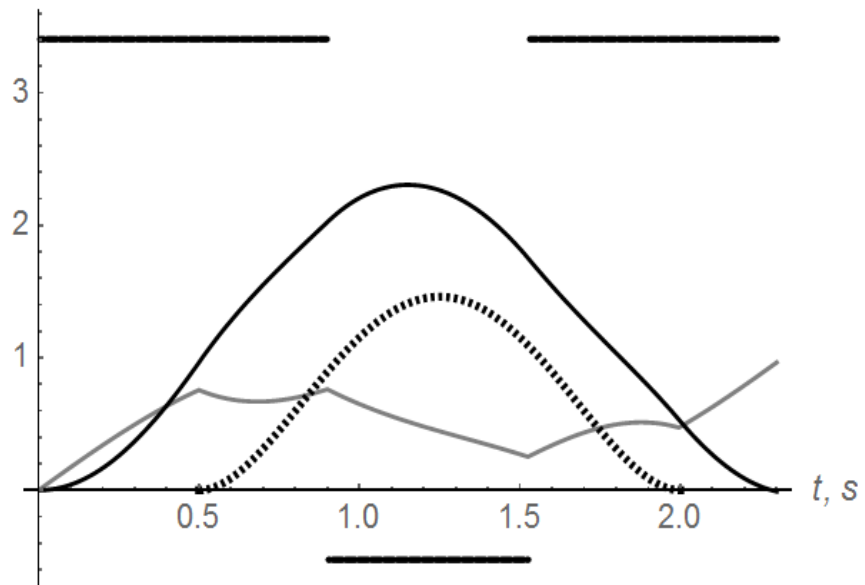


Fig. 3.6 The curves of the system's dynamics under optimal control and the wind rush

In fig. 3.6 dashed curve represents the wind force which acts to the load (it is denoted as  $F_{w,2}$ ). The black full curve relates to the deviation in positions of the load and the crane. At the end of the crane acceleration that value equals to zero. Hence, further movement of the load will be with no oscillations.

The crane velocity at the end of the acceleration equals to  $v_T$ . Thus, all the final conditions (3.32) are met. Such a result has been achieved with variation in the duration of the crane drive on-off periods.

Showed example supports the statement about invariant (to the external disturbances) property of the closed-loop optimal control [51].

### 3.3 Management and closed-loop optimal control of the system „crane-load” (minimum integral criterion control)

The handling of various loads with the help of bridge cranes is widespread. They are used in sea and river ports, factories of chemical and metallurgical industry, mechanical engineering and more. Bridge type cranes often work in unsteady operating modes (start, stop, reverse). It is known, that the default mode of motion of

the crane may be absent in the general case. Dynamic processes occurred during the transient motion of crane mechanisms may determine the efficiency of the crane, as well. The load usually is fixed on a rope and its vibrations affect the performance, reliability, and efficiency of bridge crane. The problem of eliminating of load's vibrations for port's loaders and steel valves is particularly relevant. In the first case, the elimination of load's vibrations increases crane's productivity and reduces the idle of the ship in port in the first case and increases the safety of the work in the second one.

Vibrations of the load on a rope appear during transient motion of the crane, continue during its steady movement phase and are present even after crane's stop. It is desirable to eliminate these crane's vibrations as quickly, as it is possible [52]. However, the optimal control of velocity's action to eliminate the load's vibration significantly increases the dynamic load of crane's elements and this crane can quickly fail.

One may use other methods of solving this problem. For example, one may use fuzzy-controllers [53-56]. The disadvantage of such methods is that they do not include the constraints imposed on the drive mechanism of the crane, and that load vibrations may have a big amplitude during the transient process.

One may use the passive damping devices for the elimination of load's vibrations. By the way, there are a number of ways that are patented and used by different companies [57-59]. The main drawback of these methods is that they do not provide optimal control. That's why the problem of a finding the optimal control of crane's load oscillations during its removal is very important.

One may take for the research the two-mass dynamic model of the mechanism of movement of the crane which is performed on fig. 3.3. This model is common and is used by many researchers [60-72]. The above-mentioned calculation model (fig. 3.3) is described by a system of differential equations (3.17).

One may take the system of equations (3.17) in a canonical form. Let's add one more equation for the function of control's changes:

$$\begin{cases} \dot{y}_0 = y_1; \\ \dot{y}_1 = y_2; \\ \dot{y}_2 = y_3; \\ \dot{y}_3 = u - \Omega^2 y_2; \\ \dot{u} = \varphi, \end{cases} \quad (3.26)$$

where  $y_0$  is the function proportional to the coordinate the load ( $y_0 = x_2 / \Omega_0^2$ );  $\varphi$  is the function of the rate of control change. The constraints imposed on the control  $u$  are in the form of inequalities:

$$|u| \leq u_{\max} = \frac{F_{\max} - W}{m_1}, \quad (3.27)$$

where  $F_{\max}$  is the maximum force over the crane which corresponds to the maximum torque on the motor shaft.

The movement of the crane with a load is characterized by initial conditions which are recorded for the new phase coordinates  $y_0, y_1, y_2, y_3$  as follows:

$$\begin{cases} y_0(0) = \frac{x_2(0)}{\Omega_0^2} = \frac{x_1(0) - \Delta x(0)}{\Omega_0^2} \approx \frac{x_1(0) - l\alpha(0)}{\Omega_0^2}; \\ y_1(0) = \frac{\dot{x}_2(0)}{\Omega_0^2} = \frac{\dot{x}_1(0) - \Delta\dot{x}(0)}{\Omega_0^2} \approx \frac{\dot{x}_1(0) - l\dot{\alpha}(0)}{\Omega_0^2}; \\ y_2(0) = \frac{\ddot{x}_2(0)}{\Omega_0^2} = \frac{\ddot{x}_1(0) - \Delta\ddot{x}(0)}{\Omega_0^2} \approx \frac{\ddot{x}_1(0) - l\ddot{\alpha}(0)}{\Omega_0^2}; \\ y_3(0) = \frac{\ddot{\ddot{x}}_2(0)}{\Omega_0^2} = \frac{\ddot{\ddot{x}}_1(0) - \Delta\ddot{\ddot{x}}(0)}{\Omega_0^2} \approx \frac{\ddot{\ddot{x}}_1(0) - l\ddot{\ddot{\alpha}}(0)}{\Omega_0^2}, \end{cases} \quad (3.28)$$

here  $\Delta x$  is the difference of coordinates of the crane and load ( $\Delta x = x_1 - x_2$ );  $\alpha$  – is the angle of the rope load with the vertical. The system (3.28) used an approximate estimation follows  $\Delta x \approx l\alpha$  from the fact that  $\sin\alpha \approx \alpha$ , for the small values of  $\alpha$ . This approach does not give significant errors.

The initial conditions (3.28) allow one to determine parameters of motion of the crane and of the load which must be measured. This is necessary to determine these conditions and for their default at the crane's system control. One must measure

the coordinate of crane's position and its higher derivatives in time up to the third as well, a length of rope and rope angle of the load from the vertical and its higher derivatives in time up to the third as follows from this system. These parameters are measured with a help of the three encoders. One encoder measures the length of rope. It's installed on the cable drum. The second encoder measures the position of the crane relative to zero. The third encoder measures the angle of the rope load from the vertical. Its output shaft is attached to the rope with a help of special fittings.

The following final conditions must be performed in order to eliminate load's oscillations during the moment when the crane is putting on the breaks:

$$\begin{cases} y_1(T) = 0; \\ y_2(T) = 0; \\ y_3(T) = 0. \end{cases} \quad (3.29)$$

The first condition in (3.29) is equivalent to the situation when the load's speed is equal to zero, the second condition is equivalent to the situation when the difference of coordinates of the crane and the load is equal to zero, the third condition in (3.29) is equivalent to the situation when the difference in speed of the crane and load is equal to zero. So, the amount of energy's oscillations of the load and of the crane's movement should be equal to zero just at the moment  $t=T$ . This situation means the crane's stopping and the lack of load's vibration.

In order to create the synthesis of control, one must set the criterion of optimality which will determine only the one optimal control of the entire set of alternatives. The criterion of optimality of motion of the crane during its braking may be adopted as an integral:

$$I = \int_0^T \left( \sum_{i=1}^{n=3} \delta_i y_i^2 + \delta_4 u^2 + \delta_5 \varphi^2 \right) dt \rightarrow \min, \quad (3.30)$$

where  $\delta_1, \delta_2, \delta_3, \delta_4, \delta_5$  are some coefficients. These coefficients can be calculated as follows:

$$\delta_j = k_j \tilde{I}_j, \quad j \in \overline{(1, 5)}, \quad (3.31)$$

where  $k_j$  – the weight’s coefficient that takes into account the respective importance of the  $j$ -th index in the structure of the criterion;  $\tilde{I}_j$  – a factor that brings the dimension of the  $j$ -th index in the structure of the criterion (3.30) to dimensionless form.

Criterion (3.30) is an integrated linear-quadratic integral criterion and it reflects both the phase coordinates of the dynamical system and the „costs” to its control as well.

Thus, one staged the task of the optimal control of the dynamic system „crane-load”. The problem is that the dynamic system must be converted from the original position which is characterized by initial conditions (3.28) into the final one which is characterized by finite terms of (3.29). This optimality criterion (3.30) should be the least. In addition, one imposes the constraints on the control in the form of inequality (3.27) and the end of control  $T$  is unstable.

We use the method of dynamic programming [63] for solving the problem of optimal control. This method of synthesis of optimal control allows one to obtain the control as a function of phase coordinates of dynamical systems. This control is in the closed-loop control form. The basic functional equation for this problem is written as follows:

$$\min \left( \sum_{i=1}^{n=3} \delta_i y_i^2 + \delta_4 u^2 + \delta_5 \varphi^2 + \frac{\partial S}{\partial y_0} y_1 + \frac{\partial S}{\partial y_1} y_2 + \frac{\partial S}{\partial y_2} y_3 + \frac{\partial S}{\partial y_3} (u - \Omega^2 y_2) + \frac{\partial S}{\partial u} \varphi \right) = 0, \quad (3.32)$$

where  $S$  – Bellman’s function.

The problem will be solved for the case when the control  $u$  is unconstrained (3.27). This circumstance gives one the possibility to find an analytical solution of the problem. However, we will consider the inequality (3.27) in the further content. One may search the minimum of the right side of the equation (3.32) for the function  $\varphi$ . Let’s differentiate it by the function  $\varphi$  and then equate the result to zero:

$$2\delta_5 \varphi + \frac{\partial S}{\partial u} = 0. \quad (3.33)$$

We find from equation (3.33) function:

$$\varphi = -\frac{1}{2\delta_5} \frac{\partial S}{\partial u}. \quad (3.34)$$

Let's substitute the equation (3.34) into the equation (3.32). Then we have:

$$\begin{aligned} & \delta_1 y_1^2 + \left( \frac{\partial S}{\partial y_1} + y_2 \delta_2 \right) y_2 + \left( \frac{\partial S}{\partial y_2} + y_3 \delta_3 \right) y_3 + \left( \frac{\partial S}{\partial y_3} + u \delta_4 \right) u - \\ & - \frac{1}{4\delta_5} \left( \frac{\partial S}{\partial u} \right)^2 - \frac{\partial S}{\partial y_3} y_2 \Omega^2 = 0. \end{aligned} \quad (3.35)$$

Equation (3.35) is a nonlinear differential equation in partial derivatives. We will search its solution in the form of a quadratic form (it is common practice when solving similar problems [64]):

$$\begin{aligned} S = & A_1 y_1^2 + A_2 y_2^2 + A_3 y_3^2 + A_4 u^2 + A_5 y_1 y_2 + \\ & + A_6 y_1 y_3 + A_7 y_1 u + A_8 y_2 y_3 + A_9 y_2 u + A_{10} y_3 u, \end{aligned} \quad (3.36)$$

where  $A_1, A_2, A_3, A_4, A_5, A_6, A_7, A_8, A_9, A_{10}$  – constant coefficients to be determined.

Taking the partial derivatives of expression (3.36) for functions  $y_1, y_2, y_3$  and  $u$  brings the following expressions:

$$\frac{\partial S}{\partial y_1} = 2A_1 y_1 + A_5 y_2 + A_6 y_3 + A_7 u, \quad (3.37)$$

$$\frac{\partial S}{\partial y_2} = A_5 y_1 + 2A_2 y_2 + A_8 y_3 + A_9 u, \quad (3.38)$$

$$\frac{\partial S}{\partial y_3} = A_6 y_1 + A_8 y_2 + 2A_3 y_3 + A_{10} u, \quad (3.39)$$

$$\frac{\partial S}{\partial u} = A_7 y_1 + A_9 y_2 + A_{10} y_3 + 2A_4 u. \quad (3.40)$$

Let's substitute expressions (3.37)-(3.40) in equation (3.35) and then remove common factors of the brackets. We get:

$$\begin{aligned}
 & y_1^2 \left( \delta_1 - \frac{A_7^2}{4\delta_5} \right) + y_2^2 \left( A_5 + \delta_2 - \frac{A_9^2}{4\delta_5} - A_8\Omega^2 \right) + y_3^2 \left( A_8 + \delta_3 - \frac{A_{10}^2}{4\delta_5} \right) + \\
 & + u^2 \left( A_{10} + \delta_4 - \frac{A_4^2}{\delta_5} \right) + y_1 y_2 \left( 2A_1 - \frac{A_7 A_9}{2\delta_5} - A_6\Omega^2 \right) + y_1 y_3 \left( A_5 - \frac{A_{10} A_7}{2\delta_5} \right) + \\
 & + y_1 u \left( A_6 - \frac{A_4 A_9}{\delta_5} \right) + y_2 y_3 \left( A_2 + A_6 - \frac{A_{10} A_9}{2\delta_5} - 2A_3\Omega^2 \right) + y_2 u (A_7 + A_8 - \\
 & - \frac{A_4 A_9}{\delta_5} - A_{10}\Omega^2) + y_3 u \left( 2A_3 + A_9 - 2A_3 + A_9 - \frac{A_{10} A_4}{\delta_5} \right) = 0. \tag{3.41}
 \end{aligned}$$

Equation (3.41) is true in the case when the expression in parentheses will be zero because the functions  $y_1, y_2, y_3, u$  can't be zero at the same time. Therefore, equation (3.41) can be replaced by a system of nonlinear algebraic equations:

$$\left\{ \begin{array}{l}
 \delta_1 - \frac{A_7^2}{4\delta_5} = 0; \\
 A_5 + \delta_2 - \frac{A_9^2}{4\delta_5} - A_8\Omega^2 = 0; \\
 A_8 + \delta_3 - \frac{A_{10}^2}{4\delta_5} = 0; \\
 A_{10} + \delta_4 - \frac{A_4^2}{\delta_5} = 0; \\
 2A_1 - \frac{A_7 A_9}{2\delta_5} - A_6\Omega^2 = 0; \\
 A_5 - \frac{A_{10} A_7}{2\delta_5} = 0; \\
 A_6 - \frac{A_4 A_9}{\delta_5} = 0; \\
 A_2 + A_6 - \frac{A_{10} A_9}{2\delta_5} - 2A_3\Omega^2 = 0; \\
 A_7 + A_8 - \frac{A_4 A_9}{\delta_5} - A_{10}\Omega^2 = 0; \\
 2A_3 + A_9 - \frac{A_{10} A_4}{\delta_5} = 0.
 \end{array} \right. \tag{3.42}$$

The system of equations (3.42) may be solved in analytical. But it is too difficult. So let's simplify it. The expression (3.34) may be as follows taking into account formula (3.40):

$$\varphi = -\frac{2A_4u + A_7y_1 + A_9y_2 + A_{10}y_3}{2\delta_5}. \quad (3.43)$$

Thus, in order to find the unknown function  $\varphi$  which is the first derivative of the function control of dynamic system one must find only four coefficients  $A_4, A_7, A_9, A_{10}$ . It's necessary to form four equations in order to know these coefficients. The first and fourth equations of (3.42) contain only the coefficients  $A_4, A_7, A_9, A_{10}$  so we will use them. One can get from equations (3.42) the third and fourth equation in which coefficients  $A_4, A_7, A_9, A_{10}$  are unknown. We obtain the third equation by rewriting the second equation of (3.42) and taking into account the third and sixth equations of the system. We get the fourth equation when rewrite the ninth equation of system (3.42) taking into account the third equation of the last system. As a result, we have:

$$\begin{cases} \delta_1 - \frac{A_7^2}{4\delta_5} = 0; \\ A_{10} + \delta_4 - \frac{A_4^2}{\delta_5} = 0; \\ \frac{A_{10}A_7}{2\delta_5} + \delta_2 - \frac{A_9^2}{4\delta_5} - \left( \frac{A_{10}^2}{4\delta_5} - \delta_3 \right) \Omega^2 = 0; \\ A_7 + \left( \frac{A_{10}^2}{4\delta_5} - \delta_3 \right) - \frac{A_4A_9}{\delta_5} - A_{10}\Omega^2 = 0. \end{cases} \quad (3.44)$$

The first equation of (3.44) is independent of others and we can immediately write:

$$A_7 = 2\sqrt{\delta_1\delta_5}. \quad (3.45)$$

The negative root is rejected because they can lead to unstability of the dynamical system. We can express the unknown coefficients  $A_{10}$  and  $A_9$  by the coefficient  $A_4$ :

$$A_{10} = \frac{A_4^2}{\delta_5} - \delta_4, \quad (3.46)$$

$$A_9 = \pm \left( 4 \left( \frac{A_4^2}{\delta_5} - \delta_4 \right) \sqrt{\delta_1 \delta_5} - \left( \frac{A_4^2}{\delta_5} - \delta_4 \right)^2 \Omega^2 + 4\delta_5 (\delta_2 + \delta_3 \Omega^2) \right). \quad (3.47)$$

The system of equations (3.44) leads to one algebraic equation of eighth order relative when one takes into account expressions (3.45)-(3.47):

$$A_4^8 + B_1 A_4^6 + B_2 A_4^4 + B_3 A_4^2 + B_4 = 0. \quad (3.48)$$

The last one is reduced to the equation of fourth order when we will use replacement  $A_4^2 = \tilde{A}_4$ :

$$\tilde{A}_4^4 + B_1 \tilde{A}_4^3 + B_2 \tilde{A}_4^2 + B_3 \tilde{A}_4 + B_4 = 0. \quad (3.49)$$

Equation (3.49) may be solved by Descartes-Euler's method. We will not bring solutions of these equations because they have significant volumes. We note only that equation (3.49) has two real and two complex solutions. One can find eight roots of the equation (3.48) turning to the reverse substitution  $A_4 = \pm \sqrt{\tilde{A}_4}$ . Thereafter, we choose only one - the real and positive root. Furthermore, we choose sign “+” before the root in expression (3.47) for the unambiguous determination of the coefficient  $A_9$ . Thus, all complex and negative values of coefficients  $A_4$ ,  $A_9$  that satisfy the system of equations (3.44) are rejected because they can lead to the instability of the dynamical system „crane-load”.

The expression (3.45) may be used to find a function  $\varphi$  that is the first derivative of the control's function  $u$  over time. We need to get just the same control's function in such a manner  $u=u(y_0, y_1, y_2, y_3)$ .

One must to integrate the expression (3.45) for this purpose:

$$\begin{aligned} u &= \int \varphi dt = -\frac{A_4}{\delta_5} \int u dt - \frac{A_{10}}{2\delta_5} \int y_3 dt - \frac{A_9}{2\delta_5} \int y_2 dt - \frac{A_7}{2\delta_5} \int y_1 dt = \\ &= -\frac{A_4}{\delta_5} y_3 - \frac{A_{10}}{2\delta_5} y_2 - \frac{A_9}{2\delta_5} y_1 - \frac{A_7}{2\delta_5} y_0 + C, \end{aligned} \quad (3.50)$$

where  $C$  – is the constant of integration. In order to find the constant of integration it is necessary to solve the following equation  $u(0)=u_0$  which in the expanded form will take such a form:

$$-\frac{A_4}{\delta_5} y_3(0) - \frac{A_{10}}{2\delta_5} y_2(0) - \frac{A_9}{2\delta_5} y_1(0) - \frac{A_7}{2\delta_5} y_0(0) + C = u_0. \quad (3.51)$$

One may find the solution of equation (3.51) and then substitute it in the expression (3.50). We will have finally such control's function  $u$ :

$$u = u_0 + \frac{A_4}{\delta_5} (y_3(0) - y_3) + \frac{A_{10}}{2\delta_5} (y_2(0) - y_2) + \frac{A_9}{2\delta_5} (y_1(0) - y_1) + \frac{A_7}{2\delta_5} (y_0(0) - y_0). \quad (3.52)$$

So we got control's function which depends on the initial control and on phase coordinates as well. We can set arbitrarily the initial control's function. In the particular case  $u_0=0$ . This means no dynamic efforts over the crane's drive at the beginning of its inhibition, in practice. The risk of significant current in electric and dynamic loads of the mechanical part of the crane's drive and its metal faucet is eliminated as well.

Let's build a plot (fig. 3.7) for the resulting control's law. There is also the three-dimensional phase portrait of the dynamical system (fig. 3.8). The gray point on fig. 3.8 denotes the origin of the coordinate system.

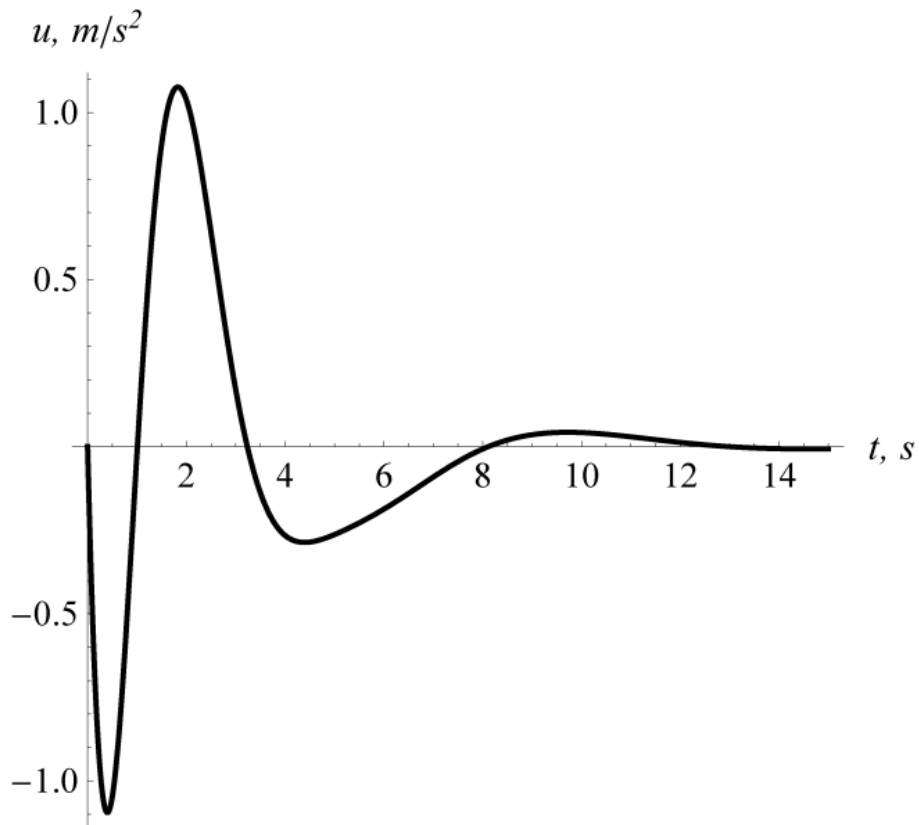


Fig. 3.7 Graph of the function of optimal control of dynamic system „crane-load”

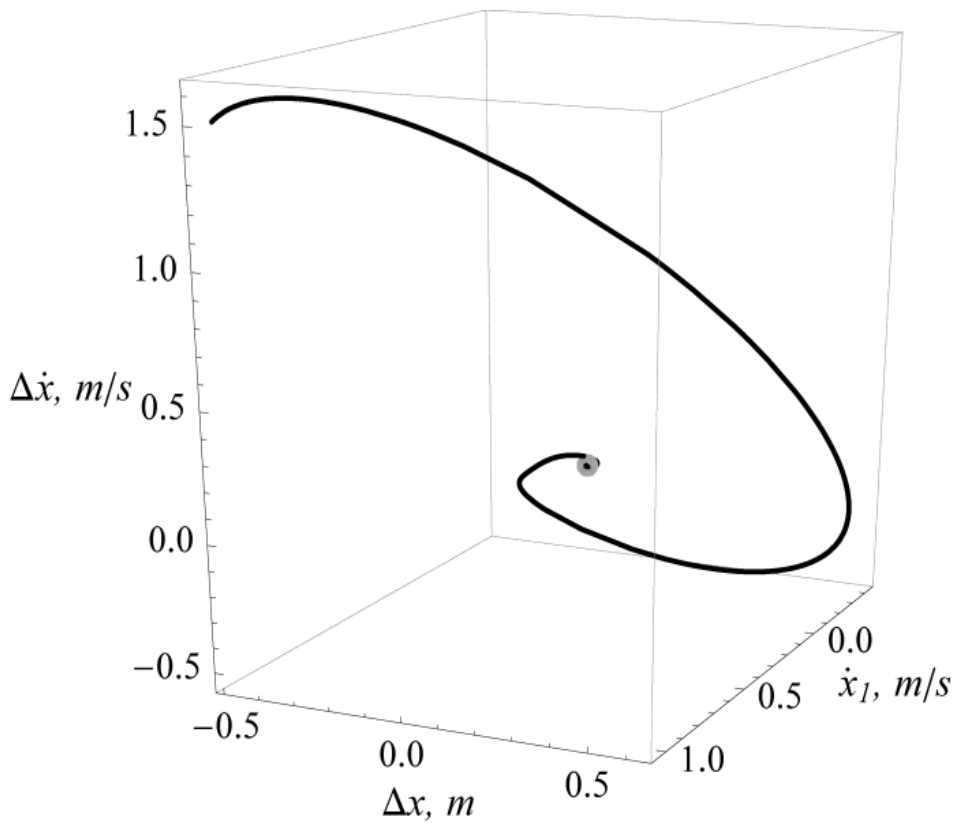


Fig. 3.8 Three-dimensional phase portrait of motion of dynamic system „crane-load”

The dynamic system has zero energy of motion in the origin of the scales i.e., crane stopped and load's oscillations on the rope are absent. Thus the problem of optimal control can be considered as a solved problem. However, we do not take into account the constraints (3.27) when solved this problem. These constraints are usually imposed on control. Physically, this means that electric drive will occasionally be transshipped and will not be able to implement optimal control. It is therefore necessary to take into account these constraints (3.27).

An easy way to take into account constraints (such as (4)) is to miss the optimal control signal through a nonlinear element such as „saturation”. Such control will be called as suboptimal control because it consists of the pieces of optimal control and of the pieces of maximum and minimum values of control. Analytically this is expressed in the following form:

$$u^* = \begin{cases} u, & \text{if } u_{\min} \leq u \leq u_{\max}; \\ u_{\min}, & \text{if } u < u_{\min}; \\ u_{\max}, & \text{if } u > u_{\max}, \end{cases} \quad (3.53)$$

where  $u^*$  – suboptimal control that satisfies constraints (3.53);  $u_{\min}$ ,  $u_{\max}$  – respectively the minimum and maximum control. Here are the graphs similar to the above in fig. 3.9 and fig. 3.10 for the case  $u_{\min}=-0,4 \text{ m/s}^2$  and  $u_{\max}=0,4 \text{ m/s}^2$ . One may see from the graphs that the control does not go to the upper limit. Let us narrow the limits of permissible values of controls:  $u_{\min}=-0,2\text{m/s}^2$  and  $u_{\max}=0,2\text{m/s}^2$ . Physically, this means that the drive motor power is reduced by half. So it is possible to project the crane's motor of less power. However, the duration of the transition process is increasing as seen from fig. 3.11 and fig. 3.12. Thus, one can reduce the crane's drive power when the duration of the transition process is increased. Fig. 3.12 shows that the lack of narrowing of the range of allowable values of control is the changing of the sign of the crane's speed. One can also specify another disadvantage of the optimal control as the suboptimal function. The control is a too small value when the phase coordinates of the dynamical systems „crane-load” are small as well. It means that at the end of the transition period control is „weak”.

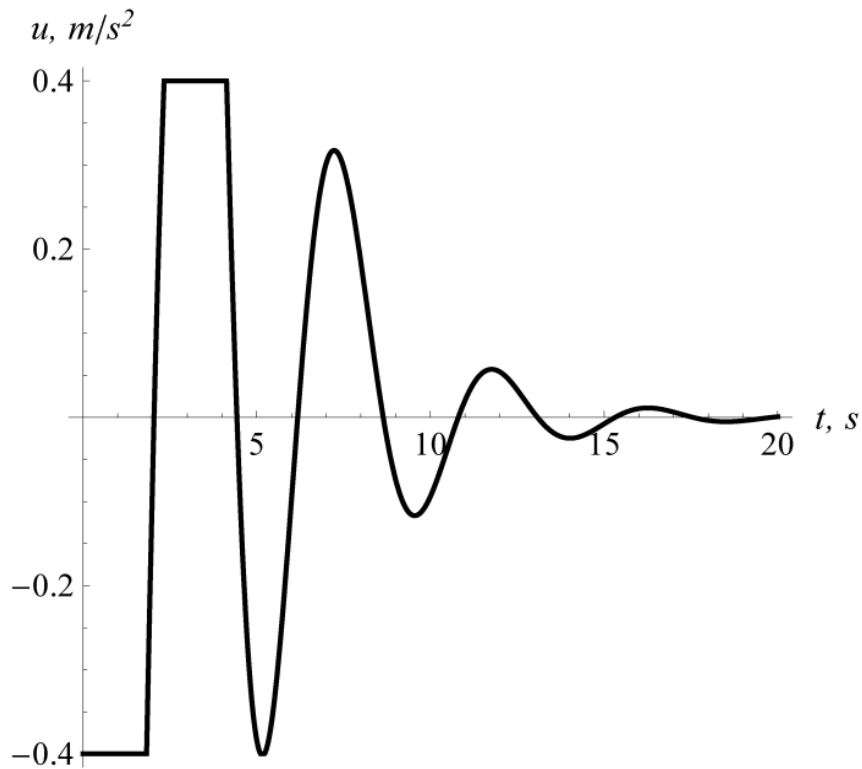


Fig. 3.9 Graph of the function of the suboptimal control of the system „crane-load” while respecting the constraints (3.27)  $u_{\min} = -0,4 \text{ m/s}^2$  and  $u_{\max} = 0,4 \text{ m/s}^2$

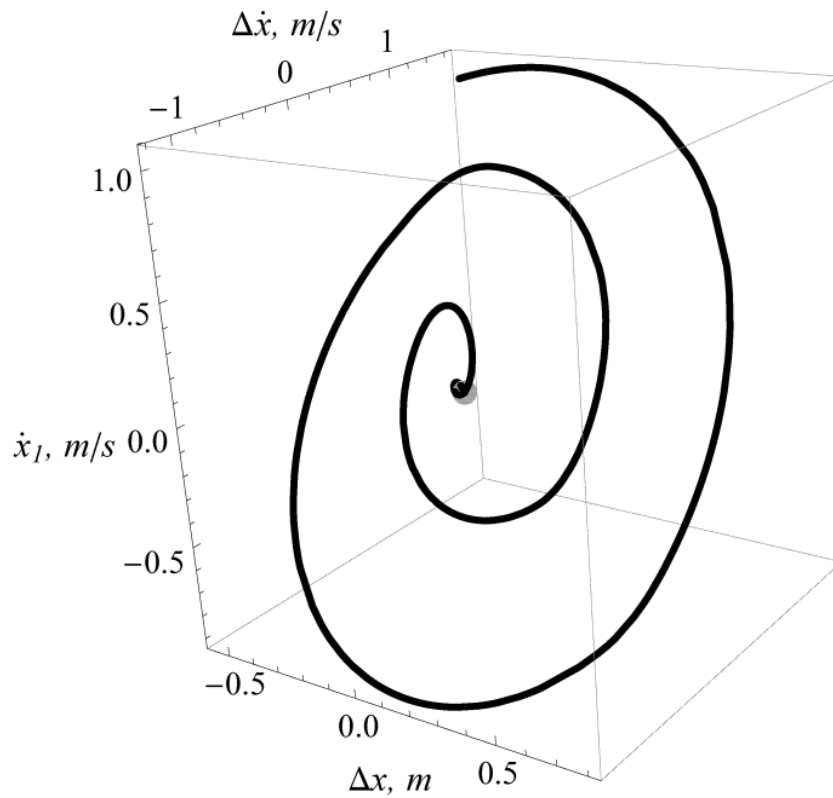


Fig. 3.10 Three-dimensional phase portrait of the motion of the dynamic system „crane-load” while control is (3.53) ( $u_{\min} = -0,4 \text{ m/s}^2$ ,  $u_{\max} = 0,4 \text{ m/s}^2$ )

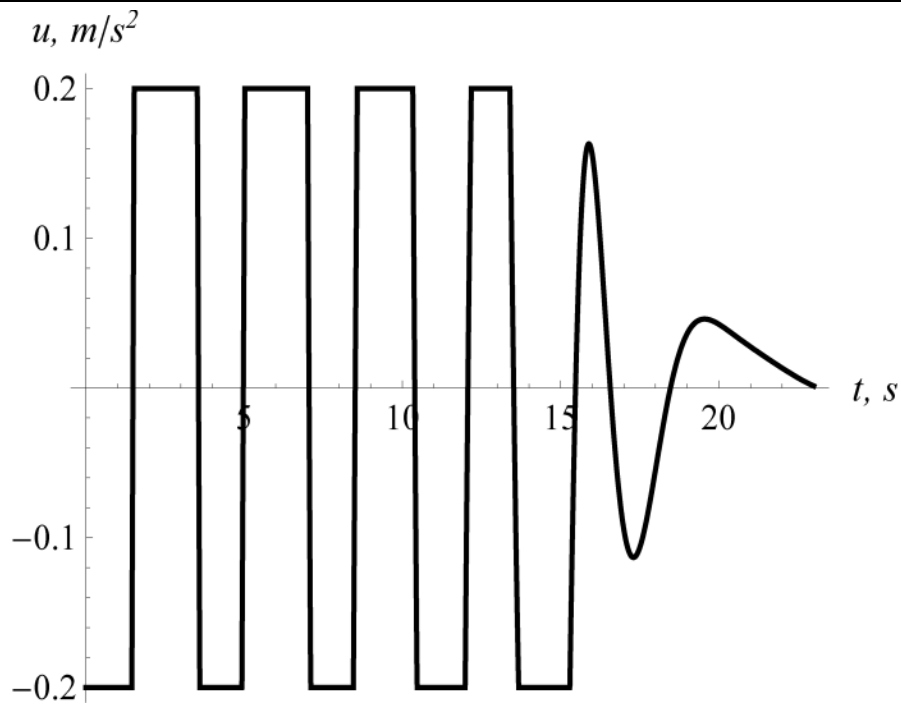


Fig. 3.11 Graph of the function of the suboptimal control system „crane-load” while control is respected the constraints (3.27) ( $u_{\min}=-0,2 \text{ m/s}^2$  and  $u_{\max}=0,2 \text{ m/s}^2$ )

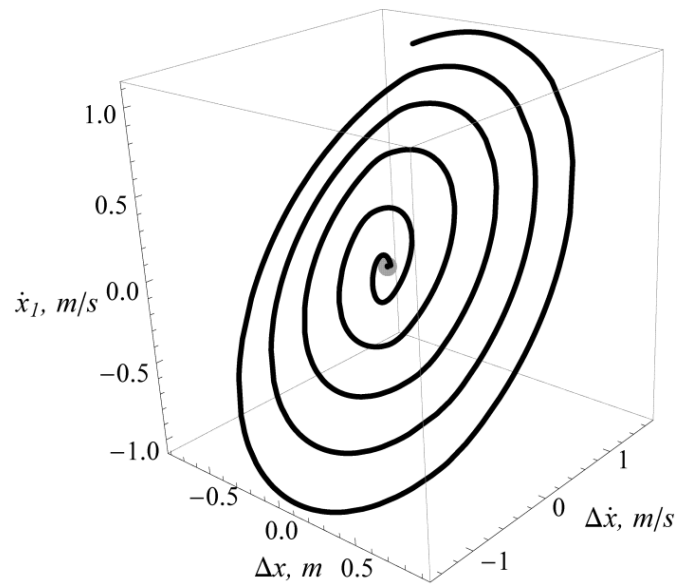


Fig. 3.12 Three-dimensional phase portrait of the motion of the dynamic system „crane-load” while control is (3.53) ( $u_{\min}=-0,2 \text{ m/s}^2$ ,  $u_{\max}=0,2 \text{ m/s}^2$ )

The possible way to solve the problem of „weak” control is to change the variety coefficients  $k_j$ , which are included in the structure of the optimization criterion of the transition process.

### 3.4 Management and optimal control of the system „crane-load” as a function of time (minimum time control)

Many studies address the problem of suppressing the oscillations of an accelerating or decelerating simple pendulum with flexible suspension in minimum time. This problem is relevant due to the desire to improve the performance of devices with suspended load such as load-lifting cranes (especially in seaports).

To solve this problem, we will use the maximum principle [66-70, 73, 74] and the method of moments [70]. Note that a feature of time-optimization problems is the presence of control constraints [72]. The maximum principle allows constraints for the control and state variables (speed, acceleration, etc.), but provides just “qualitative” information on control, saying nothing about the instants of transition from one control bound to another. To identify these instants, it is necessary to analyze the motion of system in the state space [66-68, 70, 73] or to solve transcendental algebraic equations [68, 69, 74].

Symmetric control constraints are used in [68, 72, 73, 76-78]. However, to apply in practice the solution of an optimal-control problem, or any other engineering problem [79], it is necessary to allow for friction. This necessitates using asymmetric constraints, which would complicate the problem [67].

Here, we will study the time-optimal control of a simple pendulum with a movable pivot using different problem statements and focusing on the effect of constraints on the dynamics of the system. To solve the problem, we will use both analytic and numerical methods.

Consider a system that describes the motion of a simple pendulum with a movable pivot (fig. 3.3). The linearized differential equations of motion of the reduced masses  $m_1$  and  $m_2$  (3.17) are used in the research. Assume that the speed of the point suspension does not reverse its sign acceleration (deceleration), i.e.,

$sign\left(\frac{dx_1}{dt}\right) = 1$ . If  $x_2 = s_1$  and  $u = \frac{F - W}{m_1} \cdot \Omega_0^{-2}$ , the system of differential equations

(3.17) can be represented as:

$$\begin{cases} \frac{ds_j}{dt} = s_{j+1}; & j = \overline{(1, 4)}; \\ s_5 = u - \Omega^2 s_3, \end{cases} \quad (3.54)$$

where  $\Omega$  is the natural frequency of the bob about the moving pivot

$$\Omega = \sqrt{\frac{(m_1 + m_2)}{m_1} \cdot \frac{g}{l}}; \quad \Omega_0 \text{ is the natural frequency of the bob about the fixed pivot}$$

$$\Omega_0 = \sqrt{\frac{g}{l}}.$$

The boundary conditions for the state variables of the system are:

$$\begin{cases} s_j(t_0) = s_{j,0}; \\ s_j(T) = s_{j,T}, \end{cases} \quad (3.55)$$

where  $s_{j,0}$  и  $s_{j,T}$  are the initial and final values of the  $i$ th state variable;  $t_0$  and  $T$  are the start and end times of optimal control of the system. The start time is known a priori, while the end time is determined by solving the optimal-control problem. In the case of acceleration of the pendulum, we have:

$$\begin{cases} t_0 = 0; \\ T = T_{acceler}^{opt}; \\ s_{1,0} = s_{2,0} = s_{3,0} = s_{4,0} = 0; \\ s_{1,T} = (T - t_0)v_{steady} \cdot 2^{-1}; \quad s_{2,T} = v_{steady}; \quad s_{3,T} = s_{4,T} = 0, \end{cases} \quad (3.56)$$

where  $T_{acceler}^{opt}$  is the duration of acceleration with time-optimal control of the system;

$v_{steady}$  is the steady-state speed of the suspension point.

Zero initial conditions mean that the suspension point moves from rest and the bob does not oscillate. A simple pendulum with a movable pivot goes through three stages: acceleration, steady-state motion, deceleration. To determine the duration of steady-state motion, we assume that during acceleration and deceleration, the suspension point travels equal distances equal to  $T \cdot v_{steady} \cdot 2^{-1}$ . With this approximation, we have:

$$t_{steady} = s \cdot v_{steady}^{-1} - T_{acceler}^{opt}, \quad (3.57)$$

where  $t_{steady}$  is the duration of steady-state motion of the pendulum;  $s$  is the set distance traveled by the pendulum. The distance traveled by the crane during deceleration should be refined to account for the possible stochastic perturbations that can occur during steady-state motion. In this case, the distance traveled by the pendulum during deceleration is not equal to  $T \cdot v_{steady} \cdot 2^{-1}$ . The following formulas hold for the decelerations stage:

$$\left\{ \begin{array}{l} t_0 = T_{acceler}^{opt} + t_{steady}; \\ T = T_{acceler}^{opt} + t_{steady} + T_{deceler}^{opt}; \\ s_{1.0} = s - x_1(t_0) + \Delta x; \\ s_{2.0} = \frac{dx_1}{dt}(t_0) - \Delta v; \\ s_{3.0} = \Delta x \cdot \Omega_0^2; \\ s_{4.0} = \Delta v \cdot \Omega_0^2; \\ s_{1.T} = s; \quad s_{2.T} = s_{3.T} = s_{4.T} = 0, \end{array} \right. \quad (3.58)$$

where  $T_{deceler}^{opt}$  is the duration of deceleration with time-optimal control of the system;  $\Delta x$  and  $\Delta v$  are the deviations of positions and speeds of the bob and suspension point at the beginning of deceleration;  $x_1(t_0)$  is the position of the suspension point at the beginning of deceleration. The initial conditions for system (3.58) mean that at the beginning of deceleration, there are oscillations of the bob which can be induced by a wind gust. Thus, to solve the time-optimization problem for the decelerating system, it is necessary to set  $\Delta x$  and  $\Delta v$ , position and speed of the suspension point at  $T_{acceler}^{opt} + t_{steady}$ . The final conditions (3.58) mean suppression of the oscillations and stoppage of the system at the set position  $s$ .

The optimal-time criterion is given by:

$$\int_{t_0}^T dt = (T - t_0) \rightarrow \min. \quad (3.59)$$

Since after acceleration, the suspension point moves steadily with speed  $v_{steady}$ , the time-optimization problem is solved by minimizing the durations of acceleration and deceleration.

Thus, the upper and lower limits of integration in (3.59) are different: they are given in (3.56) for acceleration and in (3.58) for deceleration.

The control constraints are asymmetric due to the reduced force  $W$ :

$$\begin{aligned} u_{\min} &\leq u \leq u_{\max}; \\ u_{\max} &= \frac{F_{\max} - W}{m_1} \cdot \Omega_0^{-2}; \\ u_{\min} &= \frac{F_{\min} - W}{m_1} \cdot \Omega_0^{-2}, \end{aligned} \quad (3.60)$$

where  $F_{\max}$  and  $F_{\min}$  are the maximum driving and braking forces determined by the overload capability of the electric drive of the system; and  $F_{\max} = -F_{\min}$  which follows from the capability of the electric drive to create electromagnetic torques equal in magnitude and opposite in direction.

Note that constraints (3.60) are the same for acceleration and deceleration of the pendulum. In what follows, we will use modified control constraints that follow from (3.60):

$$\begin{aligned} \tilde{u}_{\min}^{acceler} &\leq u \leq \tilde{u}_{\max}^{acceler}, \quad t \in [t_0, T_{acceler}^{opt}]; \\ \tilde{u}_{\min}^{deceler} &\leq u \leq \tilde{u}_{\max}^{deceler}, \quad t \in [T_{acceler}^{opt} + t_{steady}, T_{acceler}^{opt} + t_{steady} + T_{deceler}^{opt}]; \\ \tilde{u}_{\max}^{acceler} &= \frac{F_{\max} - W}{m_1} \cdot \Omega_0^{-2}; \\ \tilde{u}_{\min}^{acceler} &= \tilde{u}_{\max}^{deceler} = \frac{-W}{m_1} \cdot \Omega_0^{-2}; \\ \tilde{u}_{\min}^{deceler} &= \frac{F_{\min} - W}{m_1} \cdot \Omega_0^{-2}, \end{aligned} \quad (3.61)$$

where  $\tilde{u}_{\min}^{acceler}$  and  $\tilde{u}_{\max}^{acceler}$  are the minimum and maximum controls feasible for the acceleration of the system;  $\tilde{u}_{\min}^{deceler}$  and  $\tilde{u}_{\max}^{deceler}$  are the minimum and maximum controls admissible for the deceleration of the system. Control constraints (3.61) mean that the direction of the electromagnetic torque does not change: the motor

alternately operates and idles (is de-energized). The advantages and disadvantages of this approach will be discussed below.

Thus, two optimal-control problems for a simple pendulum with a movable pivot have been formulated. The first problem includes a mathematical model of system (3.17), boundary conditions for acceleration (3.55) and deceleration (3.57), optimization criterion (3.59), and control constraints (3.60). In the second problem, the control constraints are different: they are defined by (3.61). Note that the problems posed can be assigned to the class of problems of the stabilization of state variables [75, 81, 82] and the class of optimal-control problems [83, 84].

Time-optimal control is known [67, 71, 74] to be of relay form. Based on these data, it is necessary to solve the Cauchy problem:

$$\begin{cases} \frac{ds_j^i}{dt} = s_{j+1}^i; \\ s_5^i = u^i - \Omega^2 s_3^i; \\ s_j^{i+1} \left( \sum_{\xi=0}^i t_\xi \right) = s_j^i \left( \sum_{\xi=0}^i t_\xi \right); \\ s_j^i \in \left[ \sum_{\xi=0}^{i-1} t_\xi; \sum_{\xi=0}^i t_\xi \right], \quad i = \overline{(1, n)}, \end{cases} \quad (3.62)$$

where  $n$  is the number of stages in the motion of the system during acceleration or deceleration;  $u_i$  is the control at the  $i$ -th stage of the motion of the system equal to the minimum or maximum feasible control;  $t_i$  is the duration of the  $i$ -th stage of motion of the system;  $t_\xi$  is the duration of the  $\xi$ -th stage of motion of the system introduced as the time interval from the beginning of the controlled process to the beginning of the  $i$ -th stage of motion. The quantities  $t_\xi$  and  $t_i$  are related by:

$$t_i = \sum_{\xi=0}^i t_\xi - \sum_{\xi=0}^{i-1} t_\xi. \quad (3.63)$$

The superscript in (3.63) denotes the stage during which the state variable changes. For the  $i$ -th stage of motion of the system and for  $u_i = \text{const}$ , the solution of the Cauchy problem (3.61) has the form:

$$\left\{ \begin{array}{l} s_1^i = B_0^i + tB_1^i + t^2B_2^i + B_3^i \cos\left(\Omega(t - \sum_{\xi=0}^{i-1} t_\xi)\right) + B_4^i \sin\left(\Omega(t - \sum_{\xi=0}^{i-1} t_\xi)\right); \\ s_2^i = B_1^i + 2tB_2^i + \Omega\left(B_4^i \cos\left(\Omega(t - \sum_{\xi=0}^{i-1} t_\xi)\right) - B_3^i \sin\left(\Omega(t - \sum_{\xi=0}^{i-1} t_\xi)\right)\right); \\ s_3^i = 2B_2^i - \Omega^2\left(B_3^i \cos\left(\Omega(t - \sum_{\xi=0}^{i-1} t_\xi)\right) + B_4^i \sin\left(\Omega(t - \sum_{\xi=0}^{i-1} t_\xi)\right)\right); \\ s_4^i = \Omega^3\left(B_3^i \sin\left(\Omega(t - \sum_{\xi=0}^{i-1} t_\xi)\right) - B_4^i \cos\left(\Omega(t - \sum_{\xi=0}^{i-1} t_\xi)\right)\right), \end{array} \right. \quad (3.64)$$

where  $B_0^i, \dots, B_4^i$  – are constant coefficients:

$$\left\{ \begin{array}{l} B_0^i = s_1^i\left(\sum_{\xi=0}^{i-1} t_\xi\right) + s_3^i\left(\sum_{\xi=0}^{i-1} t_\xi\right) \cdot \Omega^{-2} - \left(s_2^i\left(\sum_{\xi=0}^{i-1} t_\xi\right) - s_4^i\left(\sum_{\xi=0}^{i-1} t_\xi\right)\Omega^{-2}\right) \cdot \sum_{\xi=0}^{i-1} t_\xi - u^i \cdot \Omega^{-4} + \\ + u^i \cdot \left(\sum_{\xi=0}^{i-1} t_\xi\right)^2 \Omega^{-2} \cdot 2^{-1}; \\ B_1^i = s_2^i\left(\sum_{\xi=0}^{i-1} t_\xi\right) + \left(s_4^i\left(\sum_{\xi=0}^{i-1} t_\xi\right) - u^i \cdot \sum_{\xi=0}^{i-1} t_\xi\right) \cdot \Omega^{-2}; \\ B_2^i = (u^i) \cdot \Omega^{-2} \cdot 2^{-1}; \\ B_3^i = (u^i) \cdot \Omega^{-4} - \left(s_3^i\left(\sum_{\xi=0}^{i-1} t_\xi\right) \cdot u^i\right) \cdot \Omega^{-2}; \\ B_4^i = -s_4^i\left(\sum_{\xi=0}^{i-1} t_\xi\right) \cdot \Omega^{-3}. \end{array} \right. \quad (3.65)$$

Since the suspension point increases its speed at the acceleration stage, control  $u_1$  for the first stage of acceleration is chosen maximum possible:  $u_1 = u_{\max}$  for problem (3.54), (3.56), (3.58)-(3.60) and  $u^1 = \tilde{u}_{\max}^{acceler}$  for problem (3.54), (3.56), (3.58), (3.59), (3.61). At the deceleration stage:  $u_1 = u_{\min}$  for problem (3.54), (3.56), (3.58)-(3.60) and  $u^1 = \tilde{u}_{\min}^{deceler}$  for problem (3.54), (3.56), (3.58), (3.59), (3.61). As the system changes over to the subsequent stages of motion during either acceleration or deceleration, control instantaneously passes from one bound of the domain of feasible controls to another, i.e.,  $u_{\max}$  and  $u_{\min}$  for problem (3.54), (3.56), (3.58)-(3.60) and  $\tilde{u}_{\max}^{acceler}$  and  $\tilde{u}_{\min}^{deceler}$  for problem (3.54), (3.56), (3.58), (3.59), (3.61) alternate. If the control  $u_1$  cannot be determined a priori, it can be chosen either maximum or minimum. If  $u_1$  is

set incorrectly, for example  $u_1=u_{\min}$ , then it will appear during the solution that the duration of the first stage is equal or close to zero. Then we should set  $u_1=u_{\max}$ . Substituting (3.55) and (3.58) into (3.64) and (3.65), we obtain functions describing the motion of the dynamic system during the first stage. Replacing  $t$  by  $t_1$  in the resulting expressions, we obtain formulas for state variables at the end of the first stage (for acceleration and deceleration). These formulas, as initial state variables, are substituted into formulas (3.64) for the second stage of motion. Continuing the calculations, we obtain the expressions  $s_j^n(T) = f_j(t_1, \dots, t_i, \dots, t_n, B_0^i, \dots, B_4^i, s_{j,0}, u_{\max}, u_{\min})$  for problem (3.54), (3.56), (3.58)-(3.60) and  $s_j^n(T) = f_j(t_1, \dots, t_i, \dots, t_n, B_0^i, \dots, B_4^i, s_{j,0}, \tilde{u}_{\max}^{acceler}, \tilde{u}_{\min}^{acceler}, \tilde{u}_{\min}^{deceler})$  for problem (3.54), (3.56), (3.58), (3.59), (3.61).

It is rather difficult to find the value of  $n$ . If the controlled dynamic system is normal and the associated roots of the characteristic equation are real, then it is possible to use Feldbaum's  $n$ -interval theorem. In this case, the number of stages of the motion of the system is no greater than its order [73]; then  $n$  should be set equal to the order of the dynamic system. The conditions of the  $n$ -interval theorem are not satisfied for the optimal-control problems under consideration because the characteristic equation of the dynamic system has complex roots.

Let  $n=5$ . Thus, the optimal-control problems (3.54), (3.56), (3.58)-(3.60) and (3.54), (3.56), (3.58), (3.59), (3.61) can be reduced to nonlinear-programming problems:

$$\begin{aligned} \sum_{i=0}^5 t_i &\rightarrow \min; \\ t_i &\geq 0; \\ s_j^5\left(\sum_{i=0}^5 t_i\right) &= s_{j,T}^5, \end{aligned} \tag{3.66}$$

which should be solved for the unknowns  $t_1, t_2, t_3, t_4$  and  $t_5$ . For the optimal-control problems (3.54), (3.56), (3.58)-(3.60) and (3.54), (3.56), (3.58), (3.59), (3.61), the expressions  $s_j^5\left(\sum_{i=1}^5 t_i\right)$  will be different. According to the Lagrangian multiplier

method, to satisfy equality constraints, we will solve the problem of finding the minimum of a composite function:

$$\sum_{i=0}^5 t_i + \sum_{j=1}^4 \lambda_j \left( s_j^5 \left( \sum_{i=0}^5 t_i \right) - s_{j,T}^5 \right) \rightarrow \min, \quad (3.67)$$

$$t_i \geq 0,$$

where  $\lambda_j$  are Lagrangian multiplier corresponding to the  $j$ -th constraint. Note that the expressions  $s_j^5 \left( \sum_{i=0}^5 t_i \right) - s_{j,T}^5$  include transcendental functions, which complicates the solution of problem (3.67). Therefore, to determine the unknowns  $t_1, t_2, t_3, t_4$  and  $t_5$ , it is necessary to use numerical methods, such as the particle swarm method [80], which allows finding the global minimum of function (3.67).

To illustrate the method proposed, we will solve problem (3.67) using the parameters of a harbor bucket unloader (Table 3.6).

Table 3.6 Values of the parameters used in the calculations

| Parameter                                       | Unit  | Value             |
|---|-------|-------------------|
| Reduced weight of crane $m_1$                   | kg    | $5.34 \cdot 10^4$ |
| Reduced weight of cargo $m_2$                   | kg    | $3.51 \cdot 10^4$ |
| Length of flexible suspension $l$               | m     | $1.00 \cdot 10^1$ |
| Steady-state speed of crane $v_{steady}$        | m/sec | $2.76 \cdot 10^0$ |
| Set distance of travel of crane with cargo $s$  | m     | $3.26 \cdot 10^1$ |
| Reduced force resisting the motion of crane $W$ | N     | $1.73 \cdot 10^4$ |
| Maximum driving force of crane $F_{max}$        | N     | $1.30 \cdot 10^5$ |

To solve problem (3.67), we will use the particle-swarm method. The swarm parameters are summarized in Table 3.7.

Problem (3.6) is solved four times: for acceleration and deceleration of the crane for classical (2.6) and modified (2.7) constraints. The values of  $t_1, t_2, t_3, t_4, t_5$  are found iteratively: setting  $n = 5$  causes two roots to be close to zero. Then  $n=5-2=3$  is set, i.e., the stages of motion corresponding to nearly zero roots are rejected.

Table 3.7 Parameters of particle-swarm method

| Parameter   | Value |
|---|-------|
| Number of iterations  | 100   |
| Number of particle in swarm                                 | 50    |
| Inertia coefficient $w$                                     | 0.72  |
| Acceleration constants $c_1=c_2$                            | 1.19  |
| Domain of searching for values of $t_1, t_2, t_3, t_4, t_5$ | 0...4 |

The values of the state variables  $s_j^3\left(\sum_{i=0}^3 t_i\right)$  are calculated again and a nonlinear-programming problem is formulated:

$$\sum_{i=0}^3 t_i + \sum_{j=1}^4 \lambda_j \left( s_j^3\left(\sum_{i=0}^3 t_i\right) - s_{j,T}^3 \right) \rightarrow \min, \quad (3.68)$$

$$t_i \geq 0.$$

The results of solving problem (3.68) are summarized in Table 3.8.

Table 3.8 Parameters of particle-swarm method

| Stages             | Acceleration duration      |                            | Deceleration constraints   |                            |
|--------------------|----------------------------|----------------------------|----------------------------|----------------------------|
|                    | Control constraints (3.60) | Control constraints (3.61) | Control constraints (3.60) | Control constraints (3.61) |
| $t_1, \text{ sec}$ | 1,45                       | 1,17                       | 1,14                       | 0,71                       |
| $t_2, \text{ sec}$ | 0,56                       | 1,18                       | 0,85                       | 1,95                       |
| $t_3, \text{ sec}$ | 1,45                       | 1,17                       | 1,18                       | 0,71                       |

It follows from Table 3.8 that the durations of stages of the motion of the system are different in different problems, which is due to the different control constraints (3.60) and (3.61).

To illustrate the solution of the problem, we will plot the phase portrait of the oscillations of the cargo (fig. 3.13) and the curve of variation in the crane speed (fig. 3.14) (the gray and black curves correspond to constraints (3.60) and (3.61), respectively).

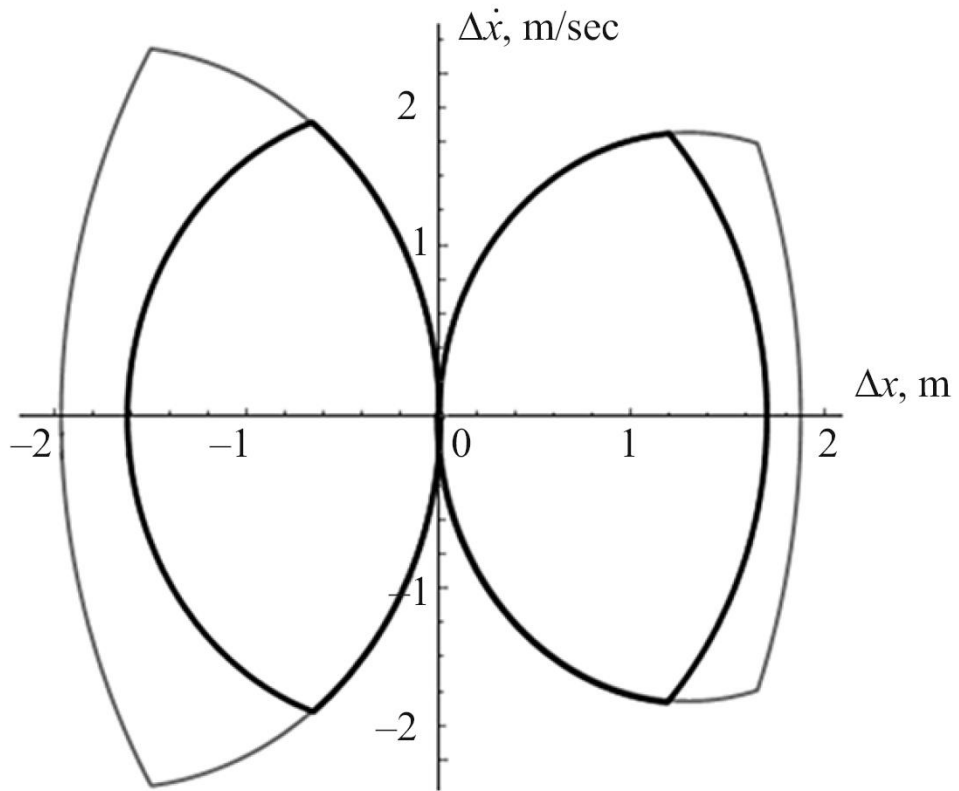


Fig. 3.13 Phase plots of the cargo (load) oscillations

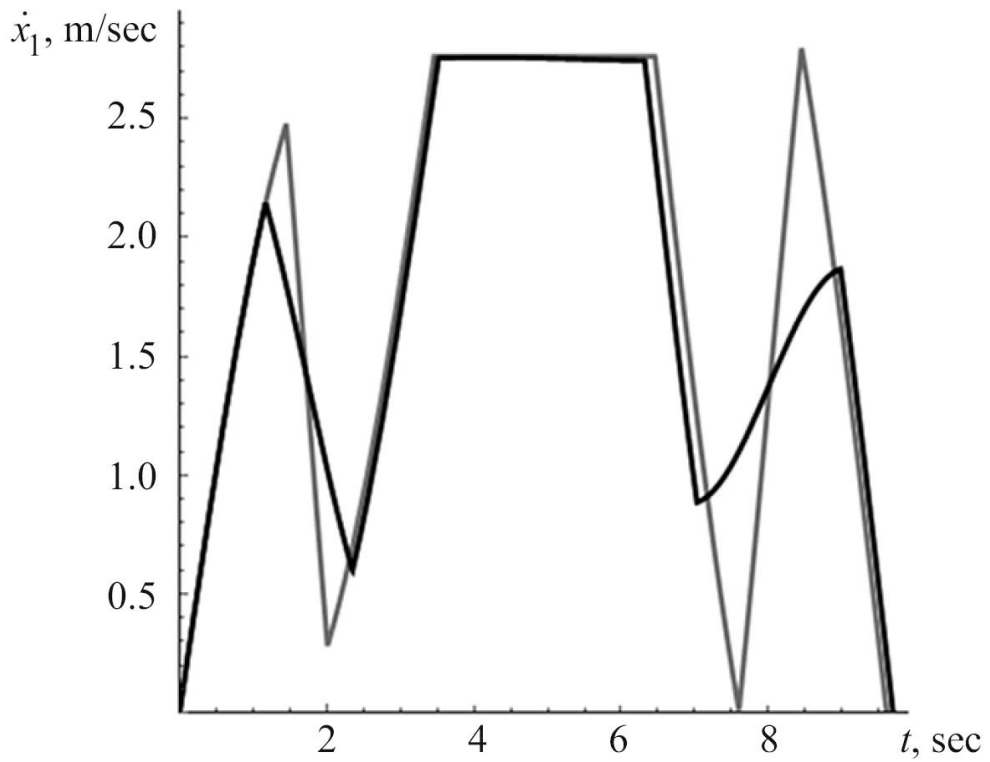


Fig. 3.14 Velocity of the crane

Figures 3.13 and 3.14 indicate that the cargo stops oscillating once the crane has stopped. The rate of variation in the crane speed and the maximum vertical deviation of the suspension are much lower when the modified constraints (3.61) are used. This reduces the dynamic loads and increases the life of the mechanisms and metalwork of the crane.

Summarizing the calculations performed, we conclude that the value of  $n$  should be found iteratively. First, a value of  $n$  based on a priori data is specified, which is decreased during solution of the nonlinear-programming problem:

$$\sum_{i=0}^n t_{\xi} + \sum_{j=1}^k \lambda_j \left( s_j^n \left( \sum_{i=0}^n t_{\xi} \right) - s_{j.T}^n \right) \rightarrow \min, \quad (3.69)$$

$$t_i \geq 0,$$

where  $k$  is the number of state variables of the system. Some of the solutions of problem (3.69) will be zero (or close to zero, depending on the accuracy of the numerical method chosen). The value of  $n$  should be decreased by the number of zero (or nearly zero) solutions of problem (3.69) and to repeat the calculations, rejecting those stages whose duration is zero (or close to zero). This allows finding the solutions of problem (3.69) for which  $t_i > 0$ . To assess the efficiency of the optimal controls obtained, it is necessary to model the motion of the system and to experimentally test the optimal control [85].

### Conclusions to chapter 3

1. It is impossible to find the exact solution of the optimal control problem for four-mass dynamical model of a crane. The efficient methods which reduce optimal control problem to the linear programming problem are direct variational techniques. It is desirable to seek the solution of the problem at limited domains of phase coordinates and dynamical parameters of a system. Obtained in the work suboptimal control of the crane movement could be implemented with frequency-controlled drive

Obtained in the work suboptimal control of the crane movement could be implemented with frequency-controlled drive [33].

2. In the study, the closed-loop problem of optimal control has been solved. Obtained optimal control of the system „crane-load” allows for minimizing the duration of the acceleration mode with taking into account the non-symmetrical control constraints. The novelty of the problem-solving approach is in reducing the initial problem to the non-linear programming problem and the using for its solving advanced PSO-based technique. Developed in the study approach may be used for the deceleration of the system „crane-load” [51].

3. One may use the method of dynamic programming which allows to synthesize the optimal closed-loop control without constraints on the control. The use of nonlinear elements such as „saturation” provides a suboptimal control that meets the limits imposed on the control. The suboptimal closed-loop control consists of pieces of optimal control and of the boundary limits of the control domain. The variation of the coefficients in the structure’s optimization criterion is the possible way to solve the problem of the synthesis of the optimal control which would always be in the acceptable control domain even when these limits are the functions of the time and of the phase coordinates of the dynamical system „crane-load” [65].

4. Time-optimization problems can be reduced nonlinear-programming problems only for systems whose equations of motion can be solved analytically (generally, linear systems of no higher than the fourth order, some linear systems of higher than the fourth order, and some classes of nonlinear systems). Using the modified control constraints allows less heavy-duty operation of the crane drive because the sign of the driving force does not change during acceleration (or deceleration). It is hoped that use of modified constraints similar to (3.61) for other problems will make it possible to determine optimal controls to improve the performance of engineering systems by slightly increasing the duration of their motion. It remains to study the influence of constraints on the speed of motion of the system. The associated problem should be rigorously formulated and solved with formal mathematical methods. By now, we can provide only purely theoretical

considerations: if the values of control constraints are infinitely large (constraints are absent), the duration of the motion of the system will be infinitesimal; if the values of control constraints are infinitely small (zero in the limit), the duration of the motion of the system will be infinitely long [85].

### **References to chapter 3**

1. Komarov M.S. Dynamics of load-lifting machines. Moscow, Mashynostroenye, 1969, 206 p. (in Russian).
2. Kazak S.A. Dynamics of overhead cranes. Moscow, Mashynostroenye, 1968, 331 p. (in Russian).
3. Gohberg M.M. Metal constructions of hoisting-and-transport machines. Moscow, Mashynostroenye, 1969, 520 p. (in Russian).
4. Gaidamaka V.F. Load-lifting machines. Kiev, Vyscha shkola, 1989, 328 p. (in Russian).
5. Sheffler M., Dresyh Kh., Kurt F. Load-lifting cranes. Book 2. [Translation with German Runov M.M., Fedoseev V.N. Under the editors Alexandrov M.P.] Moscow, Mashynostroenye, 1981, 287 p. (in Russian).
6. Lobov N.A. Dynamics of load-lifting cranes, Moscow, Mashynostroenye, 1987, 160 p. (in Russian).
7. Budikov L.Ya. Multiparametric analysis of cranes dynamics of overhead type. Luhansk, Yzdatelstvo VUHU, 1997, 210 p. (in Russian).
8. Loveikin V.S., Chovniuk Iu.V., Dikteruk M.H., Pastushenko S.I. Simulation of lifting machines mechanisms dynamics. Kyiv-Mykolaiv, RVV MDAU, 2004, 286 p. (in Ukrainian).
9. Loveikin V.S., Romasevych Yu.O. Dynamics and optimization of overhead cranes movement. Kyiv, TsP „KOMPRINT”, 2016, 314 p. (in Ukrainian).

10. Blackburn D, Singhose W, Kitchen J., Patrangenu P., Lawrence J. Command Shaping for Nonlinear Crane Dynamics. *Journal of Vibration and Control*, 00(0), 2009, pp. 1-25. DOI: 10.1177/1077546309106142.
11. Naif B. Almutairi, Mohamed Zribi Sliding Mode Control of a Three-dimensional Overhead Crane. *Journal of Vibration and Control*, 2009, 15 (11), pp. 1679-1730. DOI: 10.1177/1077546309105095.
12. Moustafa Ebeid Nonlinear Modeling and Control of Overhead Crane Load Sway. *ASME Trans. J. of Dynamic Systems, Measurement and Control*, 1998, 120, pp. 266-271.
13. Sun N., Fang Yo Nonlinear tracking control of underactuated cranes with load transferring and lowering: Theory and experimentation. *Automatica*, 2014, 50, pp. 2350–2357. doi.org/10.1016/j.automatica.2014.07.023.
14. Tuan L.A., Lee S., Dang V.H., Moon S., Kim B.S. Partial Feedback Linearization Control of a Three-Dimensional Overhead Crane. *International Journal of Control, Automation, and Systems*, 2013, 11(4), pp. 718-727. DOI: 10.1007/s12555-012-9305-z.
15. Singhose W., Kim D., Kenison M. Input Shaping Control of Double-Pendulum Bridge Crane Oscillations. *Journal of Dynamic Systems, Measurement, and Control*, 2008, 130, 034504-1–034504-6. DOI: 10.1115/1.2907363.
16. Herasymyak R.P., Leshchev. V.A. Analysis and synthesis crane electro-mechanical systems. Odessa, SMIL. 2008, 192 p. (in Russian).
17. Budikov L.Ya. Multiparametric analysis of cranes dynamics of overhead type. Luhansk, Yzdatelstvo VUHU, 1997, 210 p. (in Russian).
18. Grigorov O.V., Loveikin V.S. Optimal control of hoisting machines movement. Kiev, IZMN, 1997, 264 p. (in Ukrainian).
19. Singhose W., Porter L., Kenison M., Kriikku E. Effects of hoisting on the input shaping control of gantry cranes. *Control Engineering Practice*, 2000, 2(10), pp. 1159-1165. doi.org/10.1016/S0967-0661(00)00054-X.
20. Dhanda A., Vaughan J., Singhose W. Vibration Reduction Using Near Time-Optimal Commands for Systems With Nonzero Initial Conditions. *Journal of*

Dynamic Systems, Measurement, and Control, 2016, 138, 041006-1–041006-9. DOI: 10.1115/1.4032064.

21. Ermidoro M., Formentin S., Cologni A., Previdi F., Savaresi S.M. On time-optimal anti-sway controller design for bridge cranes. American Control Conference (ACC). Portland, Oregon, USA, 2014, pp. 2809-2814.

22. Hazriq I.J., Nursabillilah M.A., Mohamed Z., Selamat N.A., Abidin A.F.Z., Jamian J.J., Kassim A.M. Optimal Performance of a Nonlinear Gantry Crane System via Priority-based Fitness Scheme in Binary PSO Algorithm. 5th International Conference on Mechatronics (ICOM'13). IOP Conf. Series: Materials Science and Engineering, 2013, 53, 012011. DOI:10.1088/1757-899X/53/1/012011.

23. Manson G.A. Time-optimal control of an overhead crane model. Optimal control applications & methods, 1982, 3, pp. 115-120.

24. Solis C.U., Clempner J.B., Poznyak A.S. Designing a terminal optimal control with an integral sliding mode component using a saddle point method approach: a Cartesian 3D-crane application. Nonlinear Dynamics, 2016, 86, 3, pp. 911-926. DOI: 10.1007/s11071-016-2932-9.

25. Smekhov A.A., Erofeev N.Y. Optimal control of lifting and transporting machines. Moscow, Mashynostroeny, 1975, 239 p. (in Russian).

26. Loveikin, V.S., Nesterov, A.P. Dynamic optimization of the hoisting machines, Kharkiv, KhDADTU, 2002, 285 p. (in Ukrainian).

27. Kyrychenko Y., Samusia V., Kyrychenko V. Software development for the automatic control system of deep-water hydrohoist. Chapter 13. Geomechanical Processes during Underground Mining, 2012, pp. 81-86. DOI: 10.1201/b13157-14.

28. Petrov Iu.P. Variational methods of optimal control theory, Leningrad, Energia, 1977, 280 p. (in Russian).

29. Loveikin V.S., Romasevich Yu.O., Loveikin Yu.V. Analysis of the direct variational methods for solving optimal control problems, Visnyk Natsionalnoho universytetu „Lvivska politekhnika”. Optyimizatsiia vyrobnychkykh protsesiv i tekhnichniy kontrol u mashynobuduvanni ta pryladobuduvanni, 2012, 729, pp.70-79. (in Ukrainian).

30. Bronshtein I.N., Semendyayev K.A., Musiol G., Mühlig H. Handbook of mathematics [Sixth edition]. Springer, 2015, 799 p.
31. Storn R., Kenneth P. Differential Evolution – A Simple and Efficient Adaptive Scheme for Global Optimization over Continuous Spaces, Technical Report TR-95-012, ICSI, 1995, 15 p.
32. FR-E700: frequency inverter instruction manual. Art. no.: 213994. Version D. Mitsubishi Electric Industrial Automation, 2011, 524 p.
33. Loveikin V.S., Romasevych Yu.O. Optimization of Bridge Crane Movement Control. Science & technique. – Series 1. Mechanical Engineering. 2018, Vol. 17, 5, pp. 413-420.
34. Grigorov O.V., Svirgun V.P. Improving the productivity of utility cranes through optimum motion control, Soviet machine science, vol. 6, 1986, pp. 25-29. (in Russian).
35. Loveikin V.S., Romasevich Y.A., Khoroshun A.S., Shevchuk A.G. Time-Optimal Control of a Simple Pendulum with a Movable Pivot. Part 1, International Applied Mechanics, 2018, vol. 54, Issue 3, pp. 358-365.
36. Okun A., Los Y. The controllability function method, UPB Scientific Bulletin, Series D: Mechanical Engineering, 2016, vol. 78, Issue 3, pp. 3-8.
37. Martynyuk A.A., Khoroshun A.S., Chernienko A.N. Practical Stability of a Moving Robot with Respect to Given Domains, International Applied Mechanics, 2014, vol. 50 , no 1, pp. 79-86.
38. Shurub Yu.V., Dudnyk A.O., Lavinskiy D.S. Optimization of regulators of frequency controlled induction electric drives under the stochastic loadings, Journal Tekhnichna elektrodynamika, 2016, vol. 4, pp. 53-55.
39. Romasevych Yu., Loveikin V. A Novel Multi-Epoch Particle Swarm Optimization Technique, Cybernetics and Information Technologies, 2018, vol. 18(3), pp. 62-74.
40. Bulgakov V., Pilipaka S., Adamchuk V., Olt J. Theory of motion of a material point along a plane curve with a constant pressure and velocity, Agronomy Research, 2014, vol 12(3), pp. 937–948.

41. Matusko J., Iles S., Kolonic F., Lesic V. Control of 3d Tower Crane Based on Tensor Product Model Transformation with Neural Friction Compensation, *Asian Journal of Control*, 2015, 17(2), pp. 443–458. DOI: 10.1002/asjc.986.
42. Eglynas T., Senulis A., Bogdevičius M., Andziulis A., Jusis M. Krantinės kranų valdymo sistemos kompiuterinis modeliavimas optimalioms pid valdiklio vertėms nustatyti, *Statyba, transportas, aviacinės technologijos civil and transport engineering, Aviation technologies*, 2016, 8(5), pp. 540–547. DOI: 10.3846/mla.2016.962.
43. Sun N., Fang Y., Chen H., Lu B., Fu Y. Slew/Translation Positioning and Swing Suppression For 4-DOF Tower Cranes With Parametric Uncertainties: Design and Hardware Experimentation, *IEEE Transactions on Industrial Electronics*, 2015, 63(10), pp. 6407–6418. DOI: 10.1109/TIE.2016.2587249.
44. Solarz W., Tora G. Simulation of control drives in a tower crane, *Transport problems*, 2011, 6(4), pp. 69–78.
45. Tzu-Sung W., Mansour K., Wen-Shyong Y., Chien-Ting C., Ming-Guo H., Kuan-Wei W. Anti-Sway Tracking Control of Tower Cranes With Delayed Uncertainty Using a Robust Adaptive Fuzzy Control, *Fuzzy test and Systems*, 2016, 209(C), pp. 118–137. DOI: 10.1016/j.fss.2015.01.010.
46. Reza E.S., Zaharuddin M. Comparative Assessment of Anti-Sway Control Strategy for Tower Crane System, *AIP Conference Proceedings*, 2017, 1883(1), pp. 1–9. DOI: 10.1063/1.5002053.
47. Thalopil J. Input shaping for sway control in gantry cranes, *Journal of Mechanical and Civil Engineering (IOSRJMCE)*, 2012, 1, pp. 36–46. DOI: 10.9790/1684-0123646.
48. Duong S.C., Uezato E., Kinjo H., Yamamoto H. A Hybrid Evolutionary Algorithm for Recurrent Neural Network Control of a Three-Dimensional Tower Crane, *Automation in Construction*, 2012, 23, pp. 55–63. DOI: 10.1016/j.autcon.2011.12.005.

49. Carmona I.G., Collado J. Control of a Two Wired Hammerhead Tower Crane, Springer Science+Business Media Dordrecht, 2016, 84(4), pp 2137–2148. DOI: 10.1007/s11071-016-2634-3.
50. Loveikin V.S., Romasevych Y.A., Stekhno O.W. Regime Optimization of a Horizontal Gibbet Radius Varying Mechanism of a Tower Crane, Engineering, 2017, 20, pp. 11–18.
51. Romasevych Yu., Loveikin V., Stekhno O. Closed-loop optimal control of a system „Trolley-Payload”. UPB Scientific Bulletin, Series D: Mechanical Engineering, 2019, Vol. 81, Iss. 2. pp. 3-12.
52. Sakawa Y., Shindo Y. Optimal control of container cranes, Automatica, 1982 vol. 18, no. 3, pp. 257–266.
53. Hanafy M. Omar, Control of Gantry and Tower Cranes. - Ph.D. Dissertation, Blacksburg, Virginia, Virginia Polytechnic Institute, 2003.
54. Mahdieh A., Zarabadipour H., Mahdi A. S. Anti-swing control of a double-pendulum-type overhead crane using parallel distributed fuzzy LQR controller, International Journal of the Physical Sciences, 2011, vol. 6(35), pp. 7850-7856.
55. Chengyuan C., Shihwei H., Kuohung C. A practical fuzzy controllers scheme of overhead crane, Journal of Control Theory and Applications, 2005, vol 3, pp. 266-270.
56. Mohammad R., Akbarzadeh T., Amir H. “Fuzzy Modeling of Human Control Strategy for Head Crane“. In: IEEE International Fuzzy Systems Conference, 2001, pp. 1076-1079.
57. Kogure H., Tojo M. Recent developments in crain control, Hitachi Rev., 1978, vol 6, pp. 315-320.
58. SmartCrane™ Anti-Sway Crane Control Products, Product Descriptions, 2009, SmartCrane, LLC.
59. Siemens SIMOCRANE Crane Management System, System Manual, Valid for version 4.1, 2009.

60. Solihin M. I., Wahyudi “Sensorless Anti-swing Control for Automatic Gantry Crane System: Model-based Approach“, *International Journal of Applied Engineering Research*, 2007, vol.2, no.1, pp. 147-161.
61. Ahmad M.A., Raja Ismail R.M.T., Ramli M.S., Abdul Ghani N.M. , Zawawi M.A. “Optimal Tracking with Sway Suppression Control for a Gantry Crane System“, *European Journal of Scientific Research*, 2009, vol. 3, no. 4, pp. 630-641.
62. Keum-Shik H., Quang Hieu N. “Port Automation: Modeling and Control of Container Cranes“. In: *International Conference on Instrumentation, Control & Automation*, Bandung, Indonesia, October, 2009, pp. 1076-1079.
63. Bellman R., Dreyfus E. *Applied Dynamic Programming*, Princeton University Press, United States of America, Princeton, 1962.
64. Kwakernaak H., Sivan R. *Linear Optimal Control Systems*, John Wiley & Sons Inc., United States of America, New York, 1972.
65. Lovejkin V., Romasevich Yu., Chovnuk Yu. Synthesis of Quasi-Optimal Motion Crane’s Control in the Form of Feedback. *Journal of Automation, Mobile Robotics & Intelligent Systems*. 2013, Vol 7, N 3., pp. 18-39.
66. Gerasimiak R.P., Leschev V.A. Analysis and synthesis of crane electromechanical systems. 2008. Odessa. SMIL, 192 p. (in Russian).
67. Grigorov O.V. Improvement of the Performance of Crane Mechanisms, DSci Thesis: 05.05.05, 1995, Kharkov (in Russian).
68. Zaitsev Yu.I. Studying the Nonstationary Oscillations and Optimal Operating Modes of Translating Load-Lifting Machines, PhD Thesis, 01.02.06, 1981, Kharkov (in Russian).
69. Mel’nikova L.V., Microprocessor-Control Automation of the Displacement of a Mechanism with a Suspended Weight, PhD Thesis, 05.09.03, 2000, Odessa. (in Russian)
70. Pontryagin L.S., Boltyanskii V.G., Gamkrelidze R.V., Mishchenko E.F. *Mathematical Theory of Optimal Processes*, Nauka, 1969, Moscow (in Russian).
71. Smekhov A.A., Erofeev N.I. Optimal Control of Carrying-and-Lifting Machines, *Mashinostroenie*, 1975, Moscow (in Russian).

72. Strel'tsov P.M. Optimization of the Operation of Automated Harbor Cranes and Unloaders, PhD Thesis, 05.05.05, 1994, Odessa (in Russian).
73. Fel'dbaum A.A., Butkovskii A.G. Automatic-Control Methods, Nauka, 1971, Moscow (in Russian).
74. Chernous'ko F.L., Akulenko L.D., Sokolov B.N. Control of Oscillations, Nauka, 1980, Moscow (in Russian).
75. Babenko E.A., Martynuyk A.A., Stabilization of the motion of a nonlinear system with interval initial conditions, *Int. Appl. Mech.*, 2016, 52, No. 2, pp. 182-191.
76. Chen H., Fang Y., Sun N., Optimal trajectory planning and tracking control method for overhead cranes, *IET, Control Theory & Applications*, 2016, 10, No. 6, pp. 692-699.
77. Da J.J. Cruz, Leonardi F. Minimum-time anti-swing motion planning of cranes using linear programming, *Opt. Contr. Appl. Meth.*, 2014, 34, No. 2, pp. 191-201.
78. Ermidoro M., Formentin S., Cologni A., Previdi F., Savaresi M.S. On time-optimal anti-sway controller design for bridge cranes, *American Control Conf. (ACC)*, 2014, pp. 2809-2814.
79. Golub G.A., Szalay K., Kukharets S.M., Marus O.A., Energy efficiency of rotary digesters, *Progr. Agricult. Eng. Sci.*, 2017, 13, No. 1, 35-49.
80. Kennedy J., Eberhart R.C. Particle swarm optimization, *IEEE Int. Conf. on Neural Networks*, Perth, Australia, 1995, pp. 1942-1948.
81. Khoroshun A.S. Stability and speed control of a series-wound DC motor. *Int. Appl. Mech.*, 2016, 52, No. 4, pp. 432-436.
82. Khoroshun A.S. Stabilization of the upper equilibrium position of a pendulum by spinning an inertial flywheel, *Int. Appl. Mech.*, 2016, 52, No. 5, pp. 547-556.
83. Loveikin V.S., Liashko A.P., Chovnyuk Y.V. Crane's vibrating systems controlled by mechatronic devices with magnetorheological fluid: the nonlinear

mathematical model of behavior and optimization of work regimes, *Nauk. Vistn. Nats. Girn. Univ.*, 2014, No. 6, pp. 97-102.

84. Loveikin V.S., Romasevych Yu.O. Dynamic optimization of a mine winder acceleration mode. *Scientific bulletin of National Mining University Scientific and technical journal, Dnipro*, 2017, Vol. 4, pp. 55-61.

85. Loveikin V.S., Romasevich Y.A., Khoroshun A.S., Shevchuk A.G. Time-Optimal Control of a Simple Pendulum with a Movable Pivot, Part 1, *International Applied Mechanics*, 2018, 54(3), pp. 358–365.





ISBN 978-83-66567-10-8



9 788 3665 67 10 8